PLUMBAGIN-INDUCED TESTICULAR MITOCHONDRIAL-DEPENDENT CELL DEATH AND INFERTILITY IN MALE WISTAR RATS

ISAAC JAMES BELLO

MATRIC NO: 135676

PLUMBAGIN-INDUCED TESTICULAR MITOCHONDRIAL-DEPENDENT CELL DEATH AND INFERTILITY IN MALE WISTAR RATS

ISAAC JAMES BELLO

B.Sc (Hons) Biochemistry, Ilorin

M.Sc Biochemistry, Ibadan

Matric No: 135676

A thesis in the Department of Biochemistry submitted to the

Faculty of Basic Medical Sciences in partial fulfillment of the requirements for the degree of

DOCTOR OF PHILOSOPHY

of the

UNIVERSITY OF IBADAN

December, 2021

CERTIFICATION

I certify that this work was carried out by Bello, Isaac James in the Department of Biochemistry, College of Medicine, University of Ibadan, Nigeria.

……

Supervisor

Olufunso O. Olorunsogo, Ph. D, FNISEB

Professor

DEDICATION

This thesis is dedicated to God’s glory and praise for His tender mercies and faithfulness

And

also to my loving and caring father, Elder James Bello Olaoye.

ACKNOWLEDGEMENTS

God gives grace and glory! And without Him I am nothing. Therefore, I give all glory and honour to Him for his mercies, unceasing care, guidance, protection, provision and favour through the entire experience of the Ph. D project and so, I return to you all adoration for all you have done.

I sincerely appreciate my mentor and father, a teacher *per excellence*, an academic icon, professor of professors and my own supervisor- Professor Olufunso Olabode Olorunsogo for his patience, guidance, constructive criticisms, spiritual and moral support through this academic sojourn and pursuit. You refused to give up on me but put in all efforts to give the best of training to me. I feel so honoured and humbled for having your mentoring over the years. May God spare and prolong your life in good health and vigour to eat more of the fruits of your labour. You will not lack the grace of God in your life. I am saying- Thank you sir!

I also express profound gratitude to the Head, Department of Biochemistry, Professor Oyeronke Aduni Odunola for being a source of inspiration to me. I learned so much from your composed and focused disposition, discipline and doggedness. You are a mother indeed. May you be fulfilled and find grace in every area of your life.

I will remain grateful to the immediate past Head, Department of Biochemistry and Director of Molecular Drug Metabolism and Toxicology Unit, Professor Ebenezar Olatunde Farombi - an articulate and outstanding professor, for his timely and unfailing support, encouragement and accessibility to render necessary help, you have impacted in no small measure to what I become today. Thanks so much sir and may God take you higher and higher and fulfill your desires.

Professor Adekunle Oluwatosin Adaramoye remains a source of encouragement to me. I thank you for your mentoring and support in my adventure and academic pursuit. May you receive timely help and favour from God. Thank you, sir.

I will remain grateful to Professor Gbadegesin, M.A. who was then the Postgraduate Coordinator in the Department, and contributed in no small measure to the success of this research work and has always being there for me. God bless you sir.

I am indebted to the Director of Nutrition and Industrial Biochemistry Research Unit, Professor C.O. Olaiya for his contribution to this success story. Thank you, sir.

I also express sincere gratitude to my Co-supervisors Dr J.O. Olanlokun, Dr O. Oyebode and Dr O. Olowofolahan for their valuable contributions and persistent effort at ensuring the best came out of this research. You will not lack God's wisdom, presence and provision. I remain grateful for your kind gestures and support.

I appreciate other lecturers in the Department including Dr S. Nwozo, Dr O. Adesanoye, Dr A Abolaji, Dr I. Adedara, Dr (Mrs) A. Salami, Dr O. Olugbami, Dr F. Adegoke, other academic and all non-academic staff of the Department. Thanks so much.

The Director, Centre for Bio-computing and Drug Deveplopment, Adekunle Ajasin University, Akungba-Akoko, Dr Idowu Omotuyi for providing facility and logistics for the docking and simulation studies. Thanks so much.

My profound appreciation goes to the Tertiary Education Trust Fund (TETFUND) through the Management of Adeyemi College of Education Ondo and the Director, Directorate for Academic Planning and Quality Assurance for bearing the financial burden of this research.

I wish to thank my spiritual fathers and mentors: Dr D. Falade, Dr S. Adejubee, Dr B. W. Adu and other leaders of the DLCF, ACE Ondo.

I immensely acknowledge my friends and colleagues Dr A. Jonah, Dr O. Jumoke, Dr T. Daniels, Mrs O. Adeoye, Mr J. Salemcity, Dr Mrs J. Immah- Harry, Mrs I. Vining (IBK), Mrs F. Ijai, Mrs F. Olojo, Mrs O. Babarinde and host of others including the M. Sc students in the Unit for your sundry assistance and cordial company over the years. Dr J.K. Akintunde, you are also recognized. God be with you all.

I thank my father -Elder J.O. Bello, for his unceasing prayers, encouragement and financial support. Lastly, I appreciate my wife, children and siblings for their patience, understanding and prayers through the thick and thin of the programme. Thanks so much and God be with you all.

Isaac James Bello.

December, 2021.

ABSTRACT

The opening of the mitochondrial Permeability Transition (mPT) pore is an important event in mitochondrial-mediated cell death. Plumbagin, the active principle in *Plumbago zeylanica*, induces cell death in rapidly dividing cells and conditions such as prostate tumor but its effects on testicular cell death and fertility are not well understood. This study was designed to investigate the effects of plumbagin on testicular cell death and fertility in male Wistar rats.

This study was in two phases. In phase 1, twenty male Wistar rats (80-100g) were grouped into four (n= 5) and were treated once daily as follows: Group I (Control) received 10ml/kg distilled water, groups II, III and IV were orally treated with 2.5, 5.0 and 10.0mg/kg of plumbagin for 14 days. In study 2, fifteen male Wistar rats (100-120g) were grouped into three (n=5) and were orally treated once daily with 10 ml/kg distilled water (control), 30 and 100mg/kg of plumbagin for 72 hours. In study 1, testes mitochondria were isolated using differential centrifugation. The mPT pore opening, mitochondrial Lipid Peroxidation (mLPO) and mitochondrial ATPase (mATPase) were assessed using spectrophotometry. Caspases 3 (C3) and 9 (C9) activities were assessed using ELISA. Sperm count, motility and morphology were determined using microscopy. Expressions of p53, Bax, Cytochrome C Release (CCR) and Bcl-2 were determined using immunohistochemistry. In study 2, expressions of Follicle Stimulating Hormone (FSH), Progesterone Receptors (PR), Testis Specific Protein Kinase-1 (TESK-1) and aromatase were determined using polymerase chain reaction. Interactions between plumbagin, Mouse Double Minute Homolog 2 (MDM2) and Bcl-2 were assessed using docking method. Statistical analysis was done using descriptive statistics and ANOVA at $\alpha_{0.05}$

Plumbagin at 2.5, 5.0 and 10.0mg/kg induced mPT pore opening in testis by 2.3, 4.6 and 8.0 folds relative to control. Plumbagin also increased mLPO (2.3, 5.8, 8.0μmoleMDA/mg protein), mATPase (10.1, 12.7, 13.6mmolePi/mg protein/min), C3 (5.1, 7.3, 12.2ng/mL) and C9 (6.7, 8.4, 11.8ng/mL) activities respectively compared to control (1.1μmoleMDA/mg protein, 8.2mmolePi/mg protein/min, 2.6 and 1.8ng/mL), respectively. Sperm analysis revealed decrease in sperm count (63, 61, 62.5 million/mL), motility (80.1,78.3,77.0%) and increased sperm abnormality (7.2$\pm$1.41, 9.5$\pm$ 0.71, 11.5$\pm$0.71million/mL) at 2.5, 5.0 and 10.0mg/kg, compared to control (120million/mL, 98% and 4.3$\pm$0.21million/mL) respectively. Furthermore, plumbagin increased the expressions of p53 (6.3, 7.5 and 12.3%), Bax (6.1, 7.5 and 9.5%), CCR (7.2, 8.4 and 12.3%) and decreased Bcl-2 (25.0, 18.0 and 15.5%) at the same dose compared to control (5.0, 3.4, 6.0 and 27.0%,). Expressions of FSH (0.9, 0.7), PR (0.8, 0.3), TESK-1 (0.7, 0.3) and aromatase (0.8, 0.3) folds decreased relative to control. Plumbagin interacted with MDM2 and Bcl-2 (ΔG = -6.0 and -5.9kcal/mol) respectively compared to 7-hydroxy-4-methylcoumarin (ΔG = -10 kcal/mol) used as control in docking studies.

Plumbagin decreased spermatogenesis in male Wistar rats by decreasing the expressions of Follicle Stimulating Hormone and masking the Progesterone Receptor. It also decreased spermatogenesis by down-regulating the activities of Testis Specific Protein Kinase-1 and Aromatase. It caused testicular damage via mitochondrial-dependent cell death with increased sperm abnormality.

Key words: *Plumbago zeylanica,* Plumbagin, Cell death, Infertility, Testis

Word count: 492

TABLE OF CONTENTS

CHAPTER THREE: MATERIALS AND METHODS

CHAPTER FOUR: EXPERIMENTS AND RESULTS

LIST OF TABLES

LIST OF FIGURES

ABBREVIATIONS

ALT	Alanine Amino Transferase
APAF-1	Apoptosis Protease Activating factor -1
BSA	Bovine Serum Albumin
DISC	Death Inducing Signalling Complex
CASPASE	Cysteine-dependent Aspartate Specific Proteases
ELISA	Enzyme Linked Immunosorbent Assay
PCD	Programmed Cell Death
PGR	Progesterone receptor
TBARS	Thiobarbituric Acid Reactive Species
PT	Permeability Transition
PVC	Packed Cell Volume
TNFR	Tumor Necrosis Factor Receptor
7HC	7 hydroxyl methylcoumarin
Rsmd	Root Mean Square Deviation
GST	Glutathione transferase
MDA	Malonyldealdehyde
TBA	Thiobarbituric Acid
MSH	Mannose, sucrose and HEPES
HEPES	2-{4 (2-hydroxymethyl) piperazin-1 yl} ethane sulfonic acid
TCA	Trioxocarboxylic Acid
TESK-I	Testes specific protein kinase 1
NFK_B	Nuclear Factor kappa B
TA	Triggering Agent
NTA	No Triggering Agent
SOD	Superoxide Dismutase
ROS	Reactive Oxygen Species
IAP	Inhibitors of Apoptosis Proteins
2,4 DNP	2,4 – dinitrophenol
CAT	Catalase
VDAC	Voltage Dependent Anion Channel
ACUREC	Animal Care, Use and Research Ethics Committee
AST	Aspartate Aminotransferase

ALT	Alkaline Transaminase
EGTA	Ethylene gl (2-amino ethyl ether)- N,N,N,N, -tetraacetic acid
CyP D	Cyclophilin D
BAX	Bcl-2 Associated Bax Protein
FSH	Follicle Stimulating Hormone
LD_{50}	Lethal Dose 50
cDNA	Circular Deoxyribonucleic Acid
mPT	Mitochondrial Permeability Transition
PR	Progesterone Receptor
IMM	Inner Mitochondrial Membrane
OMM	Outer Mitochondrial Membrane
PL	Plumbagin
PZ	*Plumbago Zeylanica*
G-score	Gibbs free energy score
MDS	Molecular dynamics simulation
MDM2	Mouse double minute homolog 2
p53	Tumor suppressor protein 53
A1	Cyclin A1
TRIzol	Total RNA isolation reagent.
SfA	Sangliferin A
SDS	Sodium deodecyl sulphate
DPNH	2,4 dinitrophenylhydrazine
VDM	Visual molecular dynamics
C3	Caspase 3
C9	Caspase 9
CCR	Cytochrome C release
ANOVA	Analysis of variance
IMS	Inter membrane space
MMPBSA	Molecular mechanics poisson boltzman surface area

CHAPTER ONE

INTRODUCTION

The use of medicinal plants for health and healing has continued to gain increased attention over the years. This might be linked to the fact that plants are easily accessible, cheap and rarely cause allergies which are associated with the use of synthetic drugs. Plants are natural to the body and because of their preponderance in nature, there are thousands- precisely between 250,000- 400,000 species of plants and plant derived products that can promote good health and add value to life in all ramifications (Roy, 2017; Tilak, 2004).

Moreover, inherent in plants are various and varied phytochemicals with sundry health benefits. For example, plants such as carrots, potatoes, pumpkins, spinach, mangoes, cabbage, citrus fruits, water melon, cucumber and others have been found to contain photochemical with different contents of vitamins and minerals having tremendous health benefits. Basically, some phytochemicals identified and characterized from plants include: epigallocathechin gallate in green tea, quercetin in onions, capsaicin from chili pepper, resveratrol in grapes and lycopene in tomatoes among others. These and more confirm theraupeutic effects of plant pytochemicals and especially medicinal plants (Roy, 2017). More so, minerals such as potassium, magnesium, iron and sodium have been found in plants (Chen, 2003) and are of immense importance as they are found to play sundry health functions in humans, thus the saying: “let your medicine be your food and your food be your medicine”.

Advancing on myriads of health benefits derived from plants, it has been discovered that certain medicinal plants have potential to modulate the induction of pore opening in the mitochondrion – a pivotal event in cell death which is initiated through some signaling cascades and ultimately results to “safe” destruction and disposal of cells with no consequent inflammatory response-a process generally referred to as apoptosis.

Hence, phytochemicals in plants particularly medicinal plants exhibit chemotherapeutic properties by exerting toxic effects on the body cells via spontaneous response of the

mitochondrial machinery thus precipitating the apoptotic process (Crompton, 1999; Yu *et al.,* 2019, Zhao *et al*., 2014). Therefore, when the mitochondrion is made to spontaneously respond to chemotherapeutic agents in form of drugs or medicinal plants such that it results to cell death, the entire pathway or process involved is known as the mitochondrial-mediated apoptosis otherwise referred to as intrinsic pathway of apoptosis (Ray *et al*, 2016) and the entire process has a wide range of implications.

Apoptosis or in simple term cell-demise is a sequential event in developmental and as well as physiological processes where it helps to maintain tissue homeostasis and eliminate unwanted or harmful cells from the body. It has been identified in production of healthy reproductive cells in gametogenesis (Kiess and Gallaher, 1998). However, aberrant regulation of apoptosis has been identified in certain diseased conditions and pathologies including autoimmune disease, Parkinson's disease and various types of cancers among others. Since the mitochondria is central to induction of cell death via the intrinsic pathway, modulation of mitochondria to induce cell death in these conditions will pave way to examine and probe into plumbagin potential to foster health or address the aforementioned disease conditions.

There are numerous pathologies involved in the mitochondrial mediated apoptotic process which range from induction of cell death by potentiators of apoptosis which may include: toxins, hypoxia, uv light, radiations, drugs and reactive oxygen species among others to prosecutors of apoptosis featuring the caspase activities leading to formation of aggregates of apoptotic bodies (Zeng *et al.,* 2019). Interplay amongst players in the apoptotic process are initiated as they are stimulated in reaction to apoptotic signals. Such players in the pathology of cell demise may include molecules such as Bax, Bak, Bcl-2, p53, bid, cyt.c (cytochrome c) among others. Basically, balance or imbalance in the players determine the likelihood of apoptosis taking place. The next stage involves down-stream interactions of proteins which can be referred to as prosecutors of apoptosis which essentially include activation of the entire cell death process predominantly identified as the caspases such as C9, C3, C6 and C7 to ultimately precipitate cell demise in its entirety (Martin, 2006).

1.1 Rationale

Manourvering of the mMPT pore has become a core concept in pharmacological drug discovery and development and by extension a determinant factor in cell death or survival in relation to cell response to drug toxic effect. Bioactive agents in drugs are known to interact with the component of the mMPT pore to rupture the membrane and cause more absorption in the outer mitochondrial compartment leading to increased influx of water with consequent decrease in membrane potential.

Plumbago zeylanica (PZ) is an ornamental medicinal plant which has been shown to elicit multiple and varied chemotherapeutic properties. Prominent chemotherapeutic potentials of PZ among others include antifungal (Dominic, 2019), antibacterial (Aziz *et al*., 2008), anti-plasmodial (Simonsen *et al.*, 2001), abortificient (Sandur *et al*., 2006), anti-carcinogenic (Yu *et al.*, 2019), anti-inflammatory, cytotoxic (Wang *et al.*, 2015) and immunosuppressive activities (Bae, 2016). It has been used traditionally in combination with *Calliandria portoricensis* (CP) to treat prostate tumor (Oyebode, 2012).

1.2 Statement of problem

Plumbagin has been characterized from PZ and has been identified as the main bioactive principle in the ornamental plant but it is not known whether the toxic influence of plumbagin (PG) proceeds via the permeabilisation of the mitochondrial-compartment. On the other hand, CP has been experimented and studied in animal models in relation to its potential in modulating the mitochondrial membrane permeabilisation (Green, 2008). The effect of plumbagin on mitochondrial–mediated apoptosis or mitochondrial-dependent cell death especially in male reproductive cells or gamete is yet to be examined or studied.

To justify traditional use of PZ in treatment of ailments such as protate cancer, it is necessary to understand the mechanism of plumbagin toxicity and its impact on the intrinsic pathway of cell death. The reason behind its combination therapy with CP has not been empirically justified as well.

It is on this premise that the impact of plumbagin - the active principle in PZ was investigated with the view to study and understand its chemotherapeutic action in relation to mitochondrial- dependent cell-death and its probable influence on fertility machinery in male

animal model. Thus, the study focused on experimenting adverse reaction of PG on mitochondrial-dependent cell death and fertility using male Wistar rats as animal model.

1.3 Objectives

The central focus of this study was to verify whether plumbagin toxic effect in liver and testis proceeds through mitochondrial-dependent cell death and to examine its possible potential to interfere with the fertility machinery.

1.4 Specific Objectives

The major objectives of this study are to:

- Assess effect of plumbagin on the mPT pore opening in testis and liver of Wistar rats.
- Quantify levels of mLPO, mATPase and caspases 3 and 9 activities in both control and treated animals.
- Examine histopathological effects of plumbagin on testicular ultra-structure.
- Quantify effect of PG on physiological features of the sperm.
- Measure impact of plumbagin on enzyme biomarkers in liver of experimental animals.
- Determine effects of plumbagin on molecules that influence testicular functions and fertility.
- Quantify levels of promoters (proapoptotic) and anti-apoptotic proteins as a result of plumbagin administration.
- Identify potential targets that directly interact with plumbagin through docking and simulation studies.

CHAPTER TWO

LITERATURE REVIEW

The body is designed in such a way as to fight against diseased cells including cancerous cells by eliminating those cells that are unhealthy or potentially detrimental to specified functions and well being of the entire body. Machinery designed to work in this capacity where unwanted cells have to be disposed without necessarily affecting or triggering inflammatory responses from other neighbouring cells is a product of well defined and regulated process termed apoptosis or programmed cell death (Dominic *et al.*, 2019).

The term cell death or apoptosis involves a highly regulated pathway where a cell is programmed to die with no consequent inflammatory response from other neghbouring cells and was a term first used by a team of scientists in 1972. Precisely, scientists: the likes of Wyllie and Currie used the terminology to explain an energy dependent process accompanied by certain forms of morphological features involved in development and growth as well as defense mechanisms of multi-cellular organisms (Chen *et al.*, 2016). It is put in place to maintain tissue homeostasis by removing infected or damaged cells, excess population of cells and regulate the cellular preponderance of cells for the benefit and overall survival of the entire organism (Chen, 2016). It involves a process in immune response and defense against diseases as well as toxic agents which may have the propensity to overwhelm the protective factors in the cell.

From economic point of view, apoptosis fosters efficiency of the working machinery of the cell, as it helps to shed-off old and ineffective organelles so that there could either be a replacement or reduced inefficient population of senescent cells that may burden the system leading to waste or unnecessary dissipation of energy (Wacquier *et al.*, 2020).

Cells do respond to chemotherapy or certain toxic agents when assaulted and the resulting aggregates of cellular bodies are the products of a well defined and regulated pathway involving interplay of multiple and various protein molecules. Similarly, a signaling cascade

is involved in the processes leading to release of tissues of the lining of the endometrium resulting in monthly menstrual flow in women with no consequent inflammatory response. Here apoptosis also features as an essential mechanism to maintain tissue homeostasis and functionality of the entire reproductive system.

To initiate apoptotic processes involved in growth and development, defense against diseases including immune responses, proteins involved at different stages are critical factors in decision making for cell death or survival particularly in the mitochondrial-dependent pathway.

Since, apoptosis precipitates stepwise destruction and removal of cell with no consequential adverse or inflammatory reaction. This process of cell evacuation, in which mitochondrion is modulated to induce programmed cell death is known as the intrinsic pathway of apoptosis and has a wide range of implications (Li *et al*., 2019).

Obviously, apoptosis is essential in metazoans for defense against diseases as observed in tumors, necessary in maintaining tissue homeostasis, formation of foetus in pregnancy, development of reproductive cells, immune responses to foreign and toxic agents among others (Perez and Quintanilla, 2017).

2.1 Relevance of Mitochondria to Cell Survival and Functions

The mitochondrion is often referred to as *power house* of the cell; this is predicated on the basis of its energy generating activities and most importantly as the site for oxidative phosporylation among other functions. Since the existence and survival of the cell is dependent on availability of fuel in form of ATP- the energy currency of the cell, any attempt to compromise the structural integrity of the power machinery of the cell will definitely affect the survival of the entire cell. Hence, mitochondria are principal factors and tools which determine survival and functionality of the cell. Its modulation can therefore be exploited as a tool to probe for sundry activities and factors necessary for cell effective functioning and survival among others. It is worth noting that the preponderance of mitochondria population in tissues and organs is a reflection of level of energy requiring activities taking place in such tissues. This accounts for increased population of mitochondria in the heart necessitated by the unceasing pumping action and supply of blood to the entire body. Similarly, the liver is vested with preponderance of mitochondria to enable it carry out its multiple functions of detoxification, protein synthesis, production and activation of enzymes, metabolism of fats,

proteins and carbohydrates including other mechanisms in which toxicants are converted into less harmful products among others (Ruberto *et al*.,2000). Consequentially, a reduction in mitochondrial abundance in tissues and organs will affect functioning and efficiency which will in turn determines survival of cells. Hence, it suffices to say that level of physiological function, efficiency and survival of organ or tissue is dependent on the overall population of healthy mitochondria. Figure 2.1 shows detailed structure of a mitochondrion.

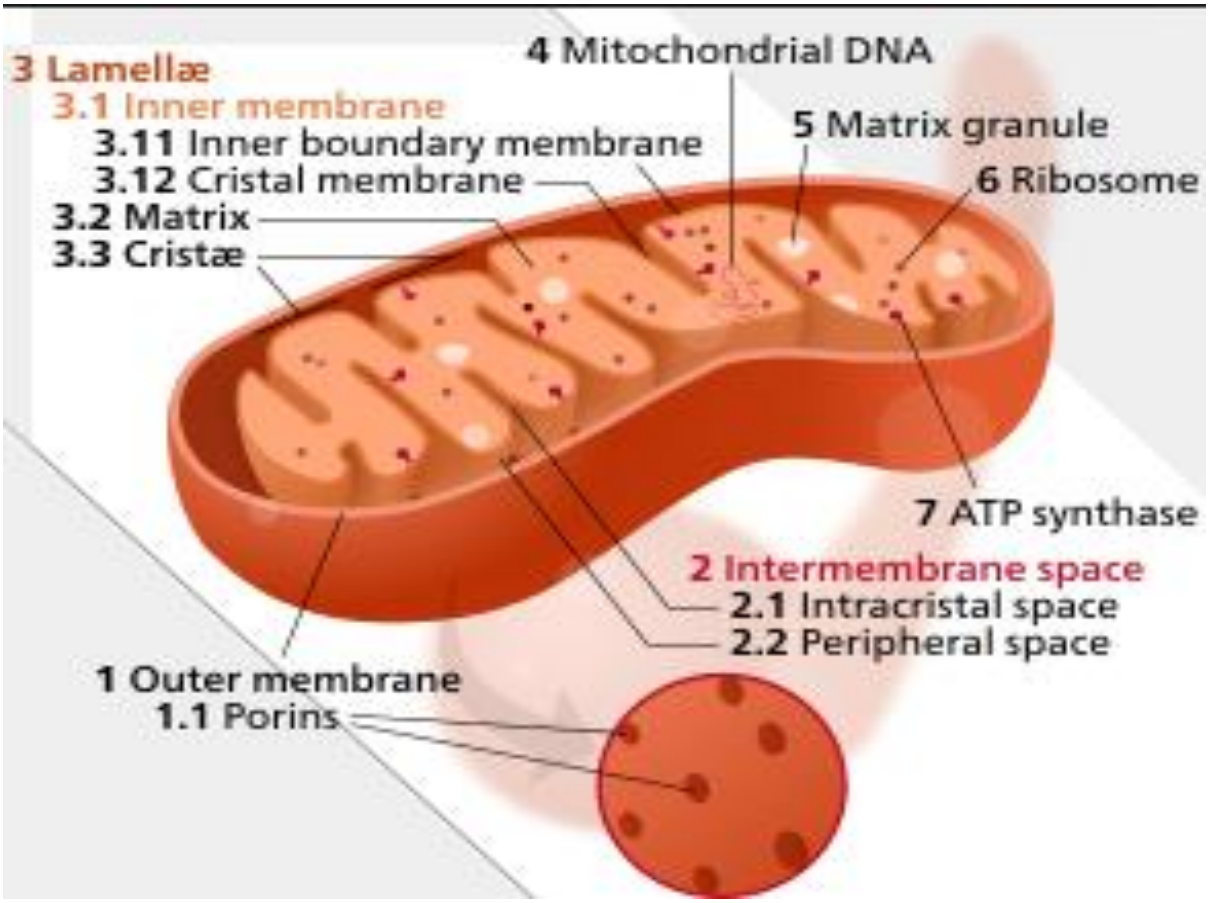

Figure 2.1 The structure of mitochondrion (Green, 2008).

2.1.1 Mitochondrial Membrane Permeability Transition Pore

Apoptosis is a highly regulated process and can occur via the intrinsic and extrinsic routes. The former requires mitochondrion which is a principal factor that regulates the pathway and it is necessary to understand this organelle as a major tool or principle regulating the apoptotic process. A probe into the structure and functions of mitochondrion would be essential to understand its role in the entire process.

Mitochondrion is a membrane bound organelle with distinct purpose of energy production among other functions. The membrane surrounding this vital organelle is only selectively permeable to certain molecules of specific size such that the integrity of the organelle is thus maintained within the enclosed and intact membrane. It consists of a double membrane layer known as outer and inner compartments (Wacquier 2020; Green, 2008).

The mitochondrial membrane permeability transition apart from being a non selective and calcium-dependent event features the permeabilisation or perforation of the innermost mitochondrial membrane as it becomes ajar in response to increased Ca^{2+} levels in the matrix and as such increase permeability of molecules that are less than 1.5 kDa in weight resulting to cell death (Crompton, 1999).

In ordinary condition, the mPT pore remains closed until Ca^{2+} concentration increases to trigger its opening. This helps to maintain Ca^{2+} heomostasis. However, prolonged exposure to Ca^{2+} influx causes mPT pore opening which results in mitochondrial expansion and the unfolding of the inner section of the mitochondria, which unequivocally leads to its outer membrane swelling, rupture and collapse of the matrix potential (Green, 2008).

Similar factors such as mitochondrial depolarization, inorganic phosphate, oxidative stress including adenine nucleotide deficit can equally influence mPT by inducing the pore to varying Ca^{2+} concentration which can stimulate various forms of cell demise. Hence, while momentary opening of the pore serves physiological function, a sustained opening will result in the discharge of cyt.c and activation of the caspases which finally culminates to cell death or the collapse of the oxidative phosporylation machinery which restricts ATP synthesis, leading to a type of cell death known as necrotic cell death (Halestrap *et al*., 2004). Pictorial representation of mPTregulation is presented in Figure 2.2.

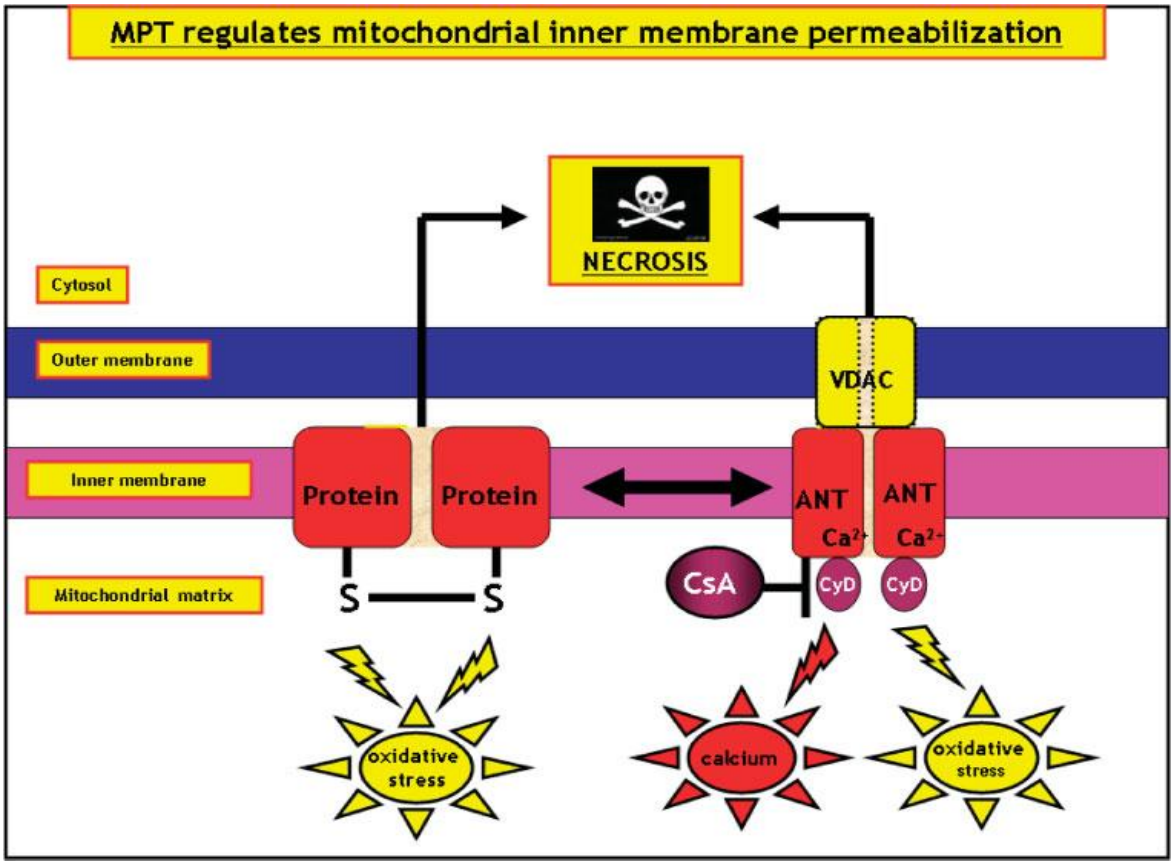

Figure 2.2: Inner mitochondrial membrane permeabilization and necrosis regulated by mitochondrial permeability transition (Jeffery, 2014).

2.1.2 Structure of mPT pore

Although the molecular architecture of mPT is still to be unraveled, relevant protein compositions which are prominent features in disease conditions show that cyclophilin D (Cyp-D), adenine nucleotide translocator (ANT) and voltage dependent anion channels (VDAC) are implicated in formation or control of mPT pore. Hence, these factors (Cyp-D, ANT and VDAC) target the mPT to selectively inhibit the components and as such have been used in the study of mPT. This invariably provides a viable therapeutic measure for a variety of health conditions. For instance, reperfusion injury in the heart is similar to situation that causes opening of the MPTP. Therefore, it presents an avenue for initial cardioprotective propensity of MPTP which is now a subject of interest to researchers. Furthermore, control of mitochondrial membrane permeability can also provide neuroprotection where it may assist to harness the functon of MPTP in conditions such as neurodegeneration (Dominic, 2019).

To unravel, the MPTP structure, the first PTPC model was put forward towards the end of 1990s. The model was conceived to consist of a supramolecular entity assembled by the juxtaposition of the internal and outer mitochondrial portion (Crompton *et al.,* 1999).

The first model suffered a substantial set back as it was challenged by genetic conceptualization and scrutiny. This is because the three distinct isoforms of VDAC (Vdac1, Vdac2 and Vdac3) failed to protect murine fibroblasts from mPT induction by hydrogen peroxide- an mPT inducer (Colombini, 2004).

Similarly, side by side removal of genes depicting two distinct ANT isoforms; Ant1 and Ant2 failed to cancel the ability of murine hepatocytes to give-up to multiple mPT inducers including the Ca^{2+} ionophore in a CsA-inhibitable manner (Bouillet and Strasser, 2002).

In the recent times, two proteins were added to the list of PTPC components namely; the mitochondrial F1F0 ATP synthase encoded by three genes in humans (ATP5G1, ATP5G2 and ATP5G3) and the SPG7 paralegin matrix AAA peptidase subunit (Ameisen 2002; Giorgio *et al.,* 2016; Bonora *et al.,* 2016) thus leaving two models shown in figure 2.3 including pictorial template of the mPTP in Figure 2.4.

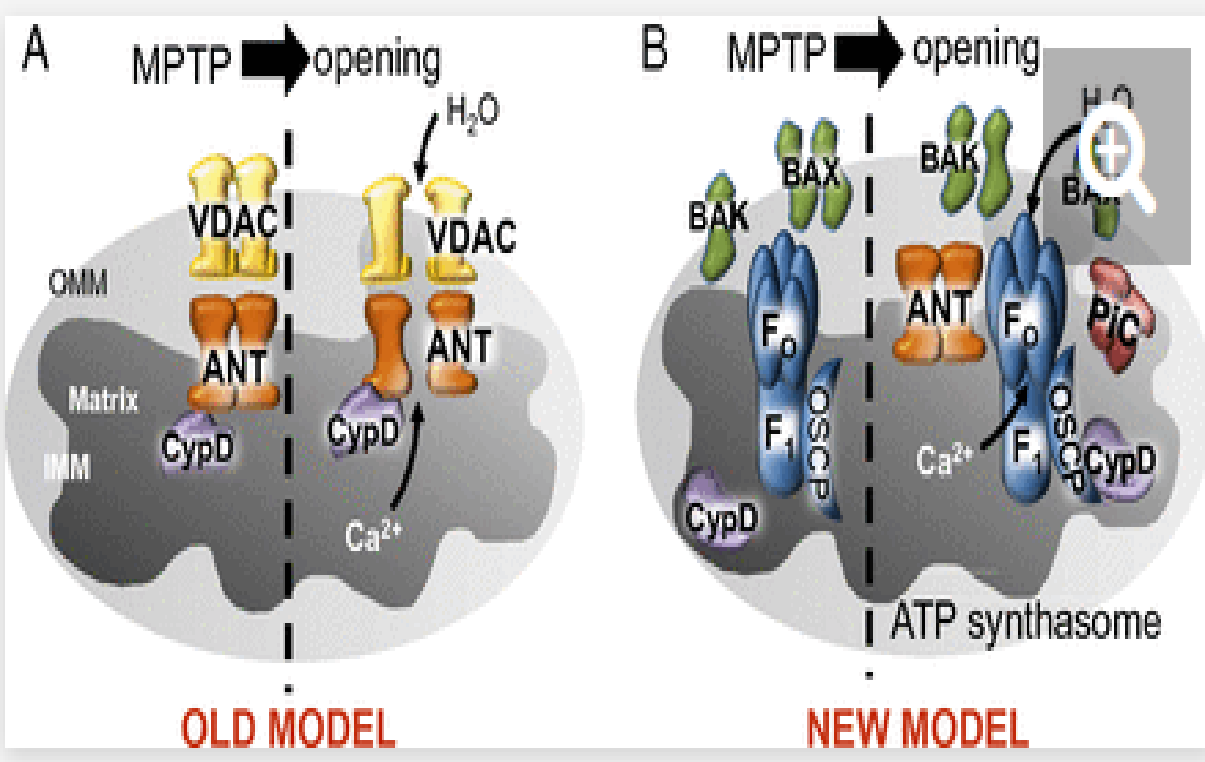

Figure 2.3: Pictorial representation of the original and new models of the mPTP (Jeffery, 2014).

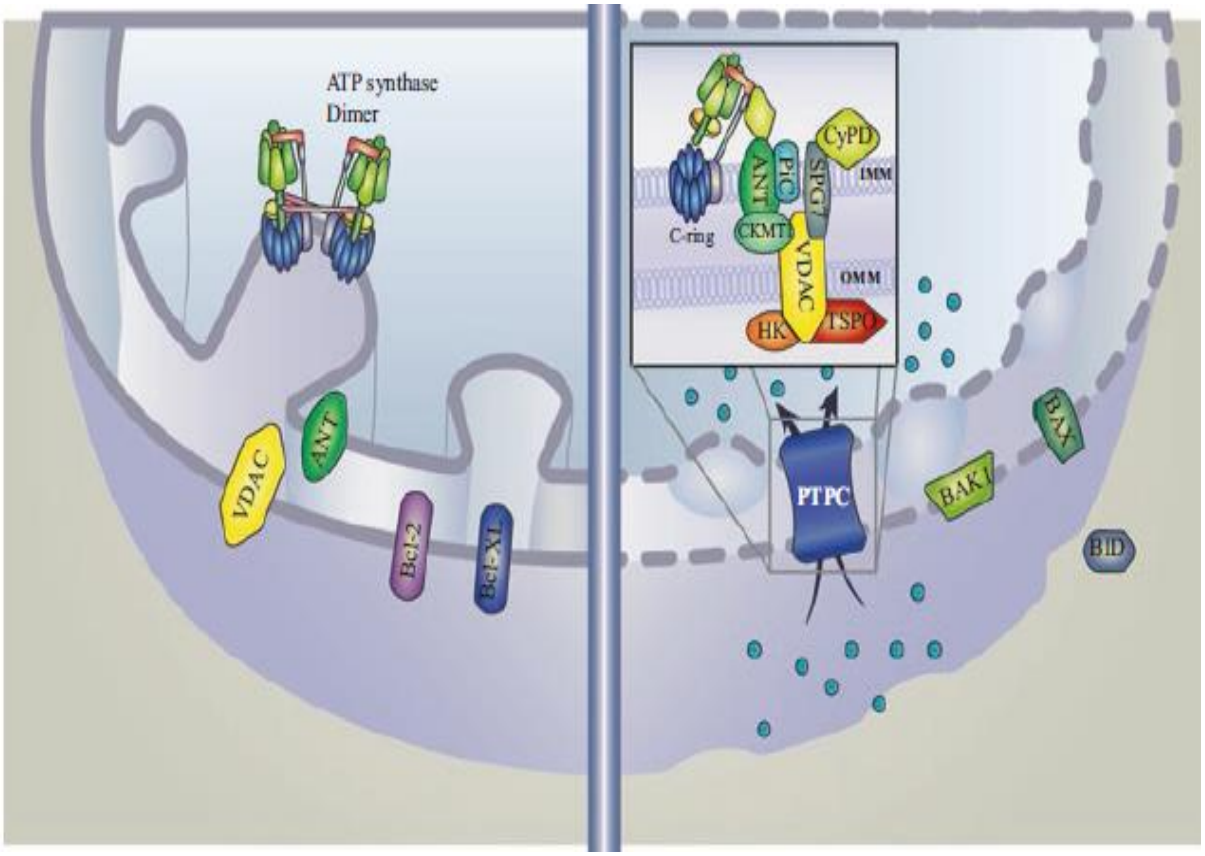

Figure 2.4: Pictorial template of the mPTP (Martin, 2006).

2.1.3 mPT Pore Components

The three key structural components of the mPTpore consist of Cyp-D localized in the matrix, ANT contained in the innermost membrane and the VDAC also called porin in the outer membrane (Halestrap *et al.*, 2004; Crompton, 1999).

Other proteins thought to perform regulatory functions in mPTP formation include surface benzodiazepine receptor, hexokinase, creatine kinase and Bcl2 family members but their involvement is said to be controversial (Halestrap *et al.*, 2004). Being part of the mPT (Walter *et al*., 2000) certain proteins including; the peripheral alestrapenzodiazepine receptor, creatine kinase, hexokinase and Bcl-2 family members have been considered to exert control function in mPTP formation, but the veracity of their involvement is uncertain (Halestrap *et al.*, 2004). Moreover, the role of ANT has been traced to be regulatory rather than structural function in pore constitution (Baines and Molkentin, 2009).

2.1.4 Adenine Nucleotide Translocator

The involvement of ANT in mPTP formation was initially conceived to have divergent regulation because ATP and ANT inhibited opening of mPTP as it decreases its reaction to Ca^{2+} while other inhibitor of ANT namely carboxyatractyloside and adenine nucleotide were able to unlock the pore by sensitising it to Ca^{2+} concentration (Halestrap *et al*., 2004). But it was later discovered that the divergent regulation of mPTP was caused by opposing orientation of ANT molecules exhibited by the inhibitors. On the whole, it has been confirmed that response of pore opening to Ca^{2+} is dependent on level of oxidative stress which inhibits adenine nucleotide binding to the ANT. Moreover, it has been established as well that CyP-D is also attracted to ANT in the presence of calcium ion to induce a conformational change subsequently leading to pore opening (Kwong and Molkentin, 2015).

2.1.5 Cyclophilin D

Cyclophilin-D being a nuclear encoded mitochondrial isoform of cyclophilin is a water-soluble protein with a molecular mass of 18 kDa (Erkkila *et al*., 2006). As at present, extensive data have been obtained to favour CyP-D as an essential component and key regulator of mPTP using various pharmacological inhibitors and genetic manipulations. The first discovery of CyP-D involvement in mPTP formation was obtained in the studies

revealing inhibitory effect of the immunosuppressant CsA widely used in tissue and organ transplantation on pore opening (Dominic *et al*., 2019).

2.1.6 Voltage Dependent Anion Channel

VDAC being an integral protein localised in the outer mitochondrial membrane is known also as mitochondrial porin. It emerges as a form of large channel with basic functions of providing transport means for anions, cations, Ca^{2+}, adenine nucleotides including other metabolites, in and out of the mitochondria. As part of the mPTP, VDAC is known to form a diffusion pore with conserved characteristic in the outer mitochondrial membrane (OMM). While VDAC is believed to be constituent part of mPTP, the OMM functions as a link between mitochondrial metabolism and the rest of the cell (Colombini, 2004).

Contemporary model suggests that PTP is constituted at contact points between inner and outer membrane via association of VDAC in the outer membrane with the ANT in the later. VDAC may also bind, perharps through a secondary interaction with the ANT. Despite other proposed models, some mitochondria are lacking all isoforms of VDAC and yet exhibit equal proportion of pore opening as ordinary mitochondria. For example, fibroblasts lack all isoforms of the VDAC yet they are highly responsive to cell death induced by oxidative stress suggesting more propensities to pore opening just as it may apply to normal mitochondria (Bauer and Murphy, 2020).

2.2 The Permeability of the Mitochondrial Membrane and its consequences

Specific effects of the opening of the mPTP are the collapse of the membrane potential and functionality which becomes disrupted with two major accompanying outcomes (Crompton *et al*., 1998).

First, is the free movement of small molecular weight protein while proteins with large molecules remain and then exert a colloidal osmotic pressure in the outer membrane causing the mitochondria to swell and bursts. However, the unfolding of the cristae in the inner membrane may allow matrix expand without necessarily allowing distruption of the inner compartment, the break in the outer membrane is sufficient to allow proteins that play critical roles, particularly cytochrome C in the apoptotic cell death to be released (Crompton *et al.*, 1999).

Second consequential outcome of the permeabilisation of the mitochondrial membrane is the free permeability of the inner membrane to protons, which uncouples oxidative phosporylation, hydrolysis of ATP rather than its synthesis with attendant sharp reduction in intracellular ATP levels which further amounts to distruption of ionic and metabolic homeiostasis with down stream activation of degradative enzymes such as proteases, nucleases and phospholipases. All these culminate to spontaneous adverse effects and irreversible damage to the cell (Juarez Rojas *et al*., 2015). This is the reason why mPTP is highly inhibited under ordinary physiological condition until otherwise required and activated under pathological conditions.

It should be noted that the key factor involved in mPTP induction is as a result of influx of Ca^{2+} and unfolds mitochondrial membrane causing leakage of mitochondrial proteins or molecules. These events are replica of those the heart experiences in post ischaemic reperfusion, and there are increasing proofs to substantiate that mPTP opening exerts important role in conversion from reversible to irreversible reperfusion injury (Bratton and Salvesen, 2010).

2.2.1 Molecular machinery of the mPTP

The core components of the mPTP consist of ANT, cyclophilin (CyP-D) that displays peptidyl-prolyl cis-trans isomerase (PPIase). Other components of mechanism include cyclosporine A (CsA) which acts as a potent inhibitor of mPTP opening by preventing CyP-D binding to the ANT (Tilak *et al*., 2004).

Until recently, Sangliferin A (SfA) was discovered as another extremely potent inhibitor of the mPTP. SfA is not related to CsA and does not prevent CyP-D binding to ANT but do inhibit PPIase activity (k 0.5< 5nM) thus preventing it from facilitating the conformational change of the ANT required for pore formation (Crompton, 1999).

One advantage of SfA is that the SfA-CyP-A complex formed has no effect on the calcium activated protein phosphatase and calcineurin. Therefore, blocking of mPTP by SfA and CsA can be by-passed at increased Ca^{2+}concentration suggesting that a change in conformation by CyP-D can easily take place in its absence (Halestrap *et al*., 2000).

Moreover, logical empirical studies have depicted that at high influx Ca^{2+} concentration level, pure ANT can undergo transformational modification to replicate a non-specific channel

without CyP-D though the response to Ca^{2+} is improved in its presence (Halestrap *et al*., 2000).

Other proteins identified to be implicated in mPTP mechanism and formation includes outer membrane VDAC also known as porin and associated benzodiazepine receptor (Crompton, 1999). Despite divergent views over whether such proteins are necessary structural components or merely exerts a crucial regulatory function, it appears that the mPTPis linked with contact sites between outer and inner mitochondrial membranes where VDAC and ANT are thought to interact. Hence, an intervention that decreases Adenine nucleotide interraction with ANT will enhance pore opening. This also includes adenine nucleotide depletion, matrix phosphate and conformational state of ANT (Crompton, 1999).

In reference to reperfusion injury in particular, it has been observed that oxidative stress also sensitizes mPTP to Ca^{2+} by simply antagonizing adenine nucleotide binding but concertedly increases CyP-D binding to the ANT. In like manner, reduced pH< 7 and Mg^{2+} restricts mPTP opening by antagonizing Ca^{2+} interraction as well (Colombini, 2004).

Although, operation of other two effective inhibitors is yet to be understood, trifluoperazine remains a strong inhibitor of mPTP in energized but not de-energised instance and may act by distrupting peripheral membrane ionic value which induces voltage response of the mPTP. It was only in the recent times that ubiquinone analogues were shown to act as either strong activators or inhibitors of mPTP possibly by association with complex 1 of the respiratory chain even though how this occurs to modify mPTP remain obscure and unclear (Walter *et al*., 2000).

2.3 Promoters and Potentiators of Mitochondrial mediated Apoptosis

Mitochondrion remains a principal factor in pathology and execution of cell death via its modulatory potentials. It has been observed that aberrant cell death or apoptosis feature in certain diseased state or health conditions in which the mitochondrion is indicted when its integrity has been compromised paving way for collapse in its functions and regulatory potentials.

Diseased state and conditions where mitochondrial integrity has been compromised include: various forms of cancers including prostate tumors, Parkinsons and Alzheimer diseases and auto-immune disorders. This implies that apoptosis regulation can be beneficial while its

aberrant regulation (up-regulation where apoptosis is in excess and down-regulation where apoptosis is inadequate) can precipitate detrimental health conditions. Therefore, there is need to have an insight to the entire apoptotic process to understand the workings and intricacies involved with a view to considering possibilities of regulating the entire process for beneficial purpose. Incidentally, certain phytochemicals have been found to posses such propensity and as such can be instrumental to modulating the mPT pore opening (Paras *et al*., 2018).

Molecules or agents in plants with the capacity to induce mPT pore opening have been employed to regulate or control aberrant apoptosis. These agents trigger apoptosis by initiating spontaneous cell death responses. Promoters and potentiators of apoptosis in this regard may range from natural toxicants of plant origin which include cyanogenic glycosides, furocoumarins, lectins, mycotoxins, solarines, chaconines and pyrollizidine alkaloids among others. These potentiators or promoters can be considered as toxicants (in form of drugs or chemotherapeutic agents) that can trigger spontaneous apoptotic responses and as such are known as inducers of MPT pore.

Experimental evidence indicates that some dietary bioactive compounds can induce apoptosis, specifically at the point of permeabilisation of the mitochondrial vesicle (Hafeez, 2012, Chen, 2016). This is a situation where cell-death is in excess and needs to be down-regulated to avert detrimental consequences.

Other forms of potentiators with propensity to trigger spontaneous or aberrant apoptosis may also be inform of radiations, hypoxia and *uv* light among others. These target cells to initiate responses from the mitochondrion through some signaling cascades and inevitably resulting to cell demise - apoptosis (Bernadi, 2018; Wang *et al*., 2015; Xu *et al*., 2016).

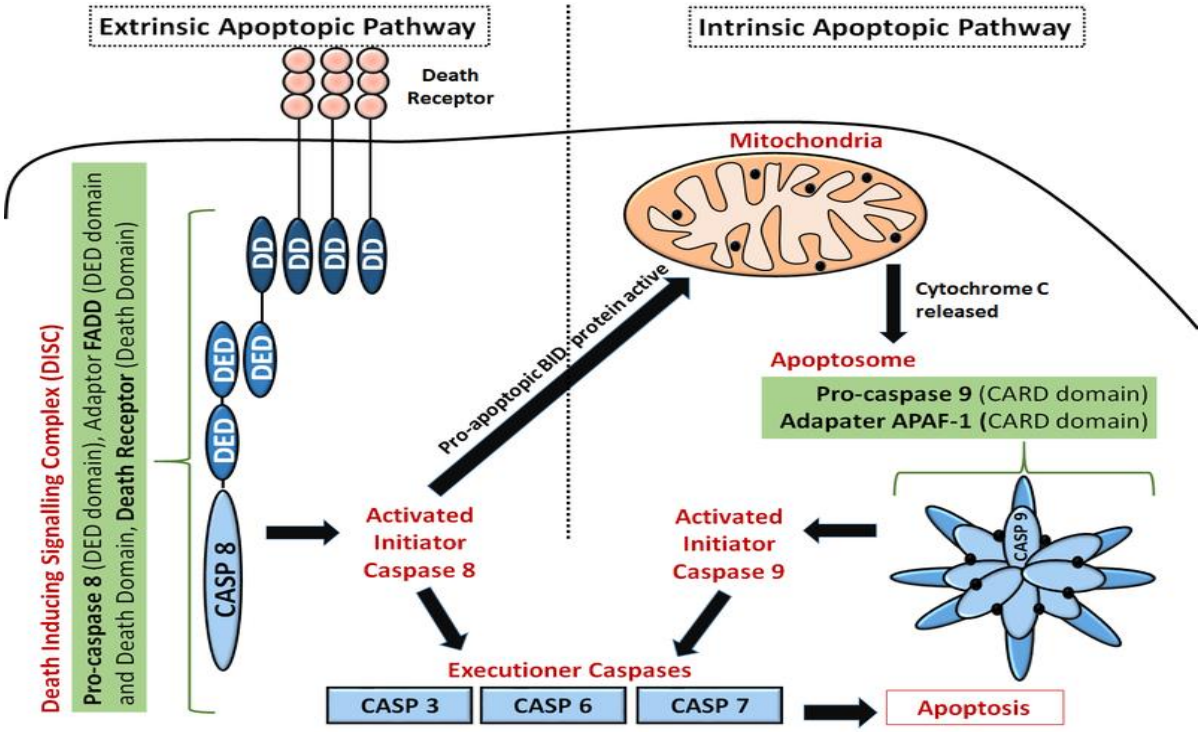

Figure 2.5: Illustration of Intrinsic and Extrinsic Pathways of Apoptosis (Dominic *et al.*, 2019)

As aforementioned, intrinsic pathway of programmed cell death (PCD) is triggered by the presence and exposure to toxicants (inform of drugs or phytochemicals), radiations, hypoxia, reactive oxygen species, hyperthermia, free radicals, viral infections and uv light which transmit non-receptor- mediated stimuli that produce intracellular signal. This happens especially when the cell loses its potential to suppress death programmes in the absence of certain growth factors, hormones and cytokines. The stimuli that produce the mitochondrial initiated event in the process precipitates pore on the mitochondrial vessel with subsequent outflow of cytochrome C from the inner mitochondrial compartment. Cells that are cancerous, injured or damaged are marked or primed to die and as such prone to the apoptotic responses triggered by inducers of cell death which forms the basis for selective cell death via the intrinsic pathway (Kwong and Molkentin, 2015).

2.4 Players and Promoters in the Intrinsic Apoptotic Responses

Preponderance of molecules (proteins in nature) is involved in cascades of events leading to cell demise. These proteins are called promoters and opposers of apoptosis and a balance or imbalance must be attained between these classes of proteins to determine whether a cell will proceed to get executed or remain intact and alive. In the mitochondrial-pathway, two pro apoptotic Bcl-2 proteins, namely: Bax and Bak are activated as they undergo structural conformation in response to cytotoxic internal stimulation. These proteins translocate to the mitochondria and homodimerise to expose the dimer-dimer binding sites and thus create channels on the surface of the mitochondria which bring about elevated membrane permeabilisation (MOMP) with consequent exit of proteins from the mitochondria intermembrane space (IMS), (Martin, 2006).

The most important protein released following the increased permeabilisation of the membrane is the Cytochrome C. It can be adduced that the outflow of cytochrome C is a rate limiting step that irrevocably commits a cell to death as it activates the reaction cascades initiating and activating other molecules coming to play roles in the entire apoptotic process. As soon as cytochrome C flows out of the membrane, it binds to Apaf-1 with the recruitment of inactive precursor procaspase-9 to form a complex calle apoptosome. The complex formed thus activates the inactive procaspase-9 to an active caspase 9 leading to a down-stream reaction in the caspase cascades (Martin, 2006).

Similarly, anti apoptotic proteins will act in antagonist to inhibit the apoptotic proteins and thus provide a regulatory mechanism to control apoptosis in the intrinsic pathway. Conversely, anti apoptotic protein which inhibits programme cell death (PCD) are sets of Bcl-2 family members and includes all apoptotic proteins. Each of these proteins hasaffinity for atleast one of the Bcl-2 family member site called homology (BH) domain. These proteins inhibit their pro-apoptotic counterparts that promote cell death. Hence, anti apoptotic Bcl-2 members stop death signals on cells in the mitochondrial pathway by constraining promoters of apoptosis proteins namely: Bak and Bax and by extension Cytochrome C release.

On the contrary, if there is a toxic stimulus on cell, the effect of Bcl-2 protein biomolecules would be suppressed and the overwhelming effect by the BH3 only proteins particularly BIM and NOXA which function to release Bax-Bak inhibition will help to precipitate MOMP and finally lead to cell death (Koff, Ramachandiran and Bernal-Mizrachi, 2015).

Another set of players in the mitochondrial mediated cell death include the Inhibitor of Apoptosis (IAPs) protein family which exert regulatory function in the intrinsic pathway. They mainly interact with caspases by binding active site of caspases through their BIR domains thus inhibiting their proteolytic function. xIAP directly targets and inhibits activation of procaspase 9 to activated caspase 9. Some IAPs target certain proteins known as effector caspases for ubiquitination and proteasomal degradation in order to weaken their executioner potentials. Other IAP in likes of cIAP contributes to activation of anti apoptotic alerts such as NF-Kb and JUNK1 (Koff, Ramachandiran and Bernal-Mizrachi, 2015).

Interplay and stimulations among these aforementioned proteins project them as key players: either promoting or inhibiting apoptosis and thus perform regulatory functions in the intrinsic pathway of programmed cell death.

2.5 Prosecutors and Products of Apoptosis

The final stage in the cascades of events culminating to reducing the cell to apoptotic bodies and products are the executioner caspases. These are group of proteins referred to as caspases and include Caspases 3 and 9 (C3 and C9) in the intrinsic pathway. Caspases facilitate precipitation of the entire cell into apoptotic bodies with no inflammatory response from neighbouring cells. They finalise the cascades of events in the pathway of apoptosis as they are activated and irrevocably committed to bring to an end the existence of the cell and as such act as prosecutors sentencing the cell to final demise by reducing it to aggregates of

apoptotic bodies ready for safe disposal. They remain the very essence of the biochemical term –apoptosis (Ray, 2016).

2.6 Fertility Potential and Mitochondria Functions in Male Gamete

Fertility implies capacity to replicate. It is the natural propensity to replicate or reproduce offsprings. It is differerent from fecundity, which can be defined as the propensity for replication via the influence of gametes uniting together in fertilization and carrying a pregnancy to term. Absence of fertility is infertility while a lack of fecundity is referred to sterility. In humans, fertility is dependent on a number of factors such as instinct, social behaviour, culture or way of life and emotions. The reproductive gamete responsible for male fertility is the spermatozoa. The sperm cell is the male gamete that fertilises the female gamete while the product called zygote is implanted in the uterus. It is essential to note that healthy and motile sperm cell would be necessary for normal reproductive process. To this end, it has been shown that semen volume, sperm motility, count and morphology decreases as male increases in age, this may be reasons why older people decline in their reproductive capabilities in most cases (Ruwanpura *et al*., 2010).

An investigation into structure and anatomy of mammalian spermatozoa indicated the presence and prominence of mitochondria and this cannot be for the fun of the structure. Moreso, the observed reduction in certain reproductive parameters such as semen volume, sperm count and motility and morphology in ageing male suggest reduced mitochondrial function characteristics of the ageing process among other health conditions including Parkinsons, neurodegenerative, Alzheimers and so on (Carreau *et al.*, 2010).

In the spermatozoa anatomy, mitochondria are found tightly packed in the mid piece where they provide energy for motility, acrosomal reaction and apoptosis. It has been revealed that a healthy and mature sperm cell has about 70 mitochondria densely packed in the mid piece region of the male sex cell structure (Mortimer, 2018).

Moreover, it has been shown in literature that there is a strong link between sperm mitochondrial function and sperm motility. Hence, if sperm motility, count and morphology are necessary parameters in assessing fertility, then mitochondrial function and contribution cannot be ruled out. In like manner, several studies attributed increased sperm mitochondrial membrane potential to corresponding increase in sperm motility and fertility potential. In other studies, mitochondrial viability and function were used as alternative method to

estimate sperm motility (Barbagallo *et al.*, 2020). All these facts show that mitochondria are central factors to survival, function and apoptotic process in male reproductive cells. In a nut shell mitochondrial membrane potential determines the fertility potential inherent in a given sperm cell considering the critical role the mitochondrion plays and exerts on the entire reproductive process where the integrity of the membrane must not be compromised.

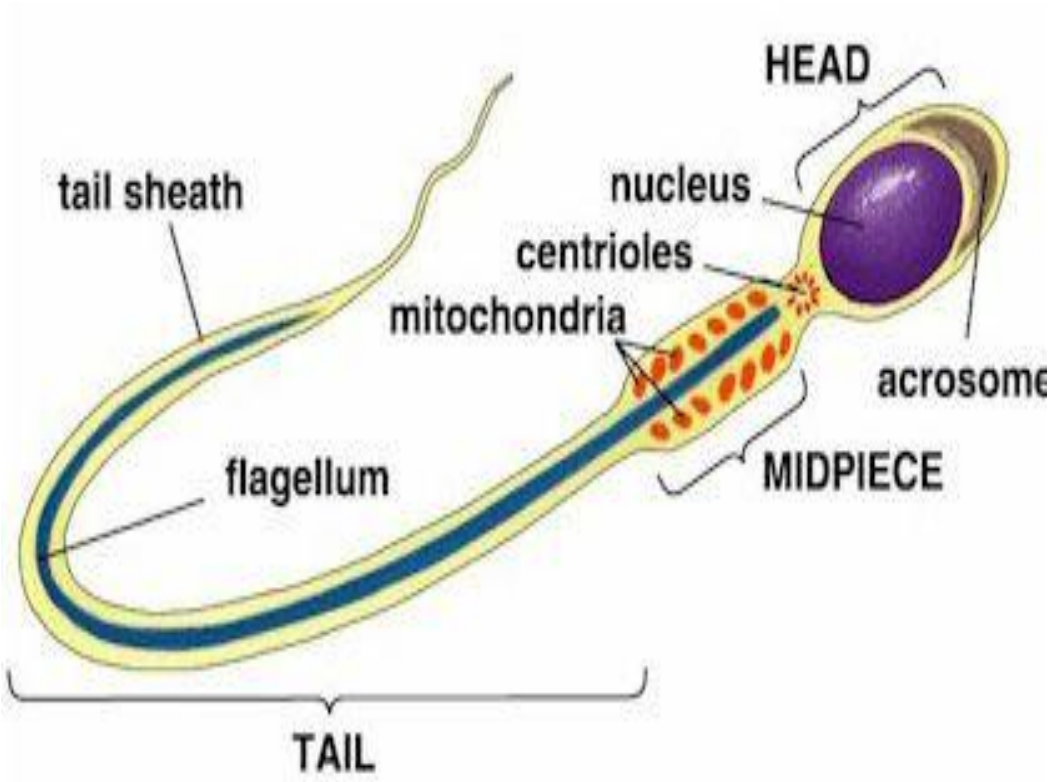

Figure2.6: Structure of the spermatozoa showing prominent location of mitochondria.

2.7 Plumbago Zeylanica - A Medicinal Plant with Multiple Pharmacological Properties

The plant Plumbago zeylanica is an onarmental plant known by its different names in various geographical zones across the world. The English name is White leadwort, Ceylon leadwort, or Plumbago. The African vernacular name especially in southwest Nigeria is Inabiri. It is widely used in India where it is called Chitrak chitramol.

The plant has been known to elicit various and varied pharmacological properties hence it has a prominent place in traditional system of medicine especially in India, Africa and Asia. It grows well in deciduous woodland, savannas and scrub lands from sea level up to 2000m altitude. The plant has a chromosome number 2n = 24. It belongs to the ornamental herb of family plumbaginaceae and consists of 10 genera and 280 species (Aditi, 1999; Tilak *et al.*, 2004; Sharma and Singh, 2015).

Figure 2.7: Locally sourced *Plumbago zeylanica* plant

2.8 Medicinal uses of *Plumbago Zeylanica*

As reported by Rajakrishnan *et al*., (2017), most parts of the plants are used although the root is said to have the highest medicinal or theraupeutic activity for effective treatment. This may be the reason why it is widely used traditionally as laxatives, expectorant, astringent, abortifacient and in dysentery (Tilak *et al*., 2004). The tincture preparation of the root bark is being used to stop period. Its traditional use is prominent in India and Chinese systems of medicine for over 2500 years where it is applied for treatment of various types of ailments (Sandur *et al.*, 2006).

The leaves of Pz are caustic in nature and are used for treating scabies. In some West African settings root or leaves of pz blended with lemon juice are ideal for use as counter-irritant and vesicant. Pulped roots or aerial parts are inserted into the vigina to induce abortion even though this is a dangerous practice which some times result to death. Other application of Pz includes; remedies for infectous and skin diseases, intestinal worms, leprosy, scabies, ringworm, dermatitis, acne, sores, ulcers of the leg, haemorrhoids and hookworm (Tilak *et al*., 2004).

Due to its potent multiple medicinal properties, it is used to treat various ailments and hence, its use in traditional medicine where the inherent potency in treating many disease and health conditions have been exploited. Some of the medicinal uses are discussed as follows:

Anti-inflammatory activity

Taking advantage of its anti-inflammatory potential, root bark methanolic extracts of pz have been used as a measure of anti-inflammatory effect where 300 and 500 mg/kg body weight produced 31.03 and 60.30% inhibition against acute inflammation respectively (Parakh *et al*., 2006). Traditionally, pz extracts boiled with milk have been used as remedy to treat inflammations of mouth, chest and throat in Zambia. Other emperical studies also attest anti-inflammatory property of phosphate buffered saline extract of root of pz. Similarly, *in vivo* experimental model using acetone extracts of pz significantly ($p<0.01$) reduced inflammation in carrageenan induced rats when compared to control group.

Lipid metabolism activity

Lipid metabolizing potential of plumbagin extracted from root of *P.zeylanica* has been demonstrated when administered to hyperlipidaemic rabbits where it lowered serum cholesterol. In another experiment it decreased serum cholesterol and LDL-cholesterol by 53% -86% and 61%-91%respectively. It also lowered cholesterol/phospholipid ratio by 45.8% (Tilak *et al*., 2004).

Healing activity

Kirtikar (1993) examine wound healing capacity of plumbago zeyaica extract in experimental rats. In those experiments, there were confirmations of wound healing activity of methanolic root extracts of Pz.

Memory-inducing activity

In their research, Itiogawa *et al*., (1991) experimented that PL on scopolamine influences amnesia for learning and memory of mice thus promising memory enhancing effect was demonstrated using chloroform extract at dose 200 mg/kg in rats. However, Pz extract significantly reversed effect of induced amnesia by scopolamine.

Blood coagulation activity

Reported blood coagulation properties of plumbagin in pz extract was determined using albino rats. The study examined and recorded bleeding time (BT), clotting time (CT) and prothrombin time (PT) among other parameters after 1-day, 15 days and 31 days treatment. In conclusion, the active principle in Pz is said to be similar to those found in vitamin k (Kirtikar *et al.,* 1993).

Anti-malarial activity

Although, the best treatments for malaria fever, is to avoid bite from Anopheles mosquitoes which are carriers of the parasites. Plants considered to ward-off malaria parasites have been employed traditionally in countries like India to treat malaria fever. Pz extract was tested for larvacidal activities in this study. The result shows that crude extract show highest larvacidal activities against Anopheles gambiae (Roy, 2017). Similar study by Wang *et al*., (2015) also confirms that extracts of pz exhibited larvacidal activity.

Allergic and modulatory effect

Plumbagin exhibits potency and modulatory effect on cellular proliferation and certain pathologies or conditions such as carcinogenesis and including radio-resistance. It is prominently reported in literature that plumbagin modulates the NF-kappa B which is a transcription factor by way of inhibition of the molecule on its activation by TNF. Hence by this act plumbagin derived from pz suppresses proliferation of unwanted or diseased cells as found in cancer cells (Sandur *et al.*, 2006).

Antifertility activity

Antifertility tendencies of plumbagin were aboundantly referenced and reported in literature but apart from work done on anti cancer and modulatory effects plunbagin is known to elicit anti fertility effect especially in the female. This claim has been confirmed in albino rats in which Pz treatment abolished uterine proteins during first 7 days of pregnancy resulting to preimplantationary loss in rats administered Pz root powder (Mahdi *et al.*, 2012).

In other research, significant anti- implantation and abortion induction activity of Pz has been depicted in wistar rats without any teratogenic effect in doses of 1mg/100g (Premkumari *et al.*, 1977). Similarly, roots of Pz have been considered to be poisonous because of its abortificient effect when applied to the ostium uteri or orally administered in experimental animals (Aditi, 1999).

Further studies in which hydroalcoholic extract of *Plumbago zeylanica* leaves were used showed highly potent (95.167 %) anti implantation activity and because of anti-estrogenic activity, which antagonizes the action of estrogen causing structural and functional changes in the uterus. The antiestrogenic effect is also supported by decrease in glycogen content, thickness of endometrium, myometrium, reduced uterine lumen with decreased pits and folds, decreased in the number and size of the uterine glands, vaginal opening and cornification (Aziz *et al.*, 2008, Erkkila *et al.*,2006).

Vassan (2011) in his work investigated that the acetone and ethanol extracts of *P zeylanica* were most effective to interrupt the estrous cycle and exhibited a prolonged diestrous stage of the estrous cycle resulting to a temporary inhibition of ovulation.

In humans, Pz has been used as family planning agent as well as an anti-implantation agent that appear to interfere with progesterone synthesis and utilization (Premkumari *et al.*, 1977; Bhargava, 1986).

Microbiological activity

High incidence of health problems prevalent in developing countries has been attributed to infectous diseases. Meanwhile, a claim for effective therapy for treating these ailments has prompted more interest in scientific quest and research. Amongst multiples and varying results, Pz root extracts showed inherent evidence of microbiological properties (Sharma and Singh, 2015).

Anti-bacterial activity

Some plants were screened and evaluated for antibacterial activity and amongst them only alcoholic extracts of Pz, Emblica officinalis, Terminalia chebula showed potential antibacterial activity (Aditi, 1999). Alcoholic extracts of roots of Pz were equally tested against multi-drug resistant of clinical origin (*Samonella paratyphi, Staphylococcus aureus, Escherichia coli and Shigelladysenteriae).* The extract exhibited anti bacterial activity against all tested bacteria (Aziz *et al*., 2008).

Anti-viral activity

Chen, (2003) examined the antiviral activities of the 4/5 methanolic extracts of *P*zagainst coxsackievirus B3 (CVB3), influenza A virus and herpes simplex virus type1 Kupka (HSV-1) using cytopathic effect (CPE) inhibitory assays in HeLa, MDCK, and GMK cells, respectively. The antiviral activity of the most active compound was confirmed with plaque reduction assays. *Plumbago zeylanica* L had marked inhibition effects on HBeAg and HBsAg which is expressed by cells. In addition, CVB3 was inhibited by the extracts of *Plumbago Zeylanica* (Martin, 2006).

Anti-oxidant activity

Anti oxidant effects and related properties were studied using aqueous/ alcoholic extracts of root of Pz equivalent to medicinal preparation (Tilak *et al*., 2004). In the entire study, plumbagin the active principle in Pz has been shown to demonstrate anti oxidant effects.

Anti cancer activity

Avalanche of reports abound where it was observed that Plumbago Zeylanica show susbstantial anti cancer properties against various and varied cancer cell lines (Chen *et al*., 2016). Anti cancer activity of Pz can further be corroborated by its traditional and age long use in treatment of prostate tumor (Kumar, 2011; Malaiyandi *et al*., 2020).

Figure 2.8: Pharmacological Activities of *P. zeylanica* (Perez *et al.*, 2017)

2.9 Plumbagin - The Bioactive Principle in *Plumbago Zeylanica*

Plumbago Zeylanica is specie of ornamental plant. It is chemically characterized by the presence of naphthoquinones, flavonoids, terpenoids and steroids, many of them being responsible for several biodynamic activites in the plant (Tilak *et al*., 2004). The common name for the plant is lead wort, not withstanding it is known by several other names in different parts of the world. For example, in India the name Chitrak is ascribed to it.

Structurally, the plant root is about 30 cm or more in length with a diameter estimated at 6 mm. It is stout, cylindrical, friable, blackish red in colour, light yellow colour when fresh and assumes redish brown colour when dried. It is often observed to posses straight unbranched or slightly branched shoots with or without secondary roots including uniform and smooth texture. Pz is also known by its characteristic odour with acrid and bitter taste (Roy, 2017).

The stem bark of Pz is usually thin and brown while the leaf is simple, alternate, 8 cm long and 3 cm broad, ovate or oblong with narrow petiole. The base is amplexicaul and often dilates into stipule-like auricles. The leaves are said to contain plumbagin and chitanone (Paras *et al*., 2014).

The flowers in Pz are white in colour, between 10 -25 cm long, inodorous, inbracteate, axillary and terminal elongated spikes and bisexual. The calyx is densely covered with stalked and sticky glands. The corolla is white, very slender with tubular stamens 5, free ovary superior, 5-gonous, and one celled ovule one basal. The flower also contains plumbagin, zeylanone and glucose (Paras *et al.*, 2014).

The entire plant (flower, fruits, leaves, stem, root and root bark) has been investigated to contain active principles which include: plumbagin, zeylanone, isozeylanone, sitosterol, stigmasterol, campesterol, dihydrofavinolplumbaginol and glucopyranoside.The bioactive compounds in pz have been evaluated and determined in different parts of *Plumbago zeylanica* and the structure elucidated (Liu *et al*, 2006; Sharma and Singh, 2015).On the whole, the predominant active principle in the ornamental plant is plumbagin (Rajakrishnan, 2017; Roy, 2017).

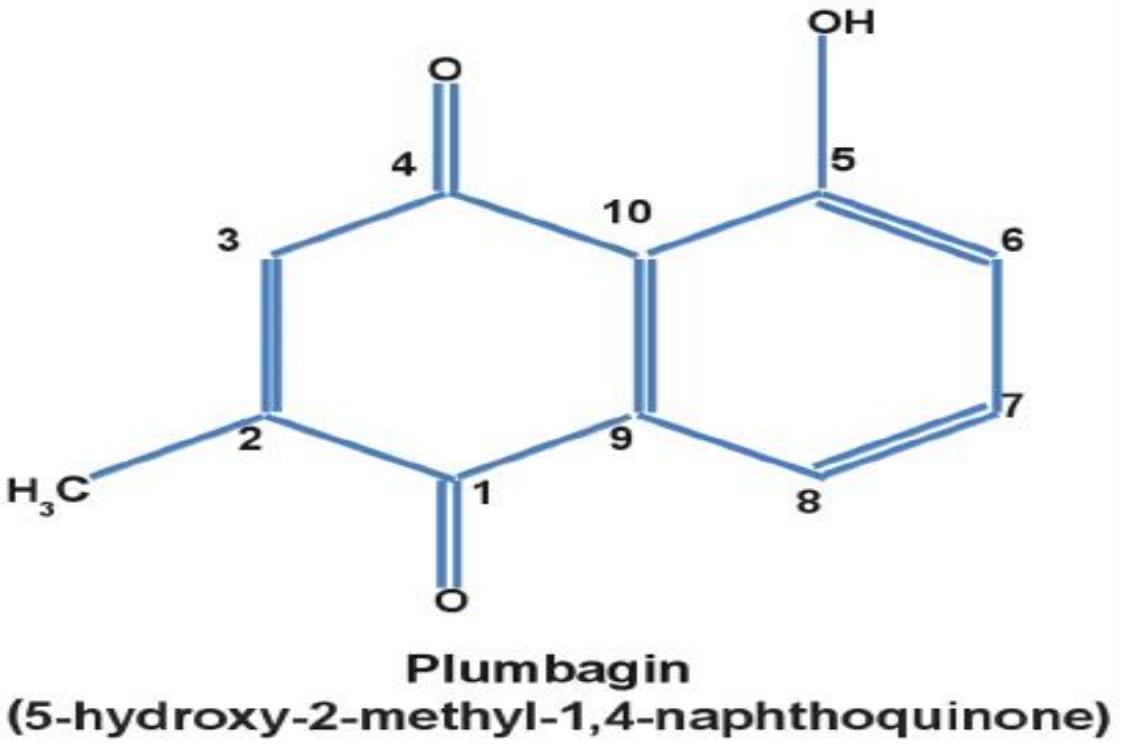

Figure 2.9: Molecular Structure of Plumbagin

Source: Sharma and Singh, 2015.

Recall that phytochemicals and potent bioactive compounds posses the propensity of eliciting or inducing the membrane permeabilisation via the mitochondrial mediated path way of cell death. This is ideal for anticancer agents in eliminating unwanted damaged or injured cells as they are primed for death. The abortificient principle of plumbagin in inducing apoptosis in the uterine wall thus causing abortion is justified in the female. However, will this happen in male considering the place of mitochondria in the sperm cell and the important role in fertility. What happens to reproductive enzymes and hormones when interacting with plumbagin the active principle in *Plumbago zeylanica*. These and other observations would be probed in the series of studies using male Wistar rats in this research.

2.10 Docking and Simulation Studies in Drug Development

A novel advancement in drug development has employed the use of computing in gaining insight to interaction between proteins and ligands and as such elucidating the structure of molecules, their orientation and possible maximum biochemical interaction to achieving a target result. This in its entirety becomes the basis for drug development. This concept is possible through docking and simulation studies. At the molecular level, there are interactions between a ligand and protein; that is potential drug and target proteins which lead to a conformational change. For example, hydrophobic, covalent bondings, electrostatic, Van der Waal forces and ionic bonds have been identified among various interactions.

Molecular docking has become a key tool in structural molecular biology and computer-assisted drug design. Docking score ranking will enable the choice of protein that will effectively interact with the ligand to produce suitable and desired results. Hence, effective drug design will require improved methods for predicting protein−ligand binding affinities to realize the ultimate goal of combating disease or infection (Yunta, 2016).

Docking score helps to determine the protein with the most effective binding affinity and hence screen out others with fewer score while proceeding with simulation studies. Simulation is an advance step taken further on docking to establish complex stability with the most effective protein-ligand complex (Dar and Mir, 2017).

In molecular simulation studies, there are various dimensions and approach. Amongst the approximate methods, the molecular mechanics/Poisson−Boltzmann surface area (MMPBSA) approach is adjudged to be most preferable (Yunta, 2016).

CHAPTER THREE

MATERIALS AND METHODS

3.1 Experimental Animals

Wistar strain male rats (90-100 g) were purchased from Veterinary Anatomy Animal House, University of Ibadan, Ibadan. They were housed in the Biochemistry Department Animal House, University of Ibadan under standard hygienic condition with ethical approval from the Animal Care and Use Reasearch Ethics Committee (ACUREC). Animals were maintained in aerated environment and fed with rat chow *ad libitum* under 12 hours light/dark cycle as they under went acclimatisation for two weeks before proceeding with experiments.

3.1.1 Animal Grouping and Treatment

Ten (10) Wistar strain (male) rats were used for *in vitro* (preliminary studies), Group A (20 male Wistar rats) for *in vivo* studies were further grouped into four (5 animals per group) viz: control, 2.5, 5.0 and 10.0 mg/kg body weight. They were orally administered the varying doses (as indicated above) of PL accordingly for 14 days.

Group (B): Fifteen Wistar strain (male) rats were used for studies on testes function and fertility employing semi-quantitative gene expression studies. They were grouped into three viz: control, 30 and 100 mg/kg body weight and were administered doses of PL accordingly for 72 hours before being euthanized.

3.2 Plumbagin (5-hydroxyl 2-methyl- 1, 4-naphthoquinone)

Plumbagin was ordered from Texas, USA (Santa Cruz Biotechnology) CAS No: 5431-34-5 packaged in ice pack to keep it stable in its crystalline dried form. The pack was received intact and preserved in the deep freezer of the Membrane Biochemistry and Biotechnology Unit of Biochemistry Department, University of Ibadan.

3.3 Procedures

Isolation of Mitochondria from Rat Liver

Animals in each group were euthanized while rat liver mitochondria were isolated using a slight modification of the methods of Johnson and Lardy, (1967) as described by Bababunmi and Olorunsogo (1976). The livers were placed on ice, quickly cut into moderate size and adjusted to remove excess tissue, and minced. The livers were cleansed in buffer C and weighed, minced with scissors in one-tenth suspension of the tissue in iced buffer C placed on ice. The suspended liver was then blended into smooth homogenate on ice using a Potter-Elvehjem glass.

Differential centrifugation was employed at 2300 rpm twice to remove cellular debris and at 12000 rpm twice to sediment and isolate purified mitochondria using buffer C and D for isolation and washing respectively. The isolated mitochondria fraction was suspended on ice for use.

3.4 Determination of Protein

Mitochondrial protein in this experiment was determined by the concept of Lowry *et al.*, (1951) and BSA was used as control.

Principle

The Lowry's method of protein determination employs the principle that phenol groups reduce certain colour reagents, precisely in this case a phospho-18-molybdictungstate compound which is a combination of several molecular forms including: $3H_2O.P_20_5.9Mo0_3$ and $3H_2O.P_2O_5.10WO_3.8MoO_3$. The complex formed is reduced by phenol groups to yield blue coloured compound at alkaline pH.

3.5 Reagents for Protein Determination

Reagent A: 0.02% Na_2CO_3 in 0.1M sodium hydroxide

Pellets of Na_2CO_3 (2 g) and NaOH (0.4 g) products of BDH Chemicals Ltd, England were introduced into volumetric flask and dissolved using standard purified water. The resulting content was made up to 100 ml mark at room temperature.

Reagent B: 2% Sodium-Potassium Tartrate

Sodium-potassium tartrate ($NaKC_4O_6.4H_2O$), 2.0g was weighed, dissolved in distilled water and made up to 100 ml in a standard volumetric flask.

Reagent C: 1% Copper Sulphate

1.0 g of Copper sulphate reagent was dissolved in water and made up to the 100ml mark in a standard flask.

Reagent D: Alkaline Solution of Copper Sulphate

The components making up this reagent was freshly prepared just before use. It consists of 20 ml of reagent A with 0.2 ml of reagent B and 0.2 ml of reagent C in the ratio 100:1:1.

Reagent E: Folin-C Reagent

This solution was prepared by adding 1ml of 2N Folin's reagent (Sigma Aldrich USA) to 5ml of distilled water.

Preparation of Folin-C Reagent

This solution consisted of sodium tungstate ($NaWO_4..2H_2O$) (100 g) and 25 g of sodium molybdate ($Na_2MoO_4.2H_2O$) which were dissolved in 700ml of water. Concentrated hydrochloric acid (100ml) and 85% phosphoric acid (50ml) were mixed and refluxed for l0 hours in all glass apparatus. To the resulting mixture, 150 g of lithium sulphate (Li_2SO_4) (Sigma Aldrich, Inc. USA.), 15 ml of water and 2-3 drops of bromine were added. The resulting mixture was heated to boiling point for 15minutes in fume hood to eliminate excessive bromine. The constituent mixture was allowed to cool and diluted to 1 liter and then filtered. The resulting mixture was preserved at 4^oC in a refrigerator.

Standard Protein Solution: lmg/mg BSA

A 1mg/ml solution of Bovine Serum Albumin (BSA) product of Sigma Company, USA. 5mg BSA in 5ml distilled water was prepared. 1ml of BSA was taken from the stock solution and mixed with 19ml distilled water.

Preparation

The preparation was made as indicated on the table 3.0 and the mixture was allowed to stand for half an hour. After which the absorbance was recorded at 750 nm wavelength in a Camspec M105 spectrophotometer. The assay was carried out in duplicates. Results from the reading were used to construct a standard protein curve.

3.6 Protein Determination in Sample

Distilled water (1000 µl) was introduced into test tube and used as blank, 10 µl of sample put in test tube, and 990µl of distilled water added to the sample. 3 ml (3000 µl) of reagent D was mixed with blank and protein specimen made to remain for l0minutes at normal temperature. Furthermore, 300 µ1 of reagent E was added rapidly to all the test tubes and mixed vigorously as shown in table 3.1

The mixture was allowed to stand for additional half an hour, after which the readings were taken at 750nm wavelength in a Camspec M105 spectrophotometer. The absorbance of the protein sample was estimated on the standard curve to derive appropriate protein concentration of sample.

Sample: Mitochondria (10µl) was taken and added to 990 µl of distilled water in a test tube to make a 1 to 100 dilution.

Dilution factor: 1:100

Blank preparation: 1000 µl of distilled water was dispensed in the test tube. The blank and the sample preparations were duplicated.

Table 3.1 Protocol for Standard Protein Estimation

Test tubes	**1(Blank)**	**2**	**3**	**4**	**5**	**6**
Standard BSA solution (µl)	-	20	40	60	80	100
Distilled H_20 (µl)	1000	980	960	940	920	900
Reagent D (µl)	3000	3000	3000	3000	3000	3000
Reagent E (µl)	300	300	300	300	300	300

Table 3.2: Protocol for Protein Estimation in Sample (Lowry *et al.*, 1951)

Duplicated Test tubes	**1 (Blank)**	**2**	**3**	**4**	**5**	**6**
Sample (Mitochondria)	-	10	10	10	10	10
Distilled H_20 (µl)	1000	990	990	990	990	990
Reagent D (µl)	3000	3000	3000	3000	3000	3000
Reagent E (µl)	300	300	300	300	300	300

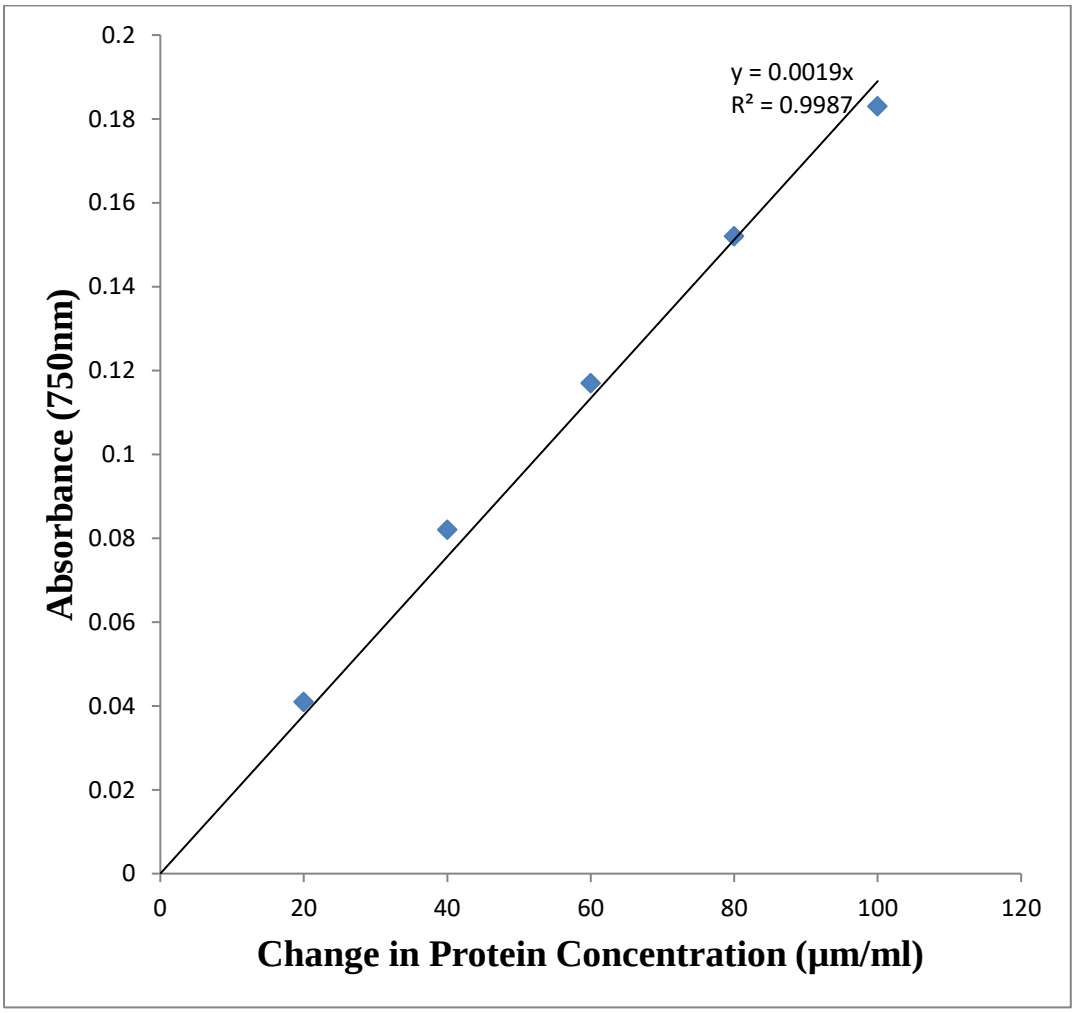

Figure 3.1: Standard Protein Solution (BSA) Curve

3.7 Preparation of Low Ionic Charged Mitochondria from Rat Testes

Low-ionic-charged testicular mitochondria were obtained from male Wistar rats using a prescribed concept described by Johnson and Lardy (1967).

Preparations of Buffers

Buffer C (Isolation buffer: 250mM Sucrose, 5mM HEPES-KOH (pH 7.4), and 1mM EDTA)

Reagents here consist of: 0.1192 g of HEPES - Sigma Aldrich Products (SAP) USA, which was initially dissolved in 70 ml distilled water, 4.56 g sucrose (BDH Chemicals Ltd, Pools, England) and 0.003 g EDTA. The entire solution was standardized to pH 7.4 with KOH (SAP, USA) made up to l00 ml. The buffer was placed in a refrigerator maintained at 4^{o}C.

Buffer D (Washing and suspension buffer: 5mM HEPES-KOH pH 7.4)

HEPES (0.1192 g) was initially dissolved in 70 ml of distilled water and standardized to pH 7.4 with KOH. The homogenous mixture was made up to l00 ml. The resulting buffer solution was kept refrigerated at 4^{o}C.

3.8 Isolation of Testicular Mitochondria

Rat testes mitochondria were obtained using a slightly adjusted method of Johnson and Lardy, (1967). Animals were euthanized and testes immediately excised, adjusted to get rid of excess tissue. The testes were washed in suspension buffer, weighed and splitted with scissors in one-tenth suspension of the tissue in ice-cold buffer C. The resulting suspension was then homogenised on ice using a Potter-Elvehjem glass homogenizer.

Nuclear fractions and other cellular components were sedimented by centrifugation twice at 2300rpm for 5 minutes using a refrigerated MSE centrifuge at 4^{o}C. Centrifugation at 2300rpm is to remove unbroken cells. Supernatant obtained was further centrifuged at 13,000rpm (10,000 g) for l0 minutes to obtain pellet of mitochondria. Mitochondria fraction (brown pellet) obtained were washed twice at twelve thousand revolution permunite (12,000rpm) for l0minutes each time with buffer D.

The mitochondria portion was re-suspended in buffer D and dispensed in pre-cold Eppendorf tubes in aliquots and used fresh. To ensure mitochondrial integrity were not compromised, all experiments were carried out on an ice-cold medium.

3.9 Preparation of Intact Mitochondria from Rat Liver

Low-ionic-strength liver mitochondria were also isolated from male Wistar rats using the modification of the procedure described by Johnson and Lardy (1967) as described for testes above.

3.10 Preparation of Buffers

Buffer C (Isolation buffer: 210mM Mannitol, 70mM Sucrose, 5mM HEPES-KOH pH 7.4, 1mM EDTA):

HEPES (0.12 g) was initially dissolved in 70 ml of distilled water, 3.83 g Mannitol, 2.4 g of sucrose and 0.038 g EGTA from Sigma Aldrich company, USA were added and standardized to pH 7.4 using KOH (Sigma Aldrich products, USA). The entire solution was made up to l00ml and was kept cold at 4^{o}C.

Buffer D (Washing buffer: 210mM Mannitol, 70mM Sucrose, 5mM Hepes-KOH (pH 7.4), 0.5%BSA):

Washing buffer was constituted using 0.12 g of HEPES (Sigma Aldrich products, USA) in 70ml of distilled water with 2.4 g of sucrose (BDH Chemicals Ltd, Pools, England), 3.83g Mannitol and 0.5 g Bovine Serum Albumin (Sigma products, USA) added and resulting solution standardized to pH 7.4 with KOH (Aldrich products). The entire mixture made up to l00ml and solution was swirled gently in order to allow BSA to dissolve completely and avoid foaming. The buffer was stored at low temperature of 4^{o}C.

MSH Buffer (Swelling Buffer210mM Mannitol, 70mM Sucrose, 5mM HEPES-KOH at pH 7.4)

HEPES (0.24 g) Sigma product, Inc. USA; was dissolved in about 100ml of distilled water. It was standardized to a pH of 7.4 with KOH (BDH Chemicals, England), Manitol (7.66 g) and 4.8g of sucrose (products of Sigma Aldrich, Inc. USA) were dissolved together in beaker and

the solution was made up to 200 ml standard flask. The solution was kept and maintained at 4^{o}C.

3.10.1 Procedure for Mitochondrial Membrane Permeability Transition Assessement in Rat Testes

According to Lapidus and Sokolove (1994), whenever mitochondrion accumulates Ca^{2+} it can be induced to undergo a process known as permeability transition and hence becomes non-selectively permeable to minute solutes. Isolated mitochondria undergoing permeability transition (PT) exhibit large magnitude swelling which causes decrease in light absorption at 540nm. Various methods and procedures have been used to study the permeability transition in separated mitochondria. In this study, measuring of mitochondrial swelling was achieved by monitoring associated decrease in light scattering capacity thus assessing membrane permeability transition.

Principle

The principle applied in this method is based on the idea that when mitochondria swell, refractive indices change and potential to scatter light decreases. This is determined by reduction in light absorbance and read with a spectrophotometer at 520 nm.

Reagents

0.1mM Spermine

Spermine (0.002g), product of Research Biochemicals International, USA was dissolved in 10ml distilled water. However, due to its photosensitive nature, it was stored in dark container and kept cold at 4°C.

Rotenone (80 nM)

Rotenone (0.0002 g) obtained from ICN Biomedicals Ltd was dissolved in 5 ml of ethanol and 5ml of distilled water. It was preserved in a dark container because of its photosensitive nature and refrigerated at 4^{o}C.

12mM Ca^{2+}

Anhydrous $CaCl_2$ (0.4234g) from Sigma Aldrich, Inc.USA, was suspended in 10 ml aqueous solution.

5mM Sodium Succinate

Sodium succinate (0.16 g) was weighed and dissolved in 10 ml of distilled water.

Swelling Buffer (Buffer D): 5mM HEPES-KOH pH 7.4

HEPES (0.1192 g) product of Sigma Aldrich, Inc. U.S.A was made into a 70 ml aqueous solution and standardized to a pH of 7.4 using KOH solution in a 100 ml standard volumetric flask. The solution was then preserved at 4^{o}C.

Procedure

Mitochondrial swelling was determined by the procedure outlined by Lapidus and Sokolove (1994). Mitochondria were sustained in swelling buffer (buffer D) and 0.80µM rotenone for three and a half minutes before the addition of 5mM succinate followed 90 seconds later by the addition of Ca^{2+} as shown on table 3.2. When Ca^{2+} was adopted as triggering agent, mitochondria were pre-incubated in the presence of buffer D and 0.8µM rotenone for 3 minutes, Ca^{2+} (25µl) was added after the 3minutes of mitochondria pre-incubation and 30 second later sodium succinate was added to make a volume of 2500 µl (see table 3.2).

Assay for spermine inhibition of swelling involves, addition of spermine (62.5µl) prior to mitochondria preincubation with swelling buffer, rotenone and allowed to stay for 3 mins after which Ca^{2+} solution was added and in the next 30 seconds sodium succinate was finally added. Temperature was maintained at 30^{o}C and swelling rate was read as a decrease in absorbance (optical density) at 540nm wavelength at 30 seconds time intervals for 12minutes in a Camspec M105 Spectrophotometer. The rate of swelling was quantified as ΔA_{540}/min/mg.

3.10.2 Measurement of Mitochondrial Permeabilisation in Rat Liver

Similar procedures for testicular mitochondria isolation and measurement of mitochondrial permeabilizationwere followed as described for testes from pages 44 to 47. The same principle also applies.

Detailed steps and protocols were as stated on table 3.3

Table 3.3: Protocol for Mitochondrial Swelling Assay at A_{540} nm (Lapidus and Sokolove, 1993)

Sample	Buffer (µl)	Rotenone (µl)	Mitochondria (µl)	Spermine (µl)	Succinate (µl)	$CaCl_2$ (µl)
Blank	2500	-	-	-	-	-
No Triggering Agent (NTA)	2380	10	60	-	50	-
+ Triggering Agent (TA)	2355	10	60	-	50	25
Inhibitor	2292.5	10	60	62.5	50	25

3.10.3 Measurement of Lipid Distortion Expressed by Peroxidation (Oxidative Stress)

Lipid distortion level in this experiment was evalauted by quantifying the amount of lipid peroxides or thiobarbituric acid reactive species (TBARS) released as a result of lipid peroxidation using rat liver and testicular mitochondria membrane as lipid enriched source as proposed by Ruberto *et al.,* (2000).

Principle

The principle applied here was to assess extent of lipid peroxidation by TBARS (thiobarbituric acid reactive species) method. The method detects malondialdehyde (MDA) produced as final product of lipid peroxidation and it is based on the reaction between 2-thiobarbituric acid (TBA) and malondialdehyde (MDA), an end product during lipid peroxidation. On heating in acidic pH, a pink coloured complex is produced which absorbs light maximally at 532 nm and which is extractable into organic solvents such as butanol. Malondialdehyde is often used to calibrate this test and thus the results are expressed as the amount of free MDA produced as shown on figure 3.2

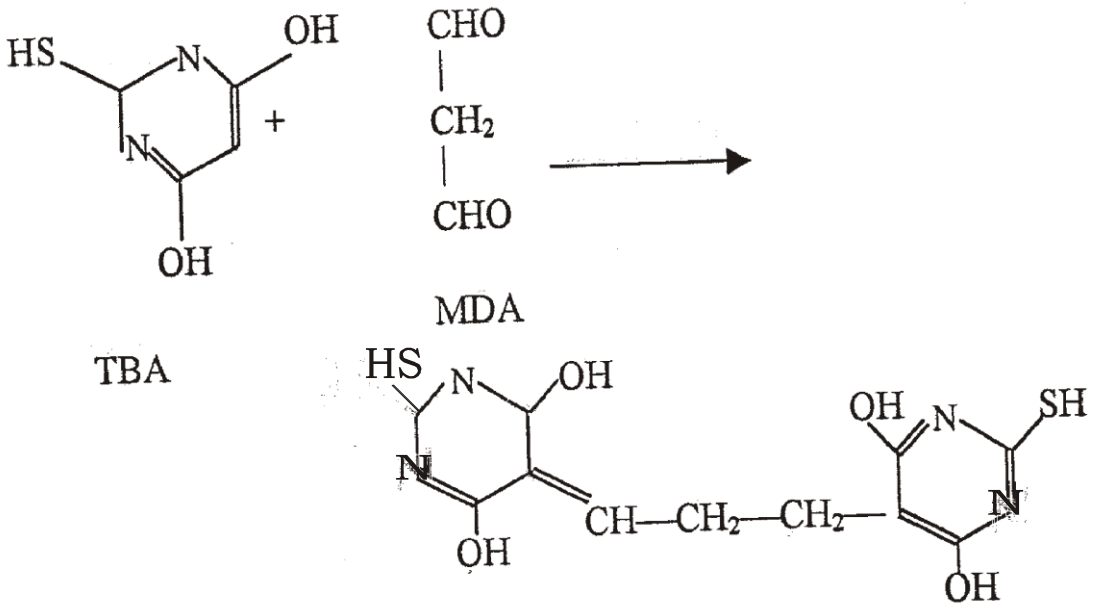

MDA-TBA (pink-coloured complex)

Figure 3.2: MDA in lipid peroxidation assay

MDA- malondialdehyde

TBA- Thiobarbituric acid

Reagents

0.1M Hydrochloric acid (HCl)

Prepared by dissolving 13µl of concentrated HCl (36.5-38%) in aqueous medium and made to 15 ml.

0.75% Thiobarbituric acid (TBA) / (1.1%)

This reagent was prepared by dissolving 0.1125 g of TBA in 0.1M HCl and made up to 15ml volume. The dissolution was aided by stirring in a hot water bath (50^{o}C).

0.15M Tris-KCl buffer (pH 7.4)

This buffer was constituted using 0.559 g of KCl and 0.909 g of Tris base which were dissolved in about 45 ml of distilled water and the pH was rectified to 7.4 with HCl and the volume made up to 50 ml.

Protocol

A drop of 0.4 ml of the test sample was mixed with 1.6 ml of Tris-KCl buffer. TCA(0.5 ml) of 30% was added and followed by 0.5 ml of 0.75% TBA. The mixture was placed in a water bath for 45 minutes at 80^{0} C. This was then cooled in ice to room temperature and centrifuged at 3000 revolutions per minutes for 10mins. The clear supernatant (organic layer) was collected and its absorbance read against reference blank of distilled water at 532 nm. The percentage inhibition was evaluated according to the concept of Ruberto *et al*., (2000).

Calculations

The MDA level was calculated using an extinction coefficient of 0.156µM^{-1}cm^{-1} (Ruberto et al., (2000).

$$\text{Lipid peroxidation (mole MDA/mg protein)} = \frac{\text{(Absorbance x volume of mixture)}}{E_{532} \text{ x volume of sample x mg protein/ml}}$$

3.10.4 Determination of ATPase activity in Mitochondria

The methods used in measuring ATPase activity are as stated by Lardy and Wellman (1953). The procedure was modified by Olorunsogo and Bababunmi (1979).

Principle

The principle here is that of a reduction process characterised by colour change of molybdic acid from yellow to a blue coloured compound when it is reduced in the presence of inorganic phosphate. Ascorbic acid is used as the reducing agent and the level of colour thus formed corresponds to the inorganic phosphate released.

Reagents

(0.25M) Sucrose Solution

This solution contains 8.56 g of Sucrose in 60 ml of aqeous solution made to 100 ml in a standard flask and maintained at $4^{o}C$ in a refrigerator.

5mM KCl

KCl solution was prepared by dissolving 37.2 mg in 60 ml of graded purified water in a standard flask and made to 100 ml volume.

0.1M Tris-HCl pH 7.4

Tris (hydroxyl methyl amino methane) of 1.2 g was added to 60 ml of distilled water. After adjusting the pH to 7.4 with HCl, the solution was made up to 100 ml in a graduated volumetric flask and preserved at $4^{o}C$

0.01M ATP at pH 7.4

The specimen was prepared by adding distilled water to 0.2757 g of disodium salt of ATP with pH rectified to 7.4. It was made to 10ml in a standard volumetric flask and suspended in Eppendorf tubes at very low temperature.

2, 4 –DNP (Uncoupler):

2, 4-dinitrophenol of 0.02g was dissolved in 10mls of 10% Ethanol.

10% SDS

About 10 g of Sodium dodecylsulphate (SDS) was made in to solution with 100 ml highly purified water in standard volumetric flask.

5%Ammonium molybdate:

Ammonium molybdate (NH_4Mb) of 5.0 g product of Hopkins and Williams Ltd England; was dissolved in 80 ml of 6.5% H_2SO_4 and then made up with the same solvent to 100 ml mark and stored in a plastic container at room temperature.

2%Ascorbate:

Ascorbic acid of 2.0 g was totally dissolved in 80ml of standard water and later made up to 100ml. The specimen solution was kept in brown reagent bottle and stored at 4^oC. This reagent is usually prepared fresh.

Procedure

Liver from experimental rats were removed after sacrifice by cervical dislocation and dissection while excess tissue was trimmed-off. Isolation of mitochondria and assessment of Permeability transition pore were as described earlier on pages 46-48).

Prepared mitochondria homogenate was immediately suspended in a solution of ice-cold of very little sucrose and then dispensed in Eppendorf tubes in aliquot and placed on ice for immediate use.

Further steps were taken as summarised on table 3.4 page 57. The medium of reaction was terminated in the presence of 1ml SDS to each test tube (except for the zero time) every thirty (30) seconds and 1ml of the reaction mixture was taken for phosphate determination.

Table 3.4: Protocol for ATPase Activity Determination (Lardy and Wellman, 1953)

Tubes	Sucrose (µl)	KCl (µl)	Tris (µl)	H_20	ATP (µl)	Mitochondria (µl)	UCP (µl)
Blank	200	200	1300	300	-	-	-
Mito only	200	200	1300	285	-	15	-
ATP only	200	200	1300	260	40	-	-
ATP + Mito	200	200	1300	245	40	15	-
UCP	200	200	1300	195	40	15	50
Zero time	200	200	1300	245	40	15	-
PO_4^{3-} Blank	200	200	1300	195	-	15	-

3.10.5 Determination of Inorganic Phosphate

The concentration of inorganic phosphate was determined by the method stated by Bassir (1963)

Principle

The principle is established on the fact that colour change does occur when a complex compound is reduced. This is similar to the principle of colour change described earlier for ATpase activity on page 54-55

Procedure

This procedure is as stated on table 3.5 and consist of ammonium molybdate (400 µl of 5% solution) and 5.0 ml of non-proteinized supernatant which were mixed in test tube, and 0.2 ml of 2% newly prepared solution of ascorbate. The tube was kept for 20 minutes after thorough mixing by gentle shaking. A standardised solution of sodium dihydrogen phosphate (0.2 mg inorganic phosphate per 5 ml) was equally treated. Distilled water was used as blank and the blue colour intensity formed was read in a spectrophotometer at 680 nm.

Calculations:

$$\text{Mg inorganic phosphate} = \frac{\text{Reading of test}}{\text{Reading of standard}} \times \frac{0.02}{1} \times \frac{1}{1000}$$

$$\text{Mole of inorganic phosphate released} = \frac{\text{mg of inorganic} \times 1000}{\text{Molecular mass of pi}}$$

Therefore, mole of inorganic phosphate (Pi) released per minute per milligram of mitochondrial protein is given by expression mole/min/mg protein.

$$\frac{\text{Mg Pi released per ml} \times 1000}{\text{Molecular mass of Pi} \times 1000}$$

$$\text{Mg protein} \times 30$$

Table 3.5: Protocol for inorganic phosphate determination

1 mM Na_2HPO_4 (µl)	H_2O (µl)	NH_4Mo (ml)	Ascorbate (ml)
-	1000	1	1
20	980	1	1
60	940	1	1
100	900	1	1
140	860	1	1
180	820	1	1

3.10.6 Determination of Caspase 9 activity using Enzyme Linked Immunosorbent Assay (Elisa) Kit

Principle

The principle used in ELISA technique involves binding of specific antigen to a specific antibody which is conjugated to a (3,3,5,5-tetramethylbenzidine) TMMB substrate.

PREPARATION OF SAMPLE AND ANALYSIS OF CASPASE 9 USING ELISA

METHODS

Rat testicles were removed from dissected animal, weighed and thoroughly rinsed with phosphate buffer to obtain a clear and clean wash. The testes were minced and homogenized on ice. The homogenate obtained was centrifuged at 8000 rpm for 5minutes and supernatant obtained was decanted into sample bottle and frozen. The frozen supernatant was allowed to thaw after 48 hours. This was repeated twice and afterward samples were assayed for caspase 9. Similar procedures were employed for caspase 3 determination using caspase 3 ELISA kit.

Liver and testes from experimental rats were isolated, weighed and sparingly washed in phosphate buffered saline until a clear and clean tissue were attained. The clean washed liver and testes were minced and homogenized on ice separately. Homogenate obtained for each organ was centrifuged (in ice-cold centrifuge) at 8,000 rpm for five minutes. The sample bottles were allowed to defroze and the process repeated.

Procedure

Experimental procedure was guided by the manufacturer's instruction which was followed in the course of the experiment. Elabscience kit consisting Samples / Standards (50µL) and 50µL antibody were added to wells in successions (mix/cocktail) in a microplate. The entire microplate was wrapped, sealed and incubated for an hour and maintained at 25^0C (room temperature) on a shaker adjusted to 400rpm; while the wells were washed repeatedly (thrice) to eliminate all unbound materials. Total separation of fluid was ensured to guarantee good outcome. The microplate was inverted after the last wash, blotted using a neat paper towel to get rid of excess fluid. This is followed by addition of 100 µl TMB substrate and thereafter incubated in the dark for 10 minutes to yield a blue-coloured compound. The reaction was consequently halted by adding 100µl stop solution thus finally transforming the initial blue

colour to yellow. The concentration or extent of colour produced is a function of the amount of bound analyte measured at 450 nm.

3.11 Sperm Analysis

Analysis carried out on the sperm include: determination of sperm motility, live-dead count, and estimation of sperm concentration as follows:

Measurement of Sperm Motility

Little quantity of suspended spermatozoa in incubation medium of trisaminomethane, citric acid and fructose was placed on a slide and a cover-slip was placed over the drop and was observed under high power magnification of x100.

Live- Dead Count

To determine live- dead preponderance of sperm cells, the principle applied is predicated on the observation that when eosin B is used to stain mixtures of live-dead sperm cells, only viable cells repel the stains while the dead cells are penetrated. It therefore requires that the staining be done without delay.

Protocol

Fresh washed semen was prepared using volumetric dilution and hemocytometry with contrast microscope and reported as millions of sperm per mL Sample drops of sperm were suspended in semen incubation medium placed on slide; 1% and 5% of eosin B and nigrosin were added respectively. Slide was observed under high (x100) magnification to count population of stained and unstained cells. To calculate sperm-count when 5 small squares within the large centre squares are counted: it is given as: Number of sperm counted x dilution.

Estimation of Sperm Concentration

To obtain an estimated value for sperm concentration, an improved haemocytometer was used with 0.9% NaCl dilution (ratio 1:200). The ruled area of the haemocytometer and special cover slip were carefully cleaned and freed from mist and grease. Cover slip was placed on the supporting ribs of the counting chamber by pressing firmly at both sides with

the thumb and sliding it over from one end. With a micropipette, the tip wastouchedwithin the space between counting chamber and the cover-lid.

The fluid filled the space by capillary movement and when the fluid had flowed three-fourths at the way cross, the pipette was withdrawn as there was enough fluid left to fill the space. After locating the central square of the nine large squares under low microscope, all the cells were numbered in 5 of the 25 small squares in the central area under high power. Each of the small squares counted was bounded by triple of single lines and divided into 16 small squares.

Epididymal Sperm Motility and Count

Caudal epididymis was dissected and incised allow drops of sperm fluid squeezed out to be observed under microscope, saline drops were added to mobilize sperm cells. Epididymal sperm motility was evaluated by calculating motile spermatozoa per unit and expressed in percentage.

Eosin/Nigrosin stain were employed to determine sperm viability after homogenized epididymis was added to 5 ml saline and counting done in counting chamber of haemocytometer

Sperm morphology

This is meant to find out the presence or occurence of morphologically deformed forms of spermatozoa possibly induced upon administration of plumbagin.

Procedure

The sperm suspension from the smear used in live dead count can be stained with the Wells and Awa stain instead of eosin B and nigrosine to identify abnormal forms of spermatozoa. Cell morphology was studied under high power (x400). Individual cells were examined and classified according to method proposed by Bloom (1948).

3.11.1 Liver Function Tests (Enzyme Assays)

Liver function tests were done by assessing levels of Aspartate aminotransferase (AST), and Alanine aminotransferase (ALT), activities with the aid of Randox Kits (Randox Laboratories, United Kingdom).

3.11.2 Determination of AST and ALT Activities

I*n vitro* determination of AST in serum was carried out using Randox kits from Randox Laboratories Ltd, United Kingdom. AST activity was read by monitoring concentration of oxaloacetate hydrazone formed with 2,4-dinitrophenylhydrazine as described by Reitman and Frankel (1957).

The measurement of AST is well guided monitoring the concentration of oxaloacetate hydrazone formed with 2,4-dinitrophenylhydrazine. The enzyme involved specializes in transferring amino group from L-aspartate to α-oxoglutarate which then results to producing oxaloacetate and L-glutamate. The unstable oxaloacetate formed is unstable and is quantitatively decarboxylated to pyruvate which is then complexed with 2,4-dinitrophenylhydrazine (DPNH) to produce highly coloured hydrazone on the addition of NaOH. This coloured complex absorbs light at 530-550 nm.

Procedure

This involves the measurement against reagent blank. 0.5 ml of reagent I (in the kits) and mixed with 0.1ml of distilled water and the solution was incubated for 30 minutes at 37^{o}C. 0.5 ml of reagent II (in the kits) was then added to the reaction mixture and allowed to stand for exactly 20 minutes at 25^{o}C. Then 5ml of NaOH was added. This was used to blank the Camspec M105 Spectrophotometer after 5 minutes at 546 nm.

To obtain the activity of AST in the serum, the absorbance read was extrapolated from the Standard Table to get the Units/Litre. For linearity, the absorbance that exceeds 0.170 from the Standard Table, there will be a reassay by diluting 0.1 ml of sample with 0.9 ml of 0.9% NaCl solution and the absorbance is then multiplied by 10.

3.11.3 Histological Assessment of Visceral Organs of Male Wistar Strain Rats

Histopathological investigation of tissue begins with surgery or autopsy followed by cutting the tissue and placed in a fixative which makes the tissue stable to avoid decay. The most frequently used fixative is formalin (10% formaldehyde in water).

Procedure

Tissues were excised, mopped and then preserved in 10% formalin except testes which was preserved in Boins solution. The tissues were subsequently cut into sections for histological assessment. The tissue section was deparaffinized by attaching it to the slide and dipping in fresh xylene in a coplar jar. This step was repeated. The tissue section was then hydrated by passing via reducing alcohol concentration baths and water (100-70 %). Hydrated tissue section was then stained and washed under running tap water and finally viewed under microscope.

3.11.4 Immunohistochemical Determination of Apoptotic Biomakers Immuno stained tissue sections

Fixed tissue section was deparaffinized by placing on the slides and deeping the slides in xylene twice for 5 min each. The slides were then removed and dipped in 100% alcohol twice for 3 min each. This was followed by passing through 95% twice and 70% alcohols once for 3 min each. The section was rinsed with Wash Buffer twice, 5 min each time and then performed antigen regaining to reveal the antigenic epitope. Other steps were sequentially carried out as specified and the staining colour of the antibody in the tissue sections was then observed under microscope.

Statistical Analysis

Unless otherwise stated, data were presented and expressed as mean ± SD, n=5: otherwise, representative data are presented. '*p*' values< 0.05 were considered significant. Microsoft Excel 2010 and Graph pad prism were used for the analysis.

3.12 Reproductive Gene Expression Procedure

Semi quantitative gene expression studies were used to quantify extent of effect of plumbagin on expression of reproductive enzymes and hormones. It features Polymerase Chain Reaction

(PCR) with agarose gel electrophoresis to separate specific genes. The process is highly sensitive and useful for detection of rare transcripts or where analysis of samples available in limited amounts are required. It features application of TRIzol (Total RNA Isolation) reagent which helps to retain integrity of the RNA while distrupting other cellular components, thus making it highly efficient and effective procedure (Omotuyi, 2015).

Principle

Semi quantitative gene expression procedure is based on expression of specific genes through amplification of RNA via Polymerase Chain Reaction. The expressions were measured with reference to standard amplicons.

Procedure

Isolation of Total RNA

Complete RNA was isolated from entire (testes) tissue after homogenization and Partioning with TRIzol (Total RNA Isolation) reagent (Zymo Resaerch, USA) and chloroform. RNA buffer was used to compliment the process after centrifugation at 15,000 rpm/15min to stabilize the pH at 6.4

cDNA conversion and Polymerase Chain Reaction

Total RNA was quantified after treatment with DNAse I to remove contamination (NEB, Cat. M0235S) as specified by manufacturer. 2ul solution containing 100 ng DNA free RNA was converted to cDNA using Reverse transcriptase kit (NEB). Reverse transcriptase was performed at 650C/20min and amplicons were resolved in 1.5% agarose gel (Cleaver Scientific Limited) in Tris reagent – Borate (JHD chemicals, China) EDTA buffer at pH 8.

Amplification of gene products was done with the primers indicated on table 3.5. where applicable amplicons were resolved to have a negative value where there is no cDNA reaction mixture.

MOLECULAR DOCKING OF PLUMBAGIN WITH TARGET PROTEINS

The study entails molecular interaction of plumbagin with some selected anti apoptotic proteins. This is known as ligand-protein docking and was chosen because it represents drug-protein target interaction with pharmacokinetic and toxicology relevance suitable for studying how drug interacts with their protein targets. Other docking types include protein-protein docking which best describes interractions between two or more proteins. Protein data bank was used to generate relevant information on properties of target proteins including amino acid involved in their interaction as obtained from the soft ware package called GROMACS (Dar and Mir, 2017).

Materials and Procedures

The study commenced with template structures of some selected anti apoptotic proteins suspected to interact with plumbagin to possibly induce apoptosis. The level of interaction of these target proteins interaction was assessed and measured. The protein includes cyclin A1, bcl 2, bcl-w, bcl-xl, Mcl-1 and MDM2. Protein interractions and amino acids involved were identified to determine the magnitude and orientation in space with reference to a standard molecule- 7-hydroxy4-methylcoumarine. The resulting plumbagin-ligand complex interractions generated coordinates and grid were measured as a function of interaction for plumbagin and 7HC. Viable standard docking tools and soft wares were deployed to arrive at the best docking pose where the most effective interaction was determined as described by Omotuyi *et al.,* (2018). Best docking pose were determined for all protein ligands and the Gibbs freee energy score were recorded accordingly.

Atomistic Simulations and kinetics

The biosystem set up for simulations of plumbagin with the ligand exhibiting the best docking oreientation and interaction score- namely MDM2 was set for kinetic simulation as complex with PL and 7HC. The conformation in the series of interractions and biophysics dynamic studies shows that in all reaction or simulation procedures, plumbagin was able to conform to similar pattern of molecular simulations with 7HC used as the standard template molecule in the study.

Post simulation Data Analysis

After the simulation routine as demonstrated in the foregoing, a package refered to as Visual Molecular Dynamics software package was used and the repective Root mean square deviations (*rmsd)* value was calculated on GROMACS soft ware (Kumari, 2014).

CHAPTER FOUR

EXPERIMENTS AND RESULTS

EXPERIMENT 1: Effects of Calcium and Spermine on Mitochondrial Membrane Permeability Transition Pore Opening in Testes of Male Wistar Rats (*in vitro)*

Introduction

Apart from cellular energy metabolism, mitochondria remain central in the intrinsic pathway of apoptosis and final collapse of the metabolic machinery of the cell. This is attained by induction of mitochondrial pore opening which uncouples mitochondria energy generation capacity and thus preventing them from providing for the energy needs of the cell. The collapse of energy generating machinery of the cell and its components are the major event in apoptosis via the intrinsic pathway.

The mechanism by which permeability occurs is still uncertain but one possible way which has attracted recent interest is induction of a permeability transition pore (PTP). Elevation of cytosolic Ca^{2+} concentration plays a role in this process (Kwong, 2015). There is uncertainty about the mechanism by which permeabilization of the inner mitochondrial membrane occurs but one possibility is the induction of the permeability transition pore (PTP).

Therefore, intact mitochondria ensure that the membrane integrity is not in any way compromised in normal situation where apoptosis is not likely to occur since the permeabilisation of the mitochondrial membrane allows the uncoupling of energy generating machinery. This experiment was designed to ascertain that mitochondrion removed from rat testes suitable for progressive studies.

Procedure

Lapidus and Sokolove (1992) method was employed to induce mitochondrial swelling. Intact isolated mitochondria were pre incubated with 0.8 μM rotenone in MSH buffer for 3.5 minutes prior to the addition of 5mM sodium succinate. The routine above was repeated and calcium added before energized by succinate in the presence of MSH buffer for 3 minutes. Spermine was also used as a standard inhibitor of mitochondrial swelling and was added prior to mitochondrial pre-incubation with rotenone. Change in absorbance was estimated at 540 nm at 30 seconds interval for 12 minutes in a T70 UV-visible spectrophotometer.

Results

As seen from Figure 4.1 mitochondria isolated from the testes of Wistar rats did not show appreciable decrease in absorbance while respiring on succinate in the absence of calcium. whereas addition of exogenous calcium caused appreciable increase in form of large amplitude swelling. Interestingly, this effect of calcium was reversed by addition of spermine - a potent inhibitor.

Conclusion

The result shows that external calcium induced the permeabilisation of the mitochondrial pore while spermine a potent inhibitor reversed pore opening. Effects of calcium and spermine show flexibility and intactness of mitochondria and thus suitability for further investigations.

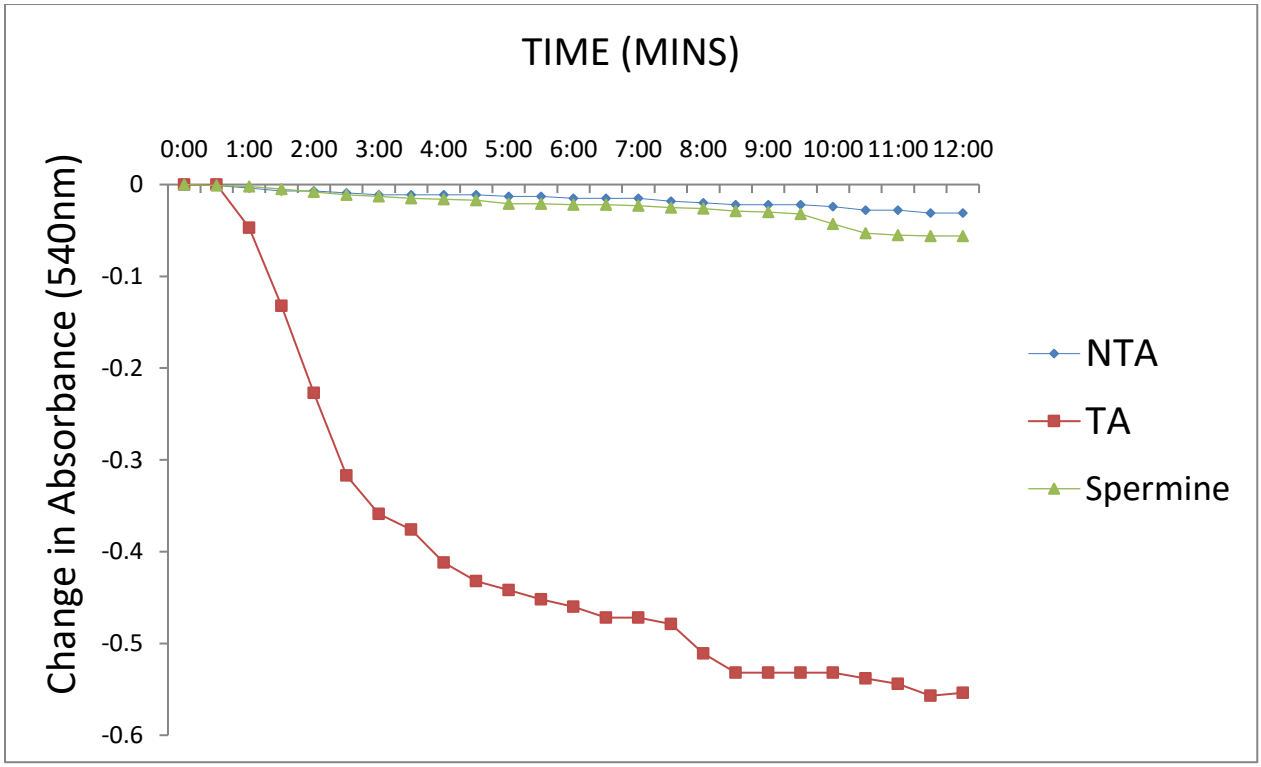

Figure 4.1: Effect of calcium (TA) and spermine on MMPT pore opening in rat testes (*in vitro)*

EXPERIMENT 2: Effects of Plumbagin on mPTPore Opening in Testes of Male Wistar Rats (*in vitro)*

Introduction

Varying concentrations of plumbagin were used to investigate whether or not plumbagin induce opening of the MMPT pore. The experiment was also to monitor the extent of opening. This is to ensure that there is independent activity of plumbagin on the mitochondrial transition pore opening with no synergistic or any form of inhibitory effect in *in vitro* situation.

Procedure

Mitochondrial samples were obtained from testes of normal Wistar rats as earlier described and swelling was determined using varying concentrations of plumbagin volumes: 20, 40, 60 and 80 μg/ml in the absence of calcium. Swelling was also determined for normal mitochondria in the presence of standard inhibitor (spermine).

Results

The results as presented on Figure 4.2 show that plumbagin has inherent capacity to induce permeabilization of the mitochondria in the absence of exogenous calcium via concentration dependent amplitude swelling of the mitochondrial membrane by 8, 10, 13 and 15 folds at 20, 40, 60 and 80 μg/ml respectively compared to control (NTA).

Conclusion

Plumbagin precipitated induction of mitochondrial membrane in a concentration dependent manner and as such exerted modulatory effect on mitochondrial membrane. Hence, plumbagin in this *in vitro* study may be a promising apoptosis inducer suitable to combat disease conditions where it is required to stop proliferation of unwanted or damaged cells.

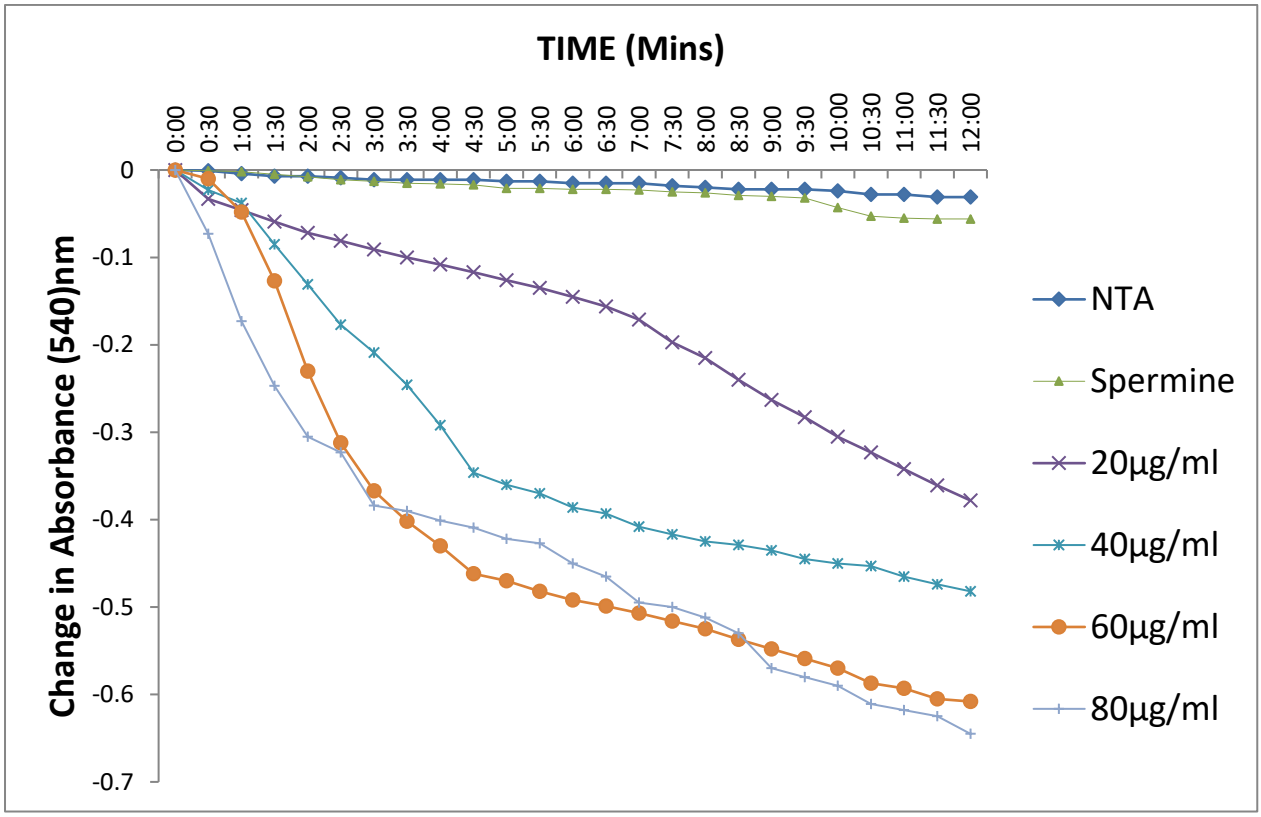

Figure 4.2**:** Effect of PL on MMPT pore opening in Absence of Calcium

EXPERIMENT 3: Effects of Plumbagin on Testicular Mitochondrial Membrane Permeability Transition Pore Opening in the Presence of Calcium (*in vitro)*

Introduction

Plumbagin has been identified as the active principle responsible for various phytochemical properties in *Plumbago Zeylanica* (PZ). Although, independent effects of plumbagin on mitochondrial membrane permeability transition pore was investigated in the preceding experiment. The present study is to examine whether plumbagin would induce or inhibit pore opening or be unaffected by varying concentrations in the presence of calcium (TA).

Procedure

The isolation of intact mitochondrial pellet was done as previously described in chapter two while mitochondrial swelling was done spectrophotometrically using 20.40, 60 and 80 μg/ml of plumbagin concentrations respectively.

Results

The results as presented in Figure 4.3 show that plumbagin exhibited further inductive effect on mitochondrial membrane permeabilisation in the presence of exogenous calcium, having induced further amplitude swelling in the mitochondrion in a concentration dependent manner.

Conclusion

Plumbagin induced pore opening with increasing concentration. Hence, plumbagin induced further permeabilisation of the pore in presence of calcium compared to its independent effect in *in vitro* studies. Therefore, pore opening by plumbagin is enhanced in the presence of exogenous calcium.

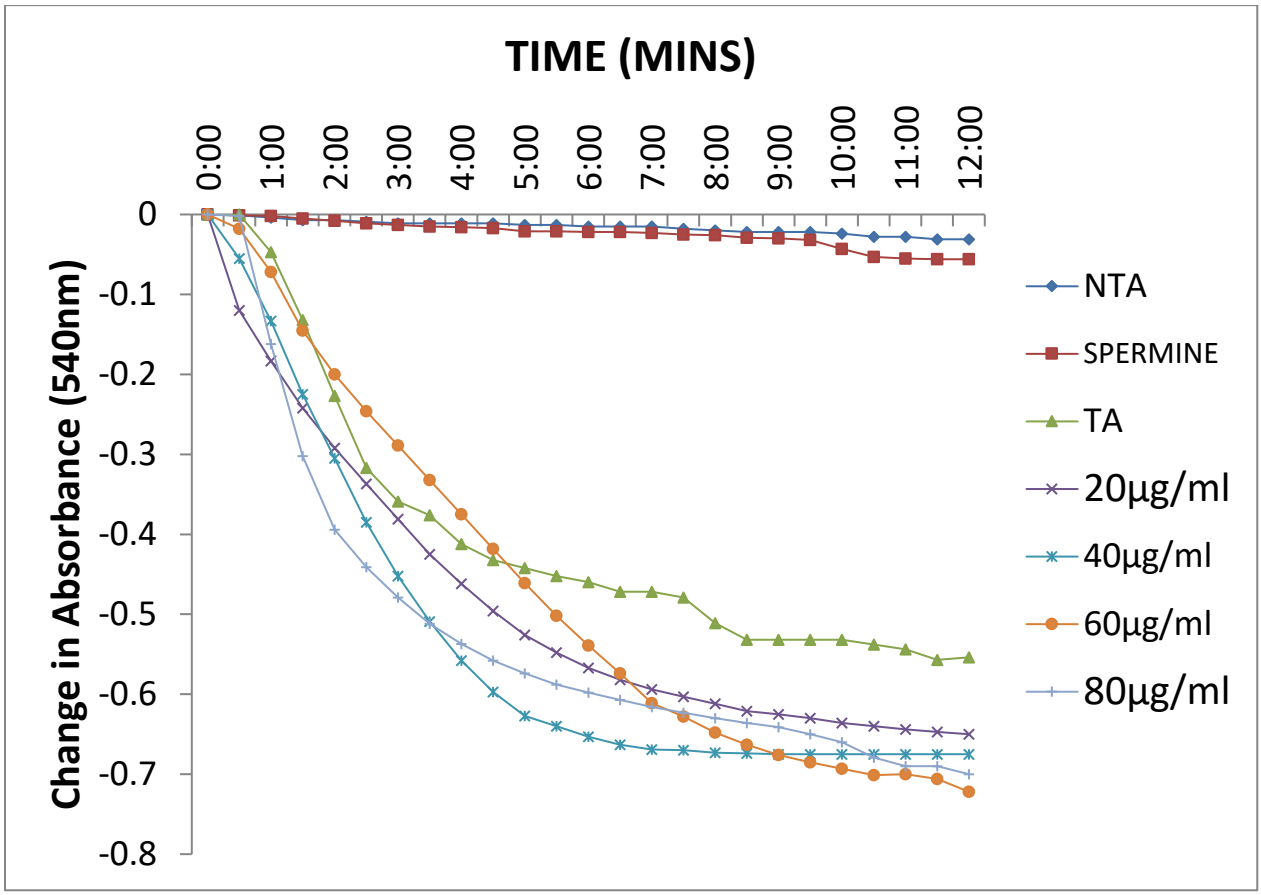

Figure 4.3: Synergistic inductive effect of plumbagin on MMPT pore opening in the presence of calcium (TA).

NTA-- No triggering agent

TA- Trigerring Agent

EXPERIMENT 4: Effects of Plumbagin on Calcium - Induced Testicular mPT Pore Opening in Untreated Wistar Rats (*In vivo*)

Introduction

This is an *in vivo* study where the effect of calcium and spermine were examined in the testicular mitochondrial of control animals which were acclimatized and kept under similar conditions with treated animals for fourteen days. It is expected that the mitochondria of health and untreated rats should be flexible or intact such that it can be made to undergo large amplitude swelling by induction and as well reversed by potent inhibitor such as spermine. This will attest to its intactness and assure that the integrity of the mitochondria has not been compromised.

Procedure

An initial assay in this study consists of MSH buffer (2380 ul), rotenone (10 ul), intact mitochondria (60ul) which is energized by 50 ul of succinate as the entire volume constitute 2500 ul (NTA). The next step proceeds by the addition of 25 ul of calcium chloride solution to the volume of assay consisting of 60ul mitochondria,10 ul rotenone and 2355 ul MSH buffer energized by 50 ul succinate to make a total of 2500 ul. The absorbance was read after pre incubation for each step taken at 540nm. The last stage involves the addition of spermine (62.5 ul) to the reacting volume such that MSH buffer was adjusted to ensure that total volume remains 2500 ul while accommodating other species involved.

Results

Result presentation in Figure 4.4 depicts prominent and significant amplitude swelling induced on mitochondrial membrane by calcium while respiring on succinate. The inductive effect was however, reversed by the standard inhibitor- spermine.

Conclusion

Calcium induced large amplitude swelling which was reversed by the inhibitor spermine in Figure 4.4 confirms the flexibility and uncompromising state of testicular mitochondria in untreated rats. It is an indication that the mitochondria of normal rats were not compromised and as such are suitable for further experiments.

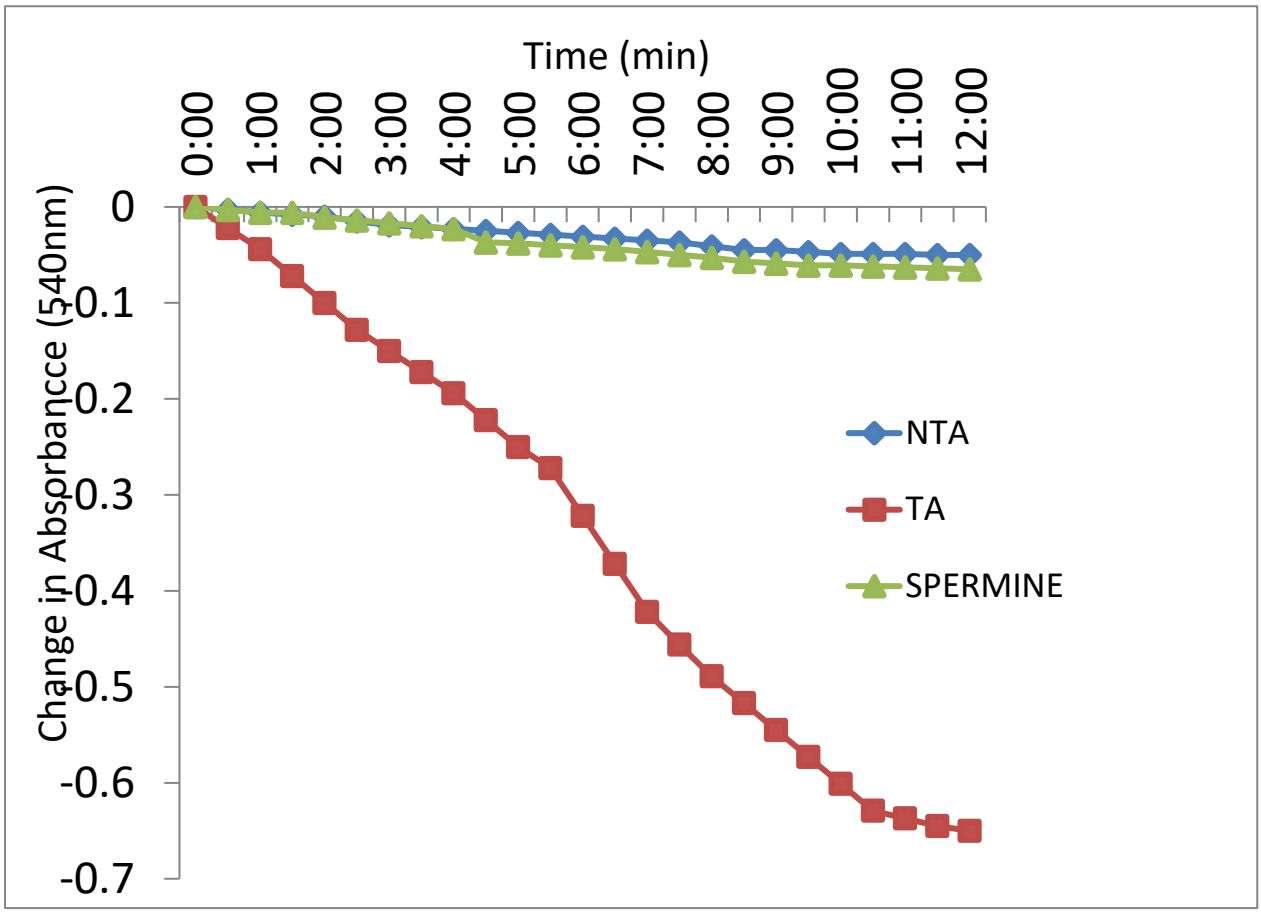

Figure 4.4: Calcium - Induced MMPT pore opening and reversal by spermine in normal rat testes.

NTA-Non triggering agent

TA- Triggering agent (calcium)

EXPERIMENT 5: Assessment of the Effects of *Plumbagin* on Testicular mPTP Opening in Wistar Rats

Introduction

Recently, mPTP has been found to be effective in the therapeutic targeting of various life-threatening diseases such as ischemia/reperfusion, diabetes, cancer and cell apoptosis. Various chemicals have been investigated for improvement of the pharmacological profile of mPTP.

Research has revealed that natural compounds possess selective potentials to kill cancer cells with mitochondrial dysfunction (Chen *et al*., 2010). mPT induction has been recognized as one of the tools for tumour cell elimination. Such natural compounds play major role in facilitating mPT induction, while others exert their action through interaction with regulators (e.g., HK II, Bcl_2- family proteins) and components (e.g., VDAC) of mPT pore.

Procedure

Plumbagin serves as the inducer (*in vivo* triggering agent) of the PTP and as such calcium was not added at all in the procedural steps. The doses include 2.5, 5.0 and 10.0 mg of PL/kg body weight treatment for 14 days and the control group (untreated) under similar environmental condition. The detailed procedure is as reported in experiment 4 and recorded results for each group were noted.

Results

Figure 4.5 presents the plot of changes in absorbance determined from varying dose of plumbagin on mPT pore of succinate-energized mitochondria. The varying dose-administration of PL at 2.5, 5.0 and 10 mg of PL/kg produced induction folds of 0.62, 0.77, and 0.84 respectively. Dose-dependent induction of mPT pore as observed in this experiment may be a toxic response of the mitochondria to plumbagin administration.

Conclusion

Plumbagin caused dose-dependent induction (toxic effect) of mPTP opening. Hence, this shows that PL was readily available to cause induction of the pore in testes of Wistar rats in the *in vivo* experiment. It can be concluded that plumbagin toxic induction of testicular

mitochondria may lead to interference and consequently distruption of reproductive machinery in experimental animals as observed in this study.

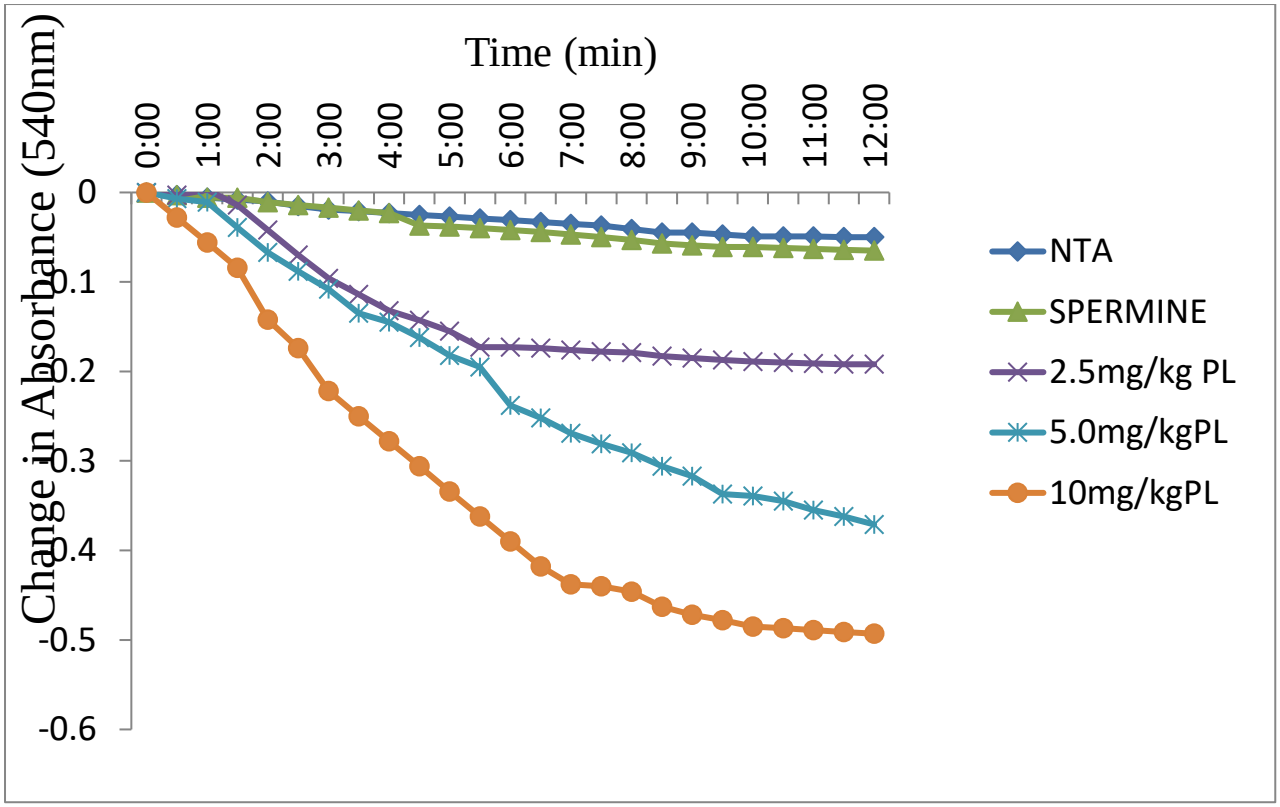

Figure 4.5: Effect of varying doses of plumbagin on mPTP opening in testes of Wistar rats

EXPERIMENT 6: Assessment of the Effect of Plumbagin on Rat Liver mPTP Opening

Introduction

The induction of mPT pore is the gate keeper in the collapse of membrane potential which gives way to apoptotic cascades. Varying doses of plumbagin administered to Wistar rats could be monitored to investigate how the doses of plumbagin will induce pore opening.

Procedure

Liver mitochondrial swelling for treated and control groups were assessed to verify extent of induction of the mPT pore opening compared to control as explained in experiment 5. The induction was determined spectrophotometrically at 540 nm and the results generated for each treatment group. This was repeated to obtain consistent readings and results tabulated for varying doses viz 2.5, 5.0 10.0 mg/kg PL and NTA (control).

Results

Results as presented in Figure 4.6 show that there was dose-dependent induction of mPT pore opening for all treated groups compared to control. The observed induction in the succinate energized mitochondria were dose-dependent in all experimental groups.

Conclusion

The result in Figure 4.6 shows that plumbagin induced dose-dependent mPT pore opening in liver mitochondria of treated Wistar rats. Thus, it can be concluded that plumbagin has potential to induce apoptosis in damaged or primed cells via mitochondrial or intrinsic pathway of cell death. Hence, toxic effect of plumbagin can be harnessed in combating unwanted rapidly proliferating diseased or cancerous cells through induction of apoptosis.

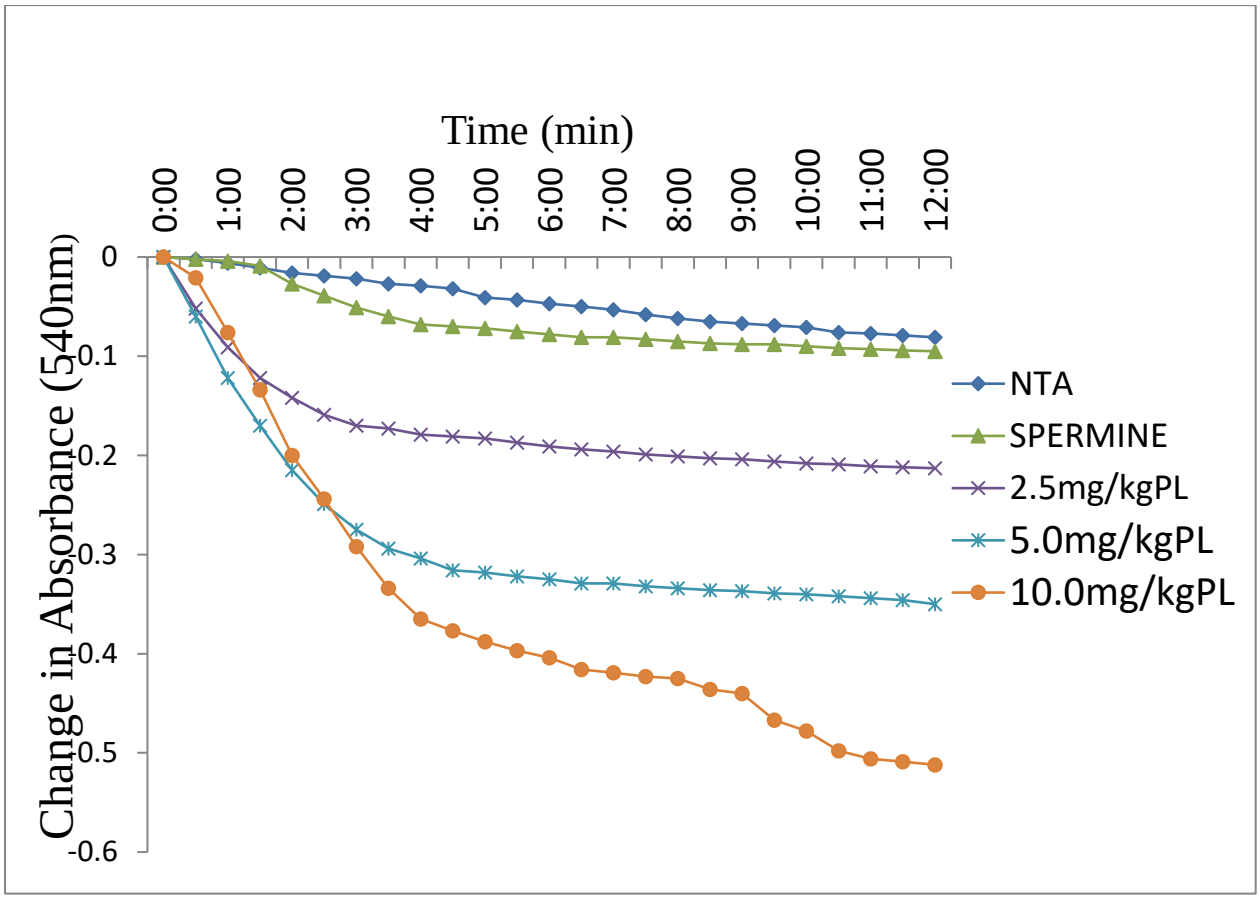

Figure 4.6: Effect of Plumbagin on mPTP opening in liver of Wistar rats

NTA-Non triggering agent

PL-plumbagin

EXPERIMENT 7: Effect of Varying Doses of Plumbagin on ATPase Activity of Testicular Mitochondria of Wistar Rats

Introduction

ATP synthase, also known as F_1F_0 ATP synthase functions to couple oxidative phosphorylation- the key step for ATP (which is a nucleotide) production which essentially involves electron transfer, electrochemical gradient and ultimately synthesis of ATP- the energy currency of the cell. Since apoptosis is an energy driven process, assessment of ATPase would further confirm mechanism of action of plumbagin in the induction of apoptosis via the intrinsic pathway (Halestrap *et al.,* 2004). Therefore, this study was structured to investigate the effects of varying doses of *Plumbagin* on mitochondrial ATPase activity in treated animals compared to control.

Procedure

Mitochondria obtained from tissue homogenate were dispensed into tubes. Mitochondria were dispensed into all the tubes at 30 seconds interval except the tube containing ATP only and 1ml of sodium dodecyl sulfate (SDS) was included in the zerotime test-tube after the addition of the mitochondria. 1000 µl was picked from each test tube and put in another set of test tubes. 1000 µl of sodium dodecyl sulfate (SDS), 1000 µl of Ammonium Molybdate and 1000µl of L-ascorbate were added into all the new set of test tubes at 30 seconds interval for 20 minutes. After the 20minutes, absorbance was taken at 660 nm.

Results

Figure 4.7 show the enhancement of mitochondrial ATPase activity in mitochondrial testes of treated animals by varying doses (2.5, 5, and 10 mg) of PL /kg body weight. The observed enhancement in ATPase activity tends to be dose-dependent in all treated groups and statistically significant for the highest dose group of 10 mg of PL /kg body weight compared to the standard uncoupler.

Conclusion

Plumbagin administration enhanced dose-dependent ATPase activity in testes of treated rats compared to control. This implies that ATPase activity is promoted by the bioactive compound in induction of apoptosis via the intrisinc pathway which is not only a cellular process but one that requires energy (Yu *et al.*, 2019).

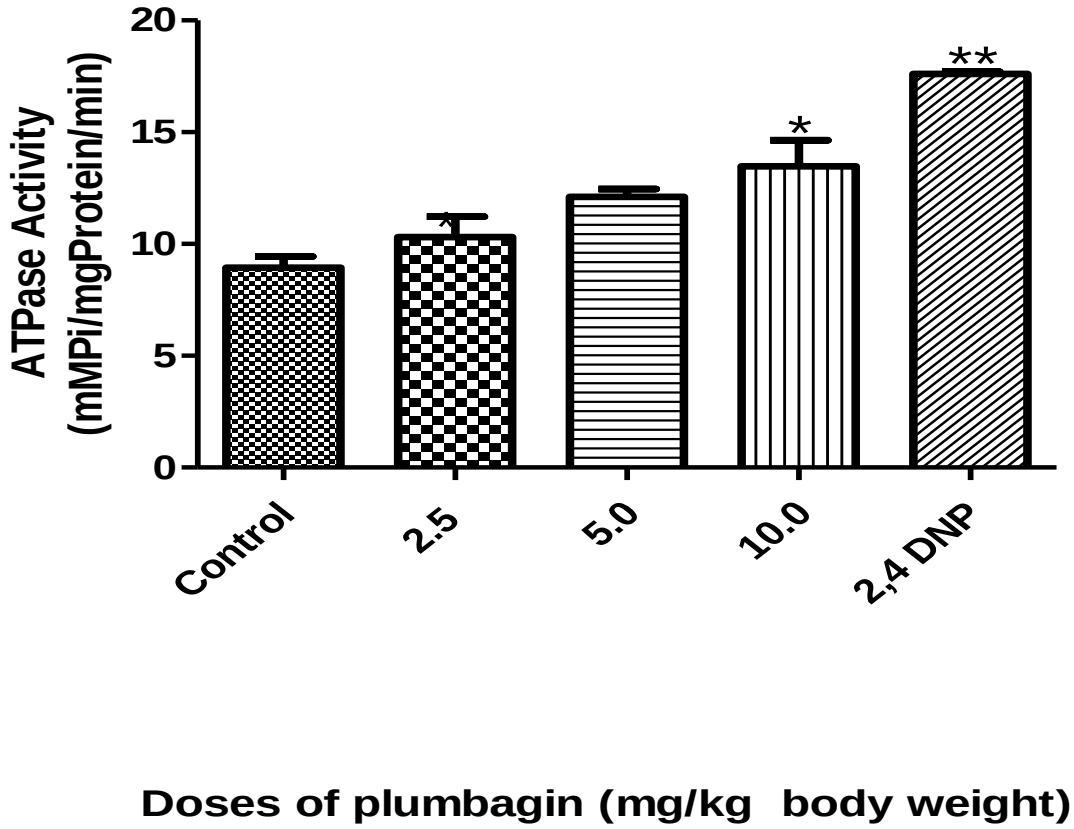

Figure 4.7: Effect of plumbagin on ATPase activity in testicular mitochondria of Wistar rats

*** p < 0.05, ** p < 0.01**

EXPERIMENT 8: Effect of Doses of Plumbagin on ATPase Activity in Liver Mitochondrial of Wistar Rats

Introduction

An energy dependent process is ATP driven and as such expends energy. Experiments on testes previously reported indicated that plumbagin promoted energy dependent activities in the cell. Moreso, the liver is the centre for various metabolic processes in the body including xenobiotics metabolism. To confirm varieties of energy requiring activities going on in the liver, the experiments will show propensity of plumbagin to promote apoptosis or otherwise. It is evident from literature that upregulation of mitochondrial ATPase activities in the cell is closely connected to the intrinsic pathway of apoptosis (Dominic *et al.,* 2019).

Procedure

Liver mitochondria were isolated as described in previous experiments by centrifugation in appropriate buffer medium and liver mATPase activity was determined via methods and procedures described by Lardy and Wellman, (1953) and as modified by Olorunsogo and Malomo (1985). The reaction was terminated using 1ml SDS and the resulting mixture kept for phosphate determination as stated in section 3.10.5 section of materials and methods. The zero-time tube was prepared by addition of ATP to the reaction vessel with immediate addition of SDS for 30 seconds intervals for other reaction vessels.

Results

Results as presented in Figure 4.8 show that mATPase activity was significantly induced in hepatocytes of experimental (treated) animals compared to standard uncoupler of oxidative phosphorylation (2.1folds). The observed enhancement was statistically significant for doses 5 and 10 mg of PL/kg body weight compared to standard uncoupler (2,4 DNP).

Conclusion

Plumbagin promoted ATPase activities in dose-dependent manner similar to what obtains for the testes. Therefore, it implies that the bioactive compound- PL can enhance the breakdown of ATP to ADP and inorganic phosphate in liver of treated animals. This is basically the feature of activities observed in an energy dependent process including those observed in hepatocytes especially for the myraids of cellular and metabolic activities in such tissues.

Therefore, it suffices to state that plumbagin promotes apoptosis -an energy dependent process which requires energy desipation in the experimental animals compared to control (untreated group).

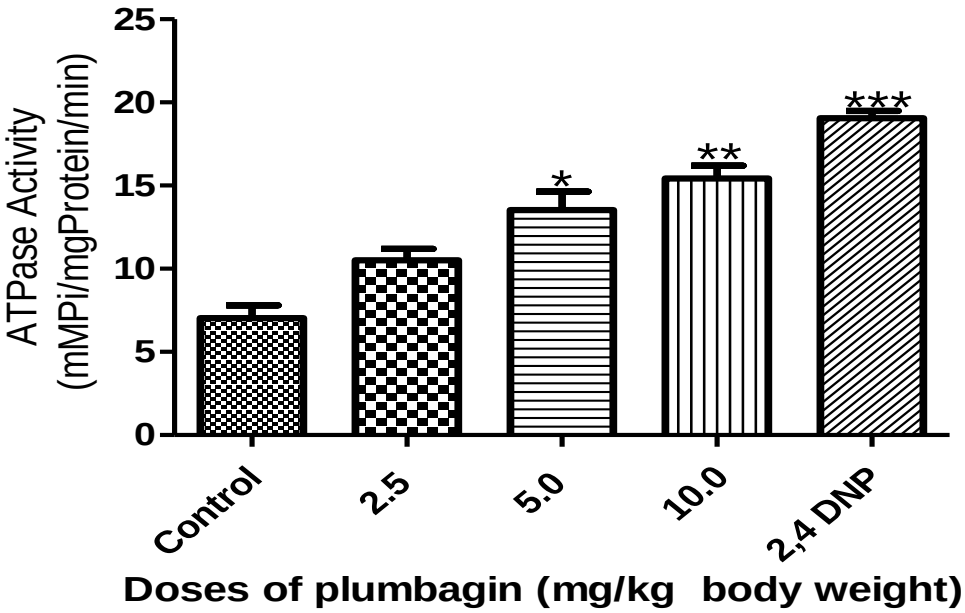

Figure 4.8 Effect of plumbagin on ATPase activity in the liver of Wistar rats

*P<0.05, **P< 0.01, *** P < 0.001

EXPERIMENT 9: Assessment of the Effects of Varying Doses of *Plumbagin* on Testicular Mitochondrial Lipid Peroxidation in Wistar Rats

Introduction

The experiment aimed to assess the lipid peroxides scavenging potential of varying doses of *Plumbagin* in rat testicular mitochondria. The peroxidation of lipid membrane marked by toxicity do alter normal functioning of organelles such as mitochondria because oxidative breakdown of biological phospholipids does occur in such cellular membranes (Sandro *et al*., 2014). This is the similar characteristic feature in nephrotoxicity, neurotoxicity and hepatotoxicity.

Procedure

Mitochondria derived from tissue homogenate following its isolation as described in Experiment 1 and procedure earlier described on pages 50-53, after incubation were allowed to stand in incubation placed in a water bath for 45minutes at 80^{o}C. This was then cooled in ice to room temperature and centrifuged at 3000rpm for 10 mins. The clean wash consisting organic layer was harvested and the absorbance recorded using distilled water as blank at 532 nm. Percentage inhibition was evaluated according to Ruberto *et al*., (2000) and as stated earlier on page 52.

Results

Figure 4.9 shows that differing amounts (2.5, 5 and 10 mg/kg bwt) of PL caused significant corresponding increase (2.3, 5.8, 8.1 umole/mg protein) in the level of MDA generated.

Conclusion

PL caused peroxidation of membrane lipids and by extension the opening of the mPT pore could be as a result of free radical production. This inevitably promotes induction of apoptosis via mPT pore opening of the mitochondria leading to the release of cytochrome C and ultimately to apoptotic cascades. Therefore, plumbagin modulates mPT via peroxidation of membrane lipid and thus cause testicular damage.

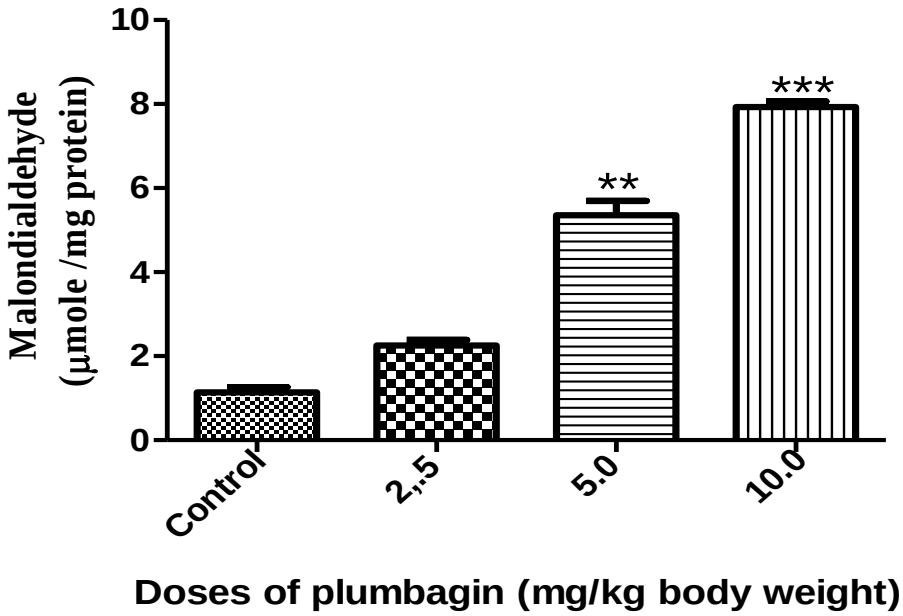

Figure 4.9**:** Effects of varying doses of plumbagin on testicular mitochondrial lipid peroxidation.

**** p < 0.01, *** p<0.001**

EXPERIMENT 10: Assessment of the Effects of *Plumbagin* on Liver Mitochondrial Lipids in Wistar Rats

Introduction

Lipid peroxidation induction potential of plumbagin was assessed as product of reaction between malondialdehyde (MDA) and thiobarbituric acid (TBA). According to research, measurement of malondialdehyde and 4-hydroxyalkenals has been used as an index of lipid peroxidation potential in membrane studies (Esterbauer *et al*., 1991). The study is to confirm peroxidation effects of plumbagin on mPTpore opening in the hepatocytes of experimental animals.

Procedure

Mitochondria isolation and incubation were done as earlier described on pages 50-53 and procedures based on the submission of Kale (1990). He estimated mitochondrial lipid peroxidation by measuring the product of thiobarbituric acid reactive substances (TBARS) present in the mitochondria derived from reaction between 2 thiobarbituric acid (TBA) and malondialdehyde (MDA) as evidence of lipid peroxides. The value is expressed:

$$\text{Lipid peroxidation} = \frac{\text{Absorbance} \times \text{volume of mixture}}{E_{532nm} \times \text{volume of sample} \times \text{mg protein/ml}}$$

Results

Results presented in Figure 4.10 show that there were dose-dependent increase in lipid peroxidation viz: 2.3, 5.8, 8.1 umole/mgprotein in the liver mitochondria of plumbagin treated rats after fourteen days of oral administration. The peroxidation is statistically significant at dose range $\geq$ 5 mg/kg body weight.

Conclusion

Increased dose of plumbagin brought about susceptibility of mitochondrial membrane to peroxidative damage (Amiesen *et al*., 2002). This is in tanderm with earlier results where plumbagin was shown to enhance lipid peroxidation and thus initiate mPT pore opening in experiment 9. Therefore, toxic effect of plumbagin can induce apoptosis in hepatocytes via

peroxidation of lipid membrane. The effect can be hearnessed in combating proliferation of diseased or primed cells.

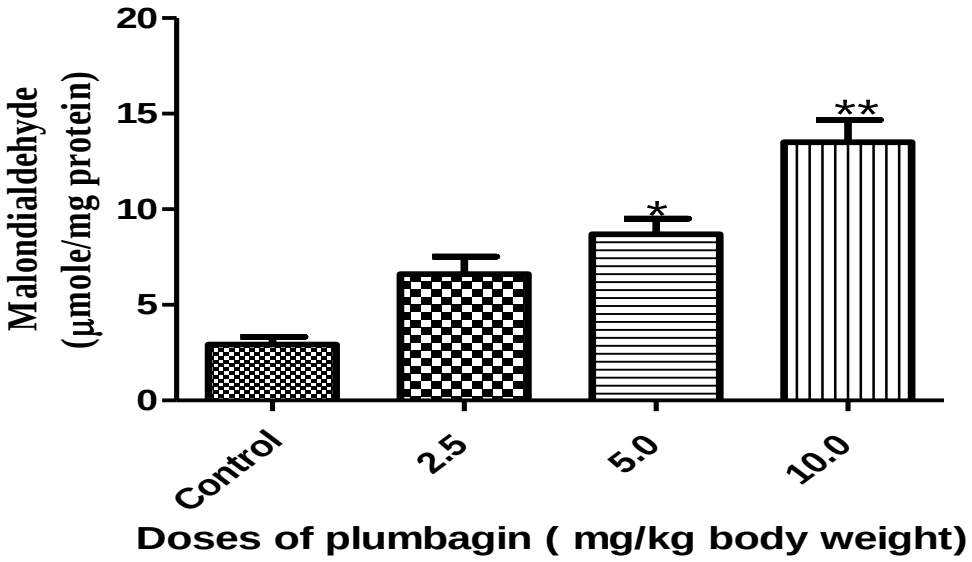

Figure 4.10: Effects of plumbagin on liver mitochondrial lipid peroxidation

*** p < 0.05, ** p < 0.01**

EXPERIMENT 11: Effects of Plumbagin Oral Administration on Caspase 9 Activity in Testicular Mitochondria of Wistar Rats

Introduction

This experiment sought to quantify the activity of caspases 9 (an initiator caspase) activation by varying doses of *Plumbagin* using testicular post-mitochondrial fraction. The principle employed is the ELISA technique where binding of specific antigen to a target antibody is conjugated to a TMMB (3,3,5,5-tetramethylbenzidine) substrate.

Procedure

As previously described on page 60 in section 3.10.7 (chapter 3) the testicular homogenate was incubated and further experimental procedures were guided by the manufacturer's instructions. The Elabscience kits consisting of samples and standard (50/50 µL) were added to wells in successions in a microplate, wrapped in seal and incubated for an hour at 25^0C in a plate shaker set at 400rpm: The wells were repeatedly washed to eliminate unbound materials. The next step was the introduction of 100 µl TMB substrate incubated for 10 minutes and allowed to yield blue colour. A stop solution was then introduced to halt the reaction which finally transforms the colour to blue. The concentration of colour produced is a function of the amount of analyte measured at 450nm using spectrophotometer.

Activity, µmol pNA/min/ml = OD x d /ε^{mM} x v x t

Where $\varepsilon = 10.5$

V= volume of sample in ml

d= dilution factor

t= reaction time in minutes

Results

Results presented in Figure 4.11 indicate that Caspases 9 activities in the experiment were expressed as 6.7, 8.4 and 11.8 folds for 2.5, 5.0 and 10.0 mg PL /kg body weight respectively. The activity is statistically significant for all treated groups compared to control (untreated).

Conclusion

Dose-dependent increase in caspase 9 activity is an indication that apoptosis is initiated by plumbagin in the testes of Wistar rats as a result of its administration, since caspase 9 is an initiator caspase in the apoptotic pathway. It is enhanced by dose-dependent administration of *Plumbagin* in the experimental animals. Hence, the potential for apoptosis is increased with increasing doses of *Plumbagin* in the testicular cells (Li *et al*., 2017).

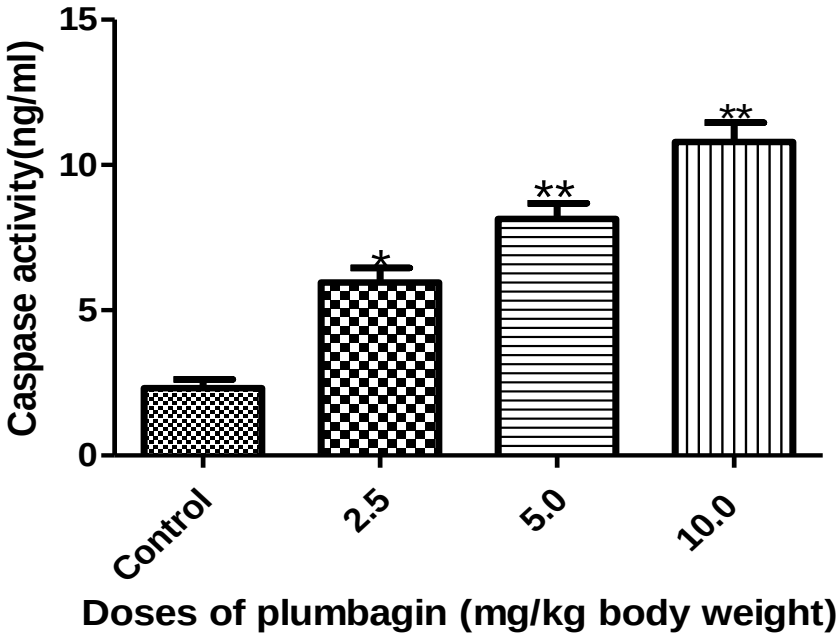

Figure 4.11: Effect of plumbagin on testicular caspase 9 activity in Wistar rats

*** p < 0.05, ** p < 0.01**

EXPERIMENT 12: Effect of Plumbagin Administration on Caspases 3 Expression in Testicular Mitochondria of Wistar Rats

Introduction

Activation of caspases 3 in the apoptotic pathway is a step in the cascade of stages involved in apoptosis. Being an apoptotic biomarker, its role in the cascade from the formation of apoptosome complex from which further reaction triggers activation of procaspase to active caspase 9 – an initiator caspase leads to recruitment of the executioner caspases such as caspases 3, 7 and 10. Hence, caspase-3 is involved in the final stage precipitating the entire cell to aggregates of apoptotic bodies. Therefore, it exerts prominent role in executing apoptosis thus it is referred to as executioner caspase particularly in the intrinsic pathway of cell demise (Xu *et al.*, 2016).

This experiment sought to quantify the activity of caspases 3 (an executor caspase) in the presence of varying doses of *Plumbagin* using testicular post-mitochondrial fraction and the principle similar for caspase 9 activity assessement.

Procedure

Similar procedures as earlier described in Experiment 11 were followed using the same post mitochondrial fraction homogenate for caspase 9 activity. The recorded absorbance of optical density for colour change were taken accordingly. Adopting the same formular for calculating caspase 9 activity in Experiment 11.

Results

Data obtained shows 5.0, 7.3 and 12.0 ng/ml increase in activity of caspases 3 as documented in Figure 4.12 for 2.5, 5.0 and 10.0 mg/ PL kg body weight administration respectively.

Conclusion

Experiment 12 confirms dose-dependent execution of apoptosis in the testes of experimental animals as a result of plumbagin administration. PL promotes the execution of apoptosis via the intrinsic pathway (Sinha *et al.*, 2003).

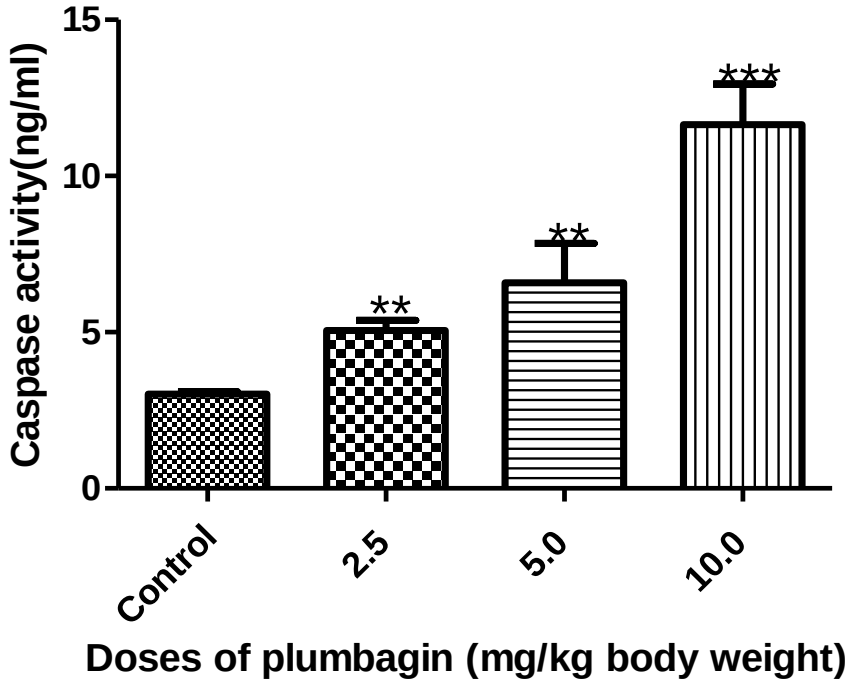

Figure 4.12: Effect of plumbagin on caspase 3 activity in testes of Wistar rats

****p<0.01 *** p<00002**

EXPERIMENT 13: Effect of Plumbagin on Caspase 9 Activity in Liver of Wistar Rats

Introduction

Caspase 9 is an initiator of cell death and a biomarker playing crucial role in the intrinsic pathway of the entire apoptotic cascade. Caspase 9 sets the stage for executioner caspases to facilitate aggregation of apoptotic bodies. Therefore, decline in the preponderance of hepetocytes population is evidence that apoptosis has been taking place as this may not likely occur in active healthy hepatocytes (Bejarano *et al.,* 2018).

The principle involved is as stated for caspase 9 activity using testicular post mitochondrial fraction of Wistar rats in Experiment 11.

Procedure

The isolation and preparation of post mitochondrial fraction of liver homogenate followed steps highlighted in Experiments 11 and 12. The assessment of caspase activity remains the same pattern used previously. Reading of absorbance for caspase 9 were taken accordingly and the formular for calculating caspase-9 activity is stated below:

Caspase-9 Activity in µmol pNA/min/ml = OD x d /ε^{mM} x v x t

Where $\varepsilon = 10.5$

V= volume of sample in ml

d= dilution factor

t= reaction time in minutes

Results

Figure 4.13 shows caspase-9 activity of 7.0, 12.0 and 16.0 ng/ml for 2.5, 5.0 and 10.0 mg/kg body weight of plumbagin administration in liver of experimental animals respectively. The activity was statistically significant at $\geq$ 5 mg / PL kg body weight.

Conclusion

Dose-dependent increase in caspase-9 in the experiment is an indication that apoptosis is promoted by initiating the cascades of events culminating to execution of the entire cell. Hence, increase in caspase 9 activities is to initiate apoptosis in the hepatocytes of wistar rats as a result of plumbagin administration and this is useful in disease conditions to get rid of diseased or malignant cells by promoting cell death (Bratton *et al*., 2010).

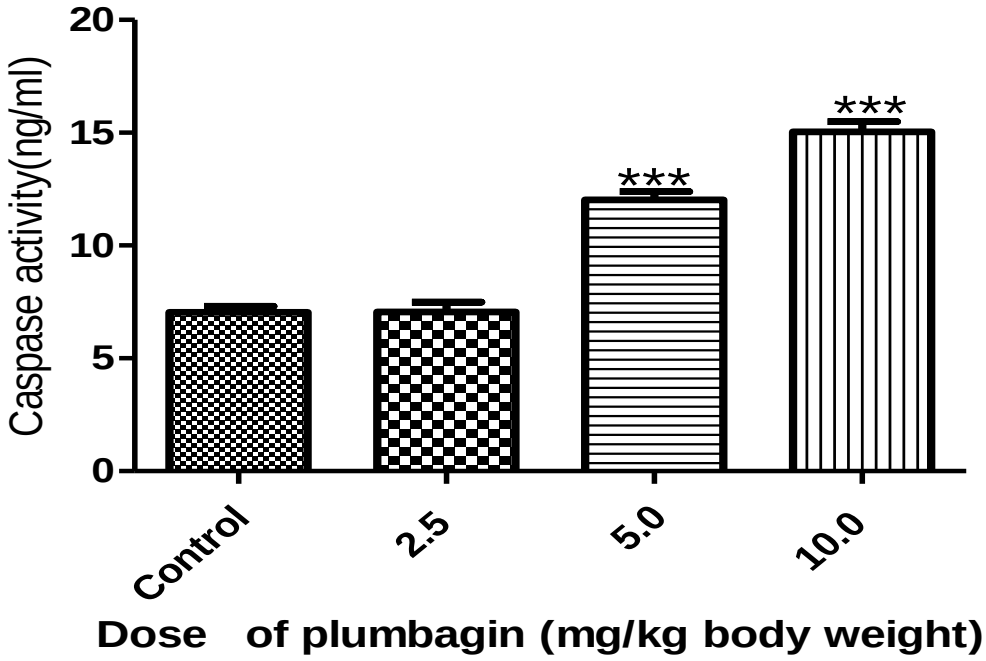

Figure 4.13: Effects of plumbagin on liver caspase 9 activity

*** p<0.001

EXPERIMENT 14: Effects of Plumbagin on Caspase -3 Activity in Liver of Wistar Rats

Introduction

As part of feature in apoptotic process, caspase-3 activity when unregulated pave avenue for indiscriminate cell death according to Boatright and Salvesen (2003). The executioner caspase-3 is inactive until it is cleaved by the initiator caspase while the activation of the extrinsic event triggers the hallmark caspase cascade where it plays dominant role.

Procedure

The procedures are the same as described in experiment 12 for caspase 3 activity in the testes. ELISA kits were used in line with manufacturer's instructions upon the isolation of liver, washing, homogenization and centrifugation at 8,000 rpm and freezing of homogenate supernatant for two days. The yellow colour product obtained was measured at 450 nm in a microplate reader and the stated formular in experiment 13 used for the calculations.

Results

Experiment 14 data and result presented in Figure 4.14 shows that caspase-3 activity in liver stands at 0.017, 0.028 and 0.031 ng/ml for doses of 2.5, 5.0 and 10 mg/kg body weight of plumbagin respectively. The activity was statistically significant at 5 and 10 mg/kg PL body weight.

Conclusion

The experiment shows that caspase - 3 activity was promoted in liver mitochondria of Wistar rats with dose-dependent increase in plumbagin administration. Hence, potential to execute cell death increases with elevated doses of PL administered.

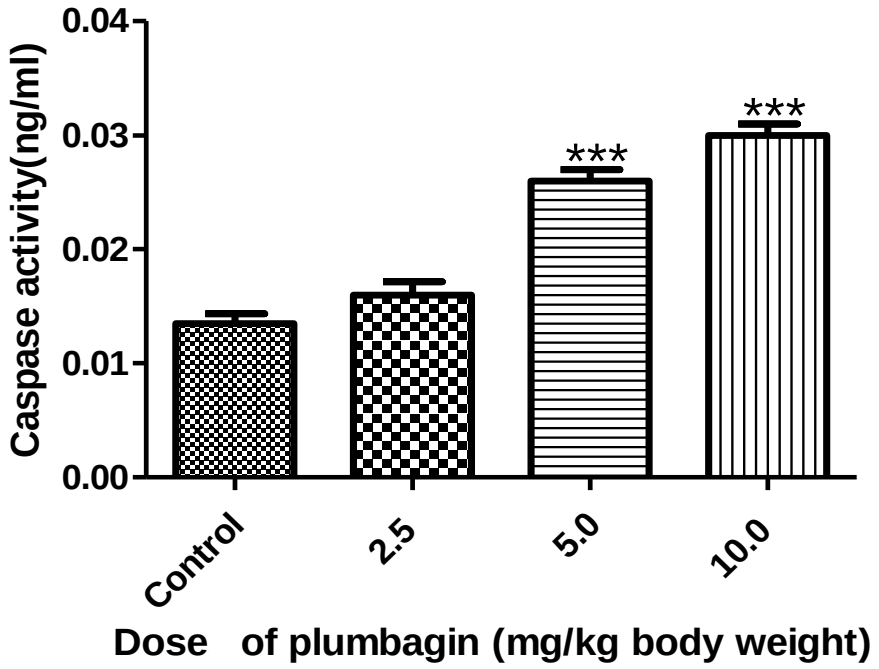

Figure 4.14: Effects of plumbagin on liver caspase-3 activity

***** p<0.001**

EXPERIMENT 15: Assessment of the effect of varying doses of *Plumbagin* on reproductive parameters

Introduction

Although, it is well known that *Plumbago Zeylanica* (PZ*)* is used in combination therapy with *Calliandra Portorinsences* (CP) in local treatment of prostate cancer. The present study aims to unravel the rationale in combination therapy employed in local treatment of prostate cancer. Hence the need to examine effect of the active compound in PZ on reproductive parameters in an attempt to understanding scientific logic in its local combination therapy with CP in treatment of prostate cancer**.**

This study investigates effect of plumbagin on male reproductive organs to determine, if plumbagin has effect on sperm count, motility, semen volume and morphology.

Procedure

Sperm analysis

Sperm sample collected from the testicular organ were examined under high power magnification.

Measurement of sperm motility

A clean dry slide was used to display drop of spem suspension. It was covered and incubated and later viewed under light microscope. The records obtained mathematically expressed *viz*:

Percentage of motile sperms = no. of motile sperms ×100% total no. of sperms (motile and immotile).

Assessement of sperm abnormalities (morphology)

Abnormal sperm viewed on light microscope as smears were inspected for deformed morphology taking to consideration: the head, neck and tail. The data were presented using the formula:

$$\% \text{ of abnormal sperms} = \frac{\text{no. of abnormal sperms} \times 100\%}{\text{Overall no. of normal and abnormal sperms}}$$

Results

Except for Figure 4.15 where the mean live/dead volume apparently shows no significant change, Figure 4.16 showed declined difference in sperm motility by 80.1, 78.3, 77.6% and Figure 4.17 features reduced sperm count (63, 61, 62.5 ml/milllitre) in PL treated Wistar rats with varying doses when compared with standard /control group. Sperm motility and count were statistically significant for all treated group compared to control as shown in Figures 4.16 and 4.17. Table 4.1 also presents details of sperm morphology expressed as mean $\pm$ S.D.

Conclusion

Increased dose of PL decreased sperm counts and sperm motility as a result of increasing apoptotic activity in the testicular cells to reduce sperm population and thus decrease fertility potential. It was clearly observed that there was dose-dependent reduction in sperm motility for all treated groups and decreased sperm count was observed as well. This implies that at higher doses of plumbagin, sperm potential to move and penetrate the ovum would be retarded and this may affect fertility. It is pertinent to note that the mean volume of sperm remains unchanged and thus unaffected in all animals.

Sperm morphology examination revealed that there were increased abnormal sperm cells particularly in all treated groups compared with the control. This morphological disorder may be as a result of plumbagin toxic effects and its anti-fertility properties.

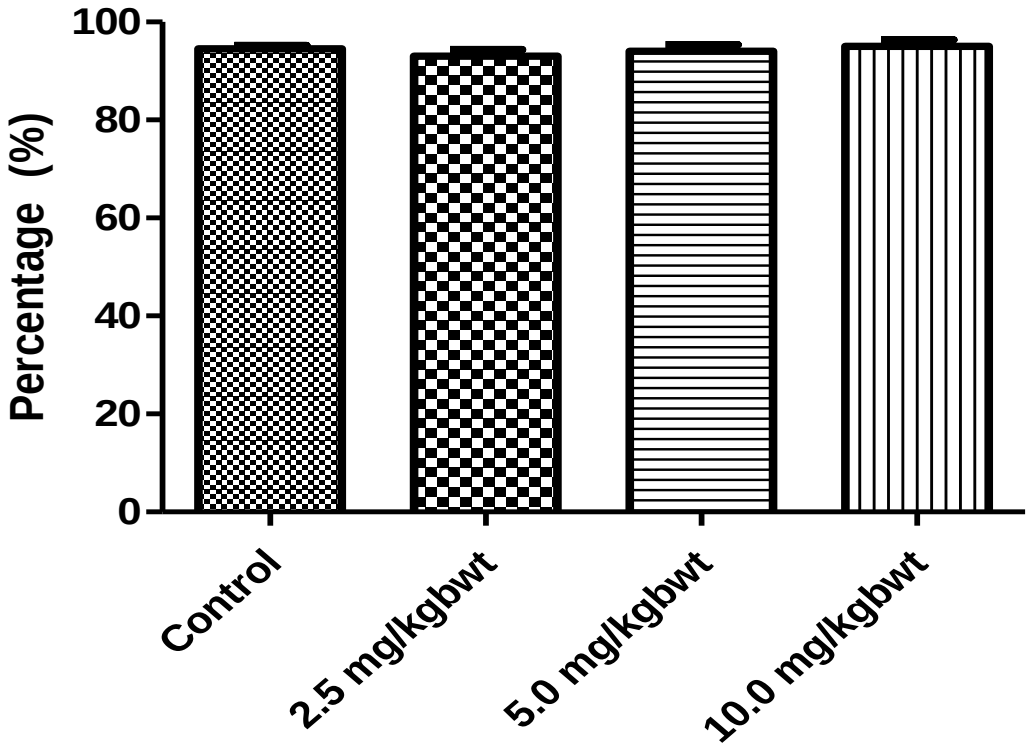

Figure 4.15: Effects of varying doses of plumbagin on mean volume of sperm.

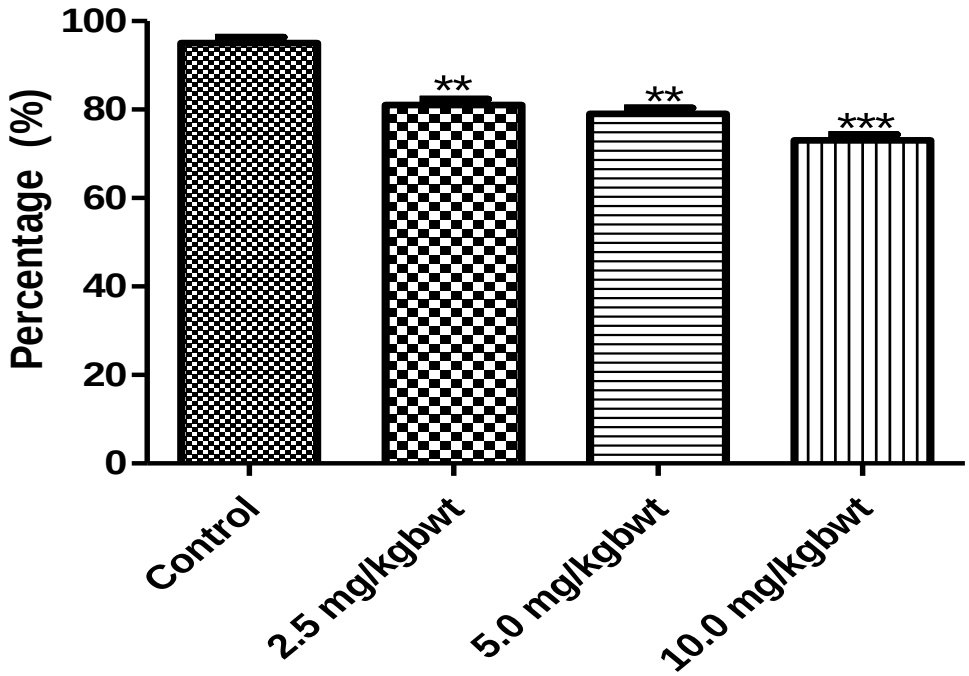

Figure 4.16: Effects of varying doses of plumbagin on sperm mean motility.

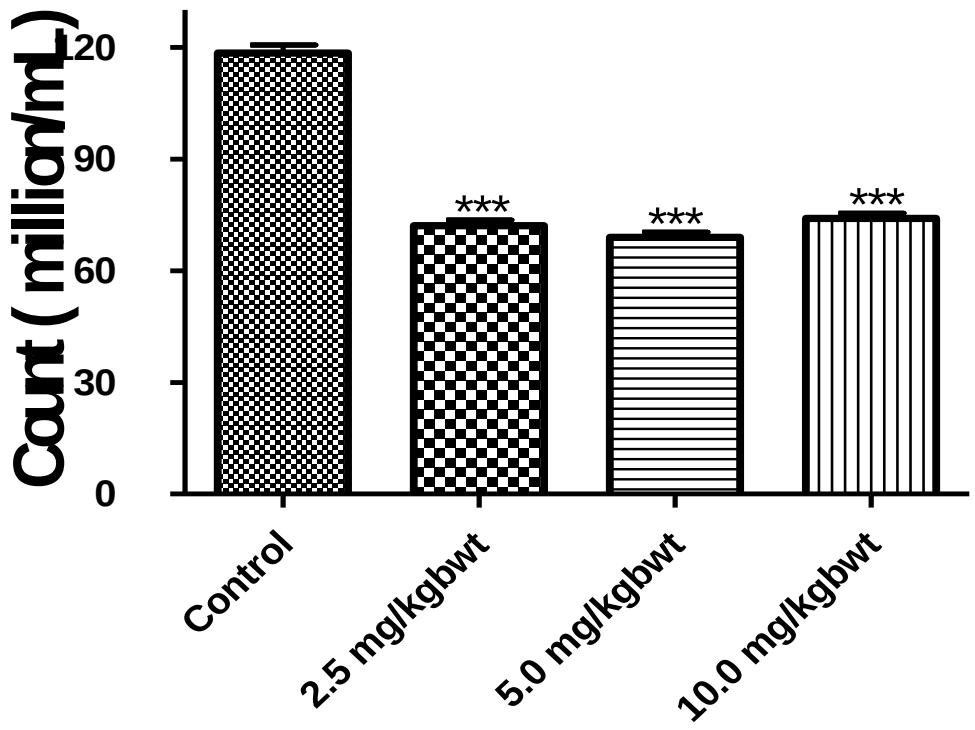

Figure 4.17: Effects of varying doses of plumbagin on mean count after oral administration

Table 4.1 Effect of plumbagin on sperm morphology

Sperm morphology	Control (M/ml)	2.50mg/kg(M/ml)	5.00mg/kg(M/ml)	10.00mg/kg(M/ml)
Tailless head	**5.00 ± 0.45**	**5.40 ± 1.31**	**6.30 ± 0.51**	**7.50 ± 0.69**
Headless tail	**3.33 ± 0.57**	**3.40 ± 0.67**	**4.60 ± 0.63**	**5.00 ± 0.00**
Rudimentary tail	**2.30 ± 1.83**	**3.10 ± 0.00**	**3.46 ± 0.60**	**2.30 ± 0.00**
Bent tail	**6.45 ± 0.47**	**6.58 ± 1.41**	**9.70 ± 0.81**	**11.50 ± 0.81**
Curved –tail	**9.32 ± 0.67**	**9.04 ± 1.31**	**11.60 ± 0.41**	**10.00 ± 1.61**
Bent mid- piece	**7.35 ± 0.57**	**11.50 ± 0.60**	**11.00 ± 0.00**	**10.00 ± 0.00**
Curved mid-piece	**7.40 ± 1.00**	**13.60 ± 0.70**	**12.46 ± 0.71**	**11.00 ± 1.22**
Looped tail	**1.57 ± 1.25**	**2.70 ± 0.81**	**3.00 ± 0.00**	**3.50 ± 0.71**
Total cell	**409.33 ± 2.98**	**415.00 ± 0.20**	**403.00 ± 7.06**	**404.50 ± 3.84**

Result expressed as mean ± S.D, statistically significant value at $P < 0.05$

EXPERIMENT 16: Effects of Plumbagin on AST and ALT in Rat Liver

Introduction

Liver function tests were done by assessing the levels of Aspartate aminotransferase (AST), and Alanine aminotransferase (ALT) activities with the aid of Randox Kits (Randox Laboratories, United Kingdom). These liver enzymes were measured in order to examine if their expressions were affected as a result of plumbagin administration in the hepatocytes.

When there is an increase in level of expressions of these enzymes, it may be indicative of toxic effect bearing in mind that the liver is the center of drug metabolism. Hence, the need to conduct this study.

Procedure

Determination of AST Enzyme Activity

Enzyme activity were measured in serum. The test was done using Randox kits product of Randox Laboratories Ltd, United Kingdom.

The activity was measured in terms of the concentration of oxaloacetate hydrazone formed with 2,4-dinitro phenyl hydrazine according to Schmidt (1963). In similar way, Aspartate amino transferate is measured by evaluation of the concentration of oxaloacetate hydrazone formed with 2,4-dinitrophenylhydrazine - DPNH (Reitman and Frankel, 1957).

The enzyme AST specializes in transfer of amino group from L-aspartate to α-oxoglutarate to form L-glutamate and oxaloacetate. However, oxaloacetate formed is an unstable complex and is converted to pyruvate and then complexed with 2,4-dinitrophenylhydrazine (DPNH) to produce a deep coloured hydrazone complex on the addition of NaOH. This coloured complex absorbs light at 530-550nm.

α-oxoglutarate + L-aspartate → L-glutamate + oxaloacetate

serum (0.1ml) was mixed with 0.5 ml of reagent I. the mixture was allowed to incubate for 30 minutes at a temperature of 37^{o}C.

In the next step, 0.5 ml of reagent II was added to the reaction mixture and also incubated for about 20 minutes and maintained at 25^{o}C. In the final step, 5 ml of NaOH was added and the absorbance was taken 5 minutes afterward at 546nm against blank using in Camspec M105 Spectrophotometer.

Activity was determined from absorbance read and extrapolated from the standard Table to get the Units/Litre. For linearity, the absorbance that exceeds 0.170 from the Standard Table, there will be a reassay by diluting 0.1 ml of sample with 0.9 ml of 0.9% NaCl solution and the absorbance is then multiplied by 10.

Measurement of ALT Activity

The quantitative determination of Alanine aminotransferase (ALT) in serum was carried out. The activity was determined as a product of intense colour of hydrazone produced on addition of NaOH because the initial oxaloacetate formed is unstable and it is decarboxylated to pyruvate afterward complexed with 2,4-dinitriphenylhydrazine (DPNH) to produce an intensely coloured hydrazone on the addition of NaOH. This coloured complex absorbs light at 530-550nm.

Reagent I (0.5ml from the kit) and 0.1ml distilled water were incubated for half an hour at 37^{o}C this was preceded by addition of 0.5 ml of reagent II and allowed to remain for 20 minutes and maintained at 25^{o}C. It was followed by addition of 5ml NaOH. The Campsec M105 Spectrophotometer was blanked at 546nm after 5 minutes.

Sample serum (0.1ml) was mixed with 0.5ml reagent I and the mixture were allowed to stand for half hour at 37^{o}C. Reagent II (0.5ml) were added to the mixture and allowed to stand for 20 minutes at 25^{o}C. NaOH was added and absorbance read against blank after 5 minutes at 546 nm.

Results

Figure 4.18 shows increased levels of AST (27, 39 and 43 IUL) for 2.5, 5.0 and 10 mg/kg body weight of plumbagin respectively. Similarly, ALT activity in Figure 4.19 was 41, 58 and 63 IUL for 2.5, 5.0 and 10.0 mg/kg body weight of plumbagin doses respectively.

Conclusion

Since enzyme activities (AST and ALT) were elicited at higher doses of plumbagin. It shows that higher doses will increase enzyme activities in response to toxic effects of the drug (PL) in the hepatocytes. Therefore, increased doses of plumbagin may tend to exert toxic burden to the liver leading to damage in the hepatocytes- the site of drug metabolism in which the mitochondria are actively involved. This is in agreement with previous results of Experiments 14 and15 revealing that increasing doses of plumbagin elicited toxic effects on the reproductive machinery.

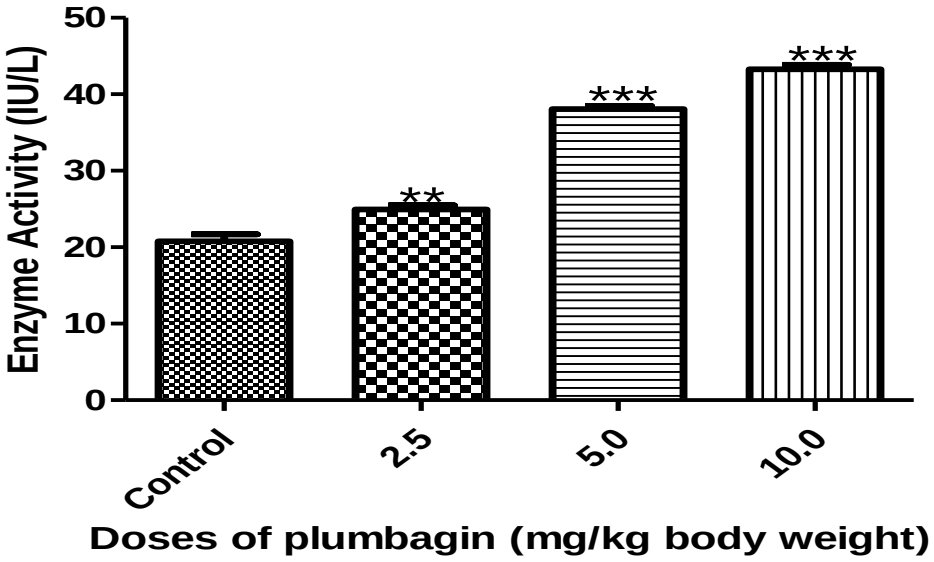

Figure 4.18: Effect of Plumbagin on AST activity

**** p < 0.01, *** p<0.001**

Result is statistically significant at p<0.01 and p <0.001

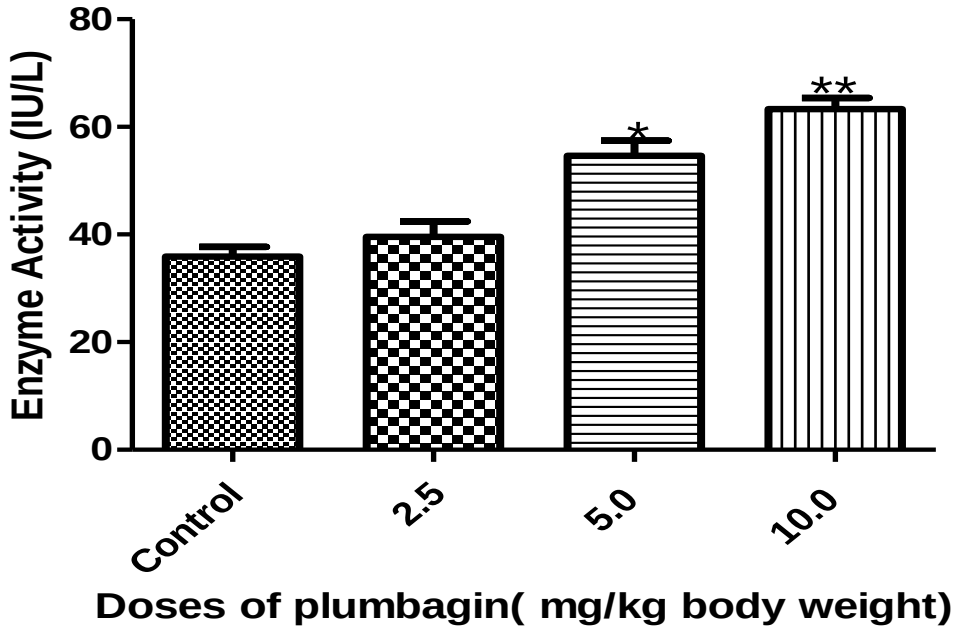

Fig 4.19: Effects of plumbagin on ALT activities after oral administration

* $p < 0.05$, ** $p < 0.01$

EXPERIMENT 17: Histological Examination of Testes on Oral Administration of Plumbagin

Introduction

In quest to assess effects of plumbagin on reproductive machinery of the animal model an experiment was designed to examine how the testicular cells are being affected as a result of varying doses plumbagin administration also considering that in previous experiments plumbagin shows propensity to promote apoptosis.

Histopathology is concerned with the study of the microscopic changes in diseased tissues. The aim of this experiment was to examine if there will be any visible lesion in the testis and liver of treated rats.

Procedure

Testicular and hepatic tissues were isolated and preserved in Boins solution and 10% formalin respectively. Grossing was carried out by cutting part of tissue into fragment about 3-4mm thick and fixed in 10% formalin for 24 hours.

Automatic Tissue Processor - Leica TP 1020 (ATPL-1020) was used to dehydrate tissue samples through stations (I & II) and levels of ethanol: 70%, 80%, 90%, 95% and absolute stations. They were also passed through xylene- containing stations 8 and 9 as they were transferred between three wax bath to facilitate infiltration and impregnation spending an hour in each station while machine works constantly for 12 hours.

The next stage is the embedding process using paraffin wax for reinforcement of tissue sample in a semi automated tissue embedding centre. Here the tissue was dipped in molten paraffin wax and pre-labelled cassettes placed on them. They were then cold to harden them into blocks which are separated out as tissue block from the mould.

Microtomy involving the use of Rotary microtome (6 µm) was employed to expose tissue surface area to cooling on ice and sectioned at 4 µm. The labelled slide was used to section on water bath at 55^{o}C.

The sectioned sample was dried by dehydration at 60^{0}C over hotplate for 60 minutes.

The sample finally stained by the modified method of Halmi known as hematoxylin (H) and Eosin (E) staining technique and viewed under microscope.

Results

Results presented in Figures 4.20 a-b and 4.21c-d show effects of PL on testicular histology. The 2.5mg/kg body wt group showed mild congestion (green arrow) of the interstitial spaces. The 5mg/kg body wt group showed multiple seminiferous tubules with vacuolations and maturation arrest (black arrow) while the 10 mg/kg body wt group showed few atrophic tubules (red arrow). The interstitial spaces show mild congestion (green arrow) and the tunica albuginea also show moderate vascular congestions. Therefore, histology results on testes show dose-dependent alterations in testicular architecture with increased vascular congestion and maturation arrest at the peak of treatment (10 mg/kg body wt plumbagin).

Conclusion

Histology results (Figures 4.20 a-b and 4.21 c-d) show dose-dependent alteration of the testicular ultra structure which ultimately proves the toxic impact of PL administration on the reproductive machinery. Therefore, the entire histology result shows that PL exerts toxic effect on the testis which may cause damage to the organ thus reducing fertility potential in the reproductive cells. This also confirms the results of previous experiments (Experiments 3, 4, 5, 6, 7 and 8) respectively.

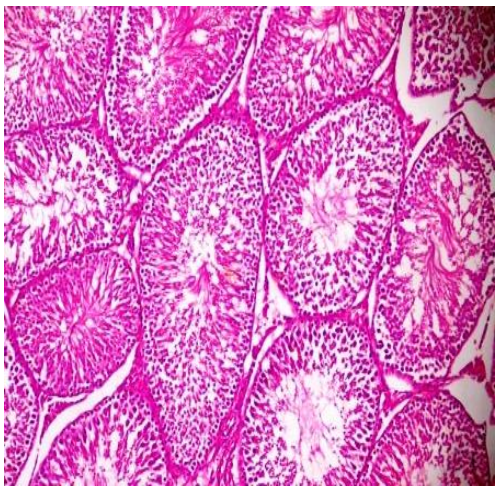

x 100 (a)

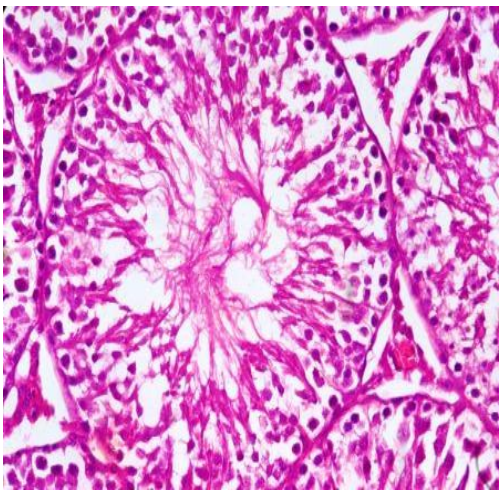

x 400(a)

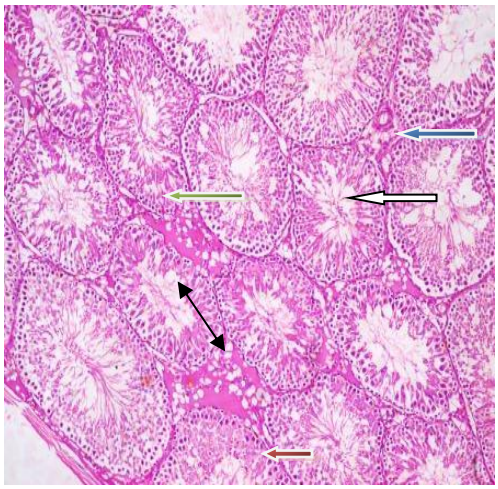

x100 (b)

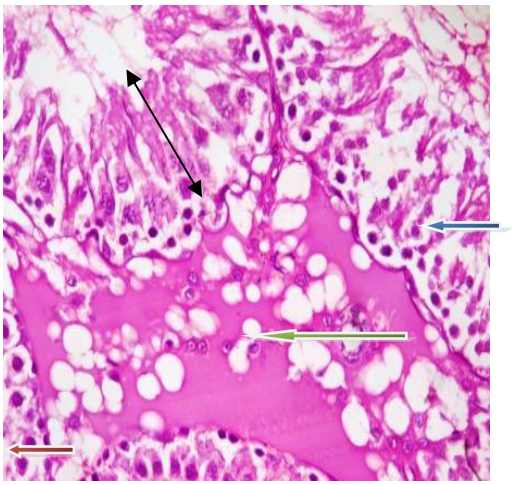

x400 (b)

Figure 4.20 a-b Showing normal to slight changes in testicular ultra structure as plumbagin dose commences from 2.5 mg/kg body wt.

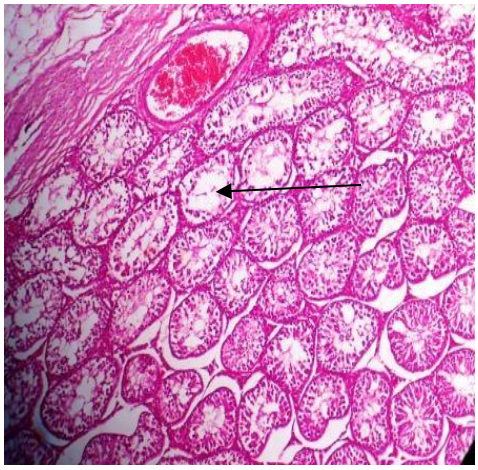

x 100 (C)

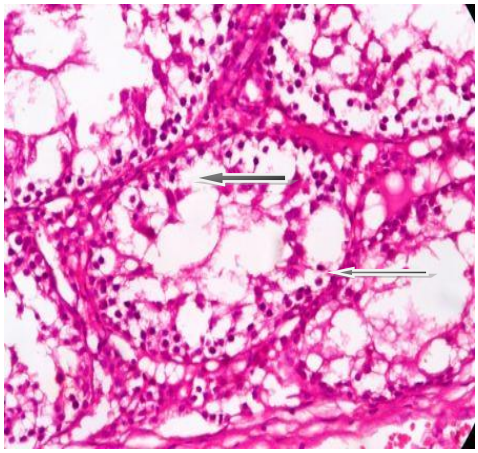

x400 (C)

x100 (d)

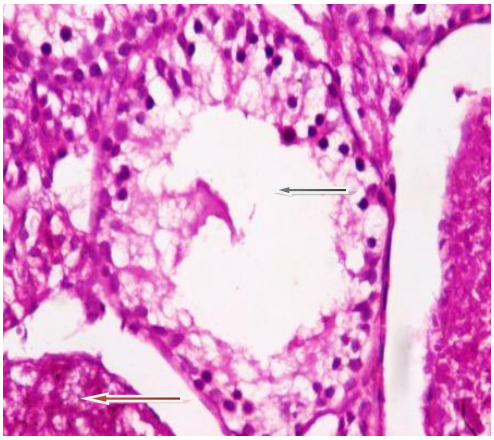

x400 (d)

Figure 4.21 c-d showing increasing vascular congestion with dose dependent alteration in testicular ultra structure from 5-10 mg/kg body weight plumbagin administration.

EXPERIMENT 18: Immunohistochemical Examination of Expresssions of Apoptotic Biomarkers in Testes of Wistar Rats

Introduction

Apoptotic biomarkers play essential roles in the cascades of reactions culminating in the consequential aggregation of cells into apoptotic bodies. They are players in the intrinsic pathways involving the mitochondria. These includes: p53, Cytochrome C, Bax and Bcl-2 proteins.

The experiment examines the expressions of these proteins as a measure of the propensity of plumbagin to induce apoptosis in the reproductive machinery of the experimental animals following oral administration by the principle of immunostaining involving interaction between antigens and antibody.

Procedure

Cytochrome C, Bax, Bcl-2 and p53 expressions were evaluated by immunostaining. Immunohistology techniques utilizes exogenously labelled antibodies to target specific antigens in tissue section thereby forming antigen-antibody complex fixed on slides. Paraffin was separated by immersing slides into xylene twice for 5 minutes. Slides were further transferred to absolute alcohol for 180 seconds and passed through immersion of 95% alcohol twice with subsequent 70% alcohol once for 3 minutes separately. This was transferred into wash buffer repeatedly for five minutes and antigenic epitope exposed by executing antigenic recapturing in succeeding steps. Chromogenic colour stain of the antibody-antigen complex was examined microscopically and captured into photomicrographs. Photomicrographs of the stained coloured complex was quantified by image J and expressions statistically analysed using Graph pad prism 5 package on computer system.

The intensity of the coloured complex was quantified as level of anti apoptotic/ apoptotic protein expression and further converted to percentage by the package.

Results

Results as indicated in Figures 4.22 a-d and statistically presented in Figure 4.23 indicates that plumbagin induced dose–dependent decrease in Bcl-2 expressions by 25%, 18% and 15.5% respectively in the testes of experimental animals relative to control and since Bcl-2 is an anti apoptotic protein, its decrease relative to increasing dose of plumbagin is indicative of its potential to promote cell death via the intrinsic pathway. Moreover, results as presented in Figures 4.24 a-d and statistically analysed in Figure 4.25 shows 6.3%, 7.5% and 12.34 % increase in expressions of p53 for doses 2.5, 5.0 and 10.0 mg/kg body weight of plumbagin respectively. Thus, indicating dose-dependent increase in p53 expression.

Similarly, photomicrographs in Figures 4.28 a-d quantified and statistically presented in Figure 4.29 show dose-dependent increase in Cytochrome C release by 7.2, 8.4 and 12.3% for doses of 2.5, 5.0 and 10.0 mg/kg body wt of plumbagin administration respectively.

Lastly, Figures 4.26 a-d presents photomicrographs of Bax expressions which were quantified and statistically analysed using Graph pad prism 5 in Figure 4.27 indicate dose-dependent increase by 6.1, 7.5 and 9.5% for doses: 2.5, 5.0 and 10.0 mg/kg body wt of plumbagin administration respectively in testes of experimental animals.

Conclusion

Results of quantified photomicrographs and analysis of immunohistochemistry expressions of apoptotic biomarker in the testes of experimental animals show that pro apoptotic biomarkers- Bax, p53 expressions and Cytochrome C release were increasingly expressed in a dose-dependent manner whereas Bcl-2 anti apoptotic biomarker expressions decreased as dosage regimen increases from 2.5, 5.0 and 10.0 mg/kg body wt. respectively relative to control. It is thus unequivocally established that plumbagin induces apoptosis from the expressions and realease of these biomarkers playing significant roles in the intrinsic pathways of apoptosis (Benardi, 2018).

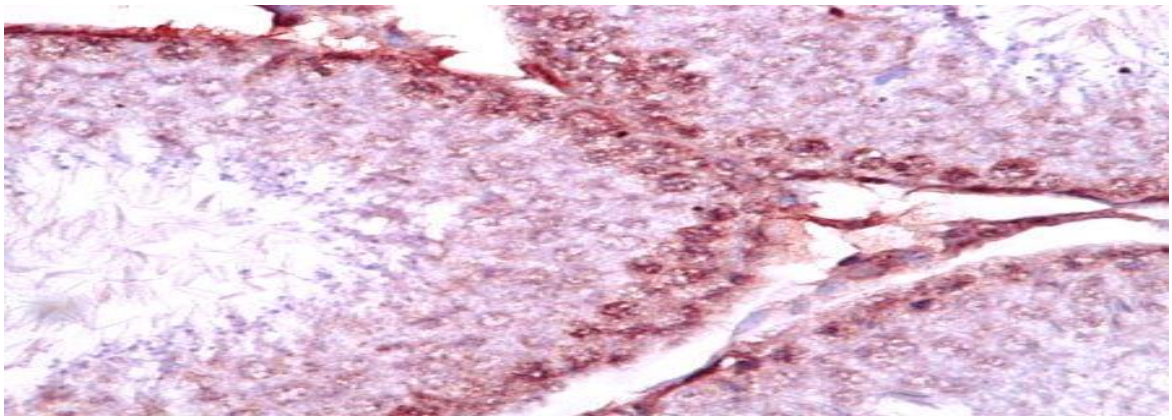

Fig 4.22 (a) x400: Representation of Bcl-2 expression in testes of normal rats (control).

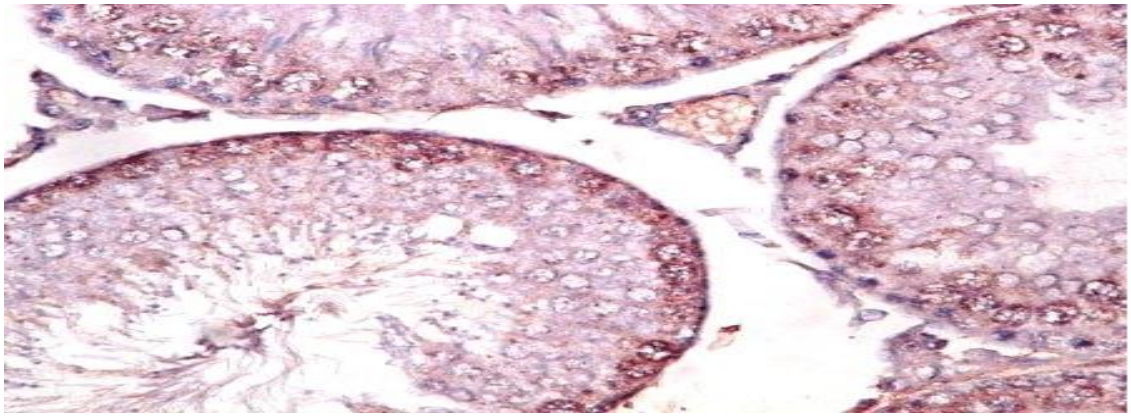

Figure 4.22 (b) x400: Effect of 2.5mg/kg body wt plumbagin on Bcl-2 expression in testes of Wistar rats.

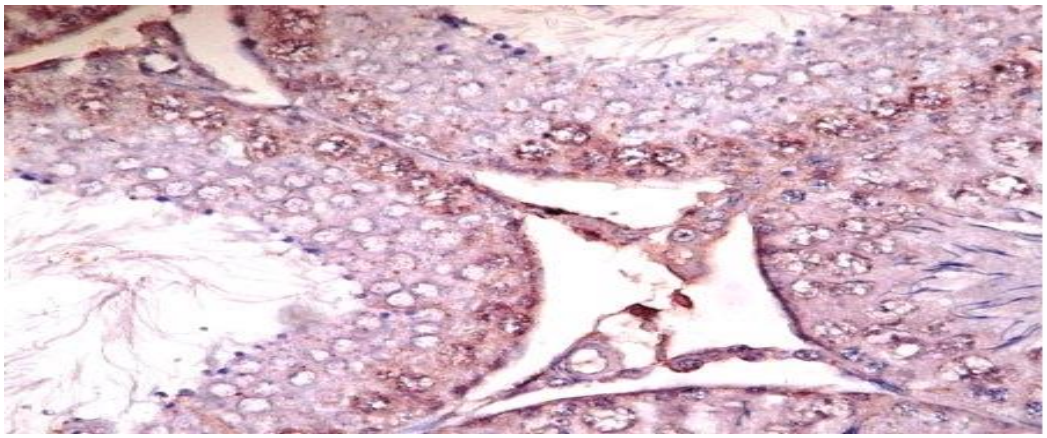

Figure 4.22 **(c)** x400: Effect of 5mg/kg body wt plumbagin on Bcl-2 expression in testes of Wistar rats.

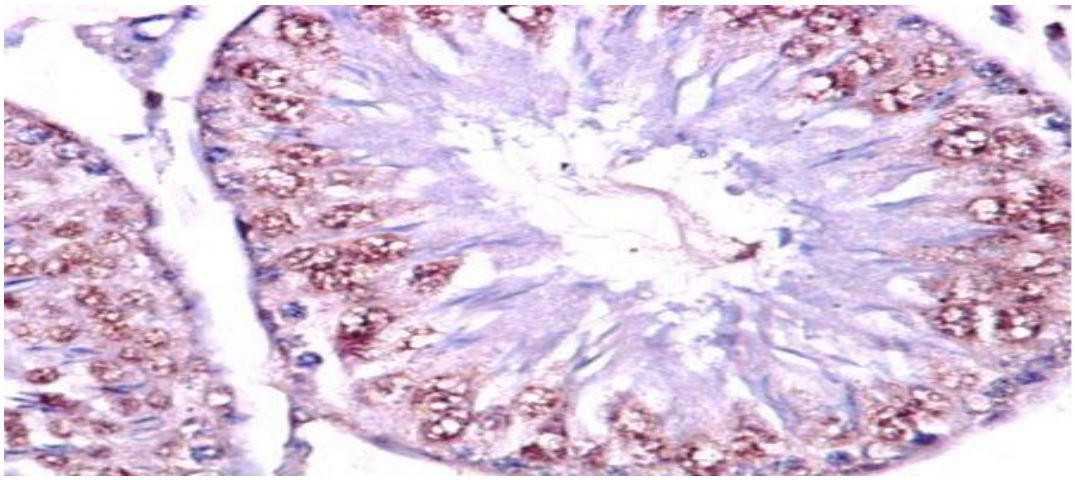

Figure 4.22 **(d)** x400: Effect of 10mg/kg bodywt plumbagin on Bcl-2 expression in testes of Wistar rats

Figures 4.22(a-d) Photomicrographs showing effects of varying doses of plumbagin on Bcl- 2 expressions in the testes of Wistar rats after 14 days of oral administration.

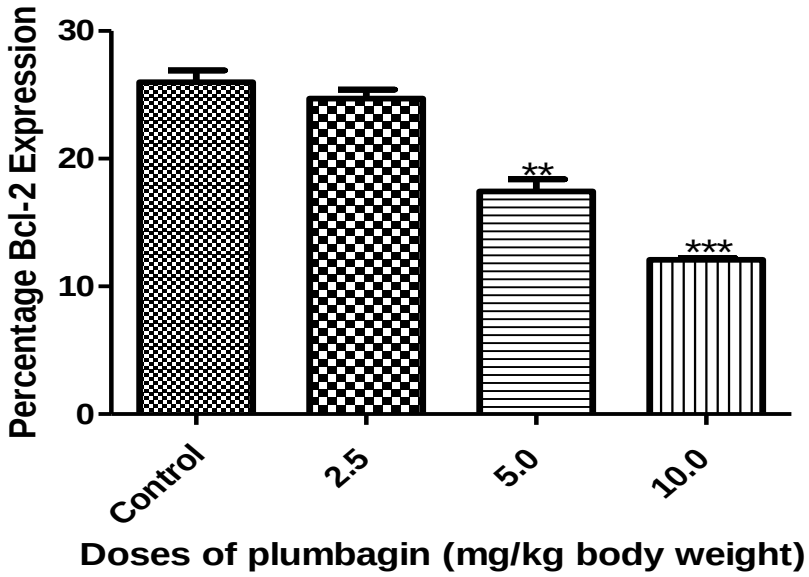

Figure 4.23: Effect of plumbagin on Bcl-2 Expression in testes of Wistar rats

*** P < 0.05, ** p < 0.01, *** p<0.001**

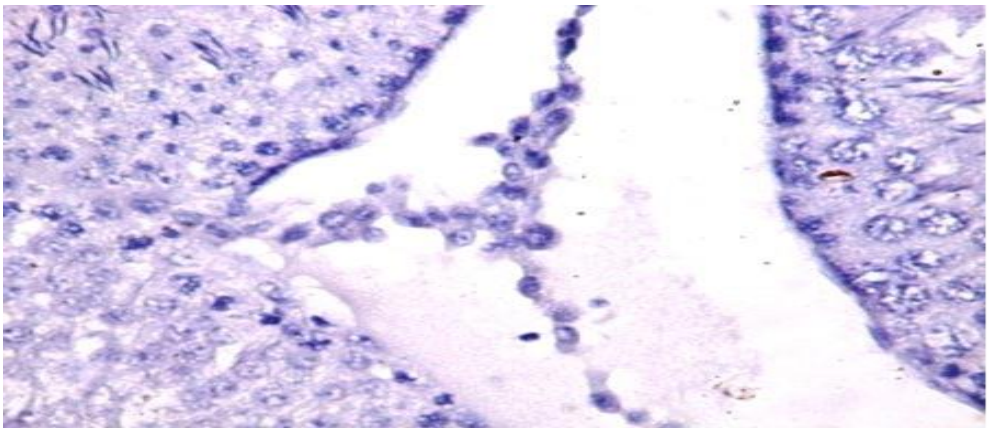

Figure 4.24 (a) x400: Expressions of p53 protein in testes of normal Wistar rats (Control).

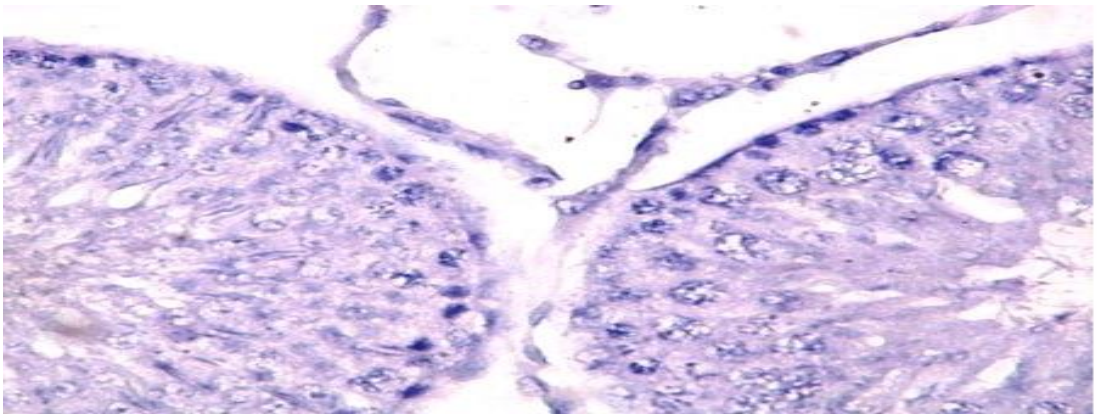

Figure 4.24 (b) x400: Effect of 2.5 mg/kg body wt plumbagin on p53 expression in testes of Wistar rats.

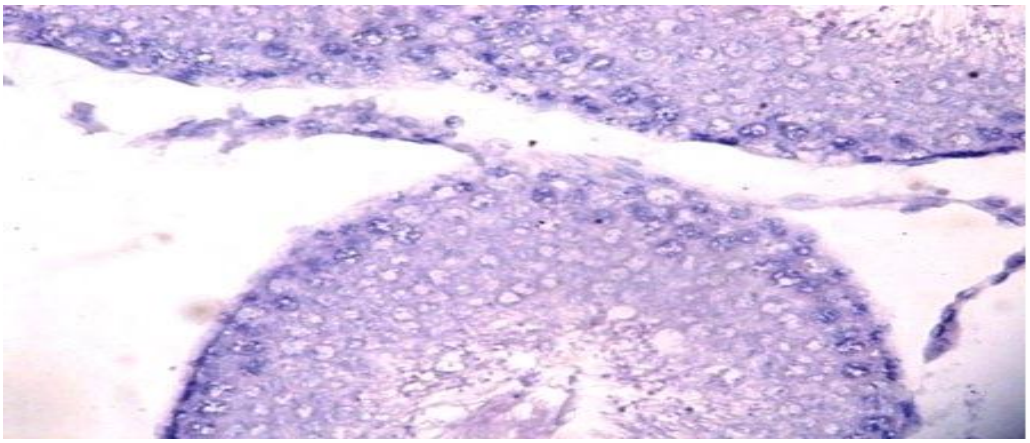

Figure 4.24 (c) x400: Effect of 5.0mg/kg body wt plumbagin on p53 expression

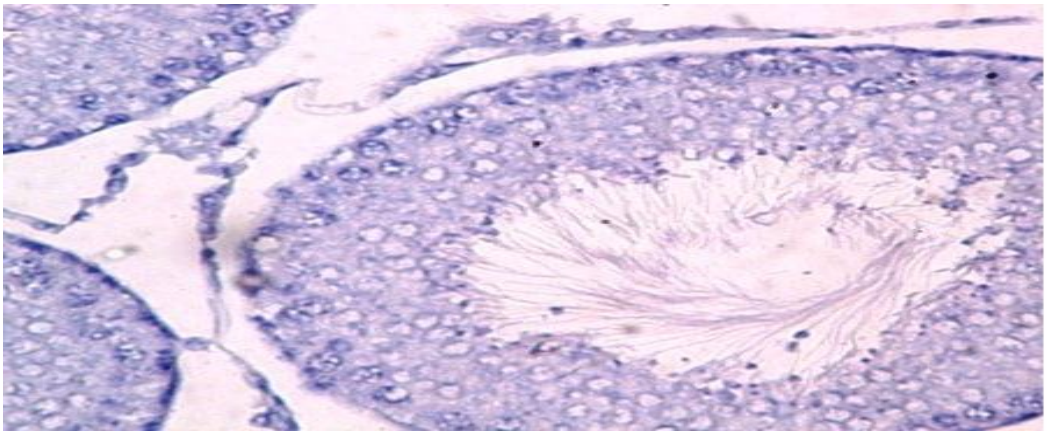

Figure 4.24 (d) x400: Effect of 10.0mg/kg body wt plumbagin on p53 expressions in testes of Wistar rats

Figures 4.24 **(**a-d): Photomicrographs showing effect of varying doses of plumbagin on p53 expression in testes of Wistar rats.

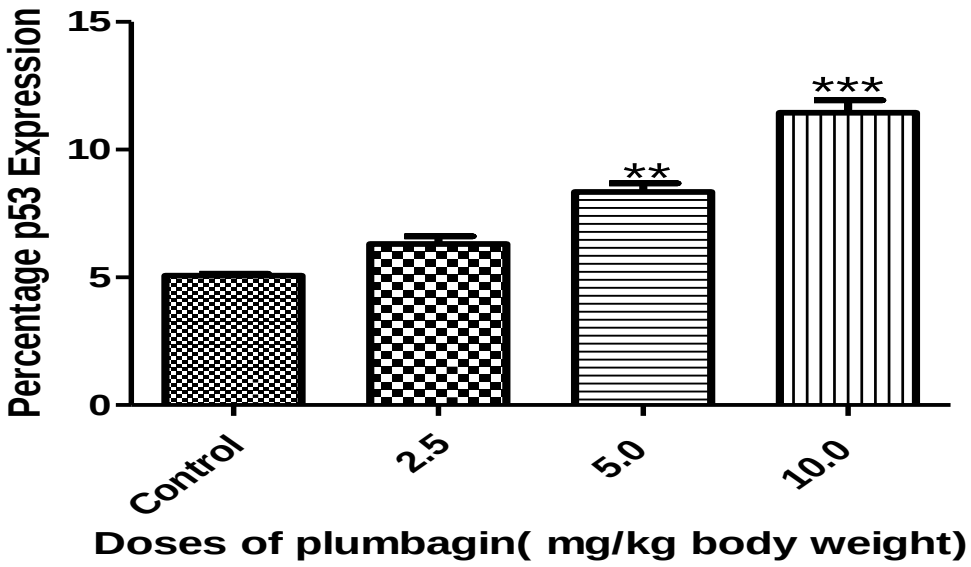

Figure 4.25: Effect of plumbagin on p53 expression in testes of Wistar rats

*** p < 0.05, ** p < 0.01, *** p<0.001**

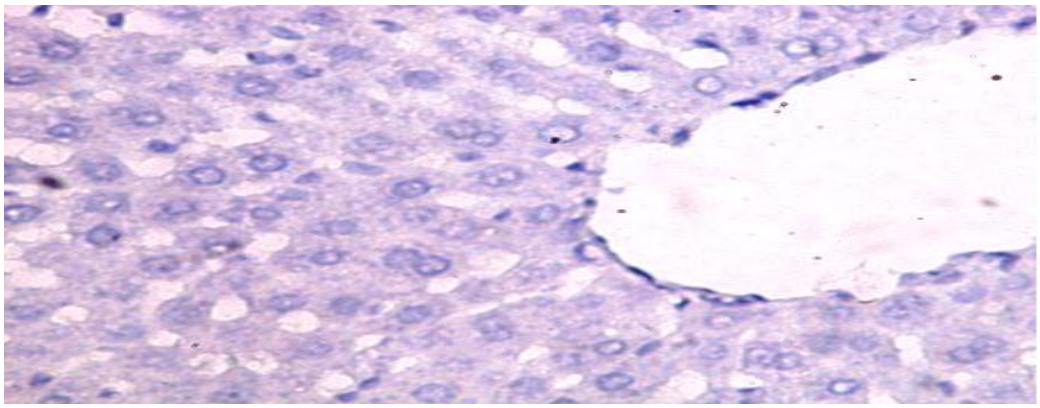

Figure 4.26 (a) x400: Bax expression in testes of normal rat (control).

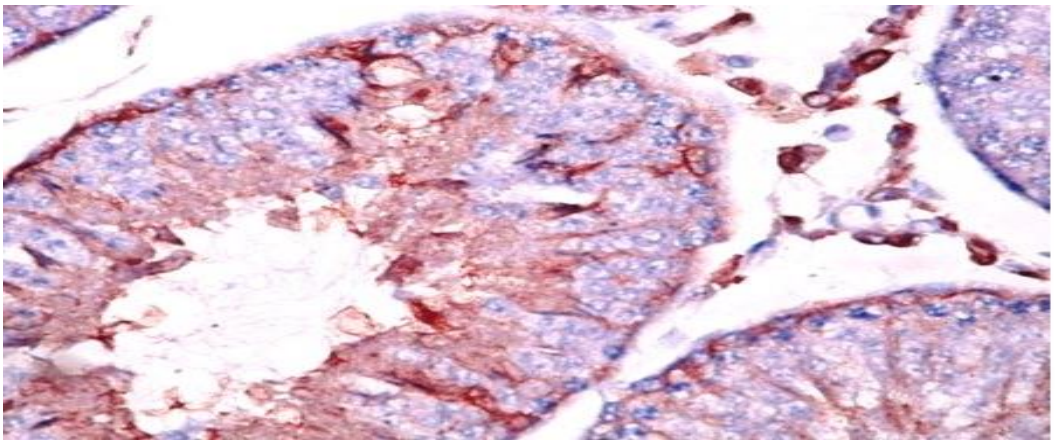

Figure 4.26 (b) x400: Effect of 2.5 mg/kg body wt plumbagin on Bax expression in testes of Wistar rats.

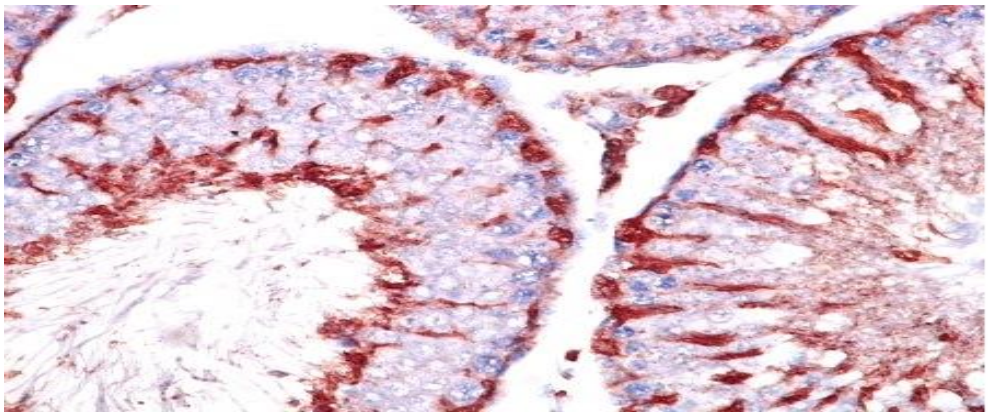

Figure 4.26 (c) x400: Effect of 5.0 mg/kg body wt plumbagin on Bax Expression in testes of Wistar rats.

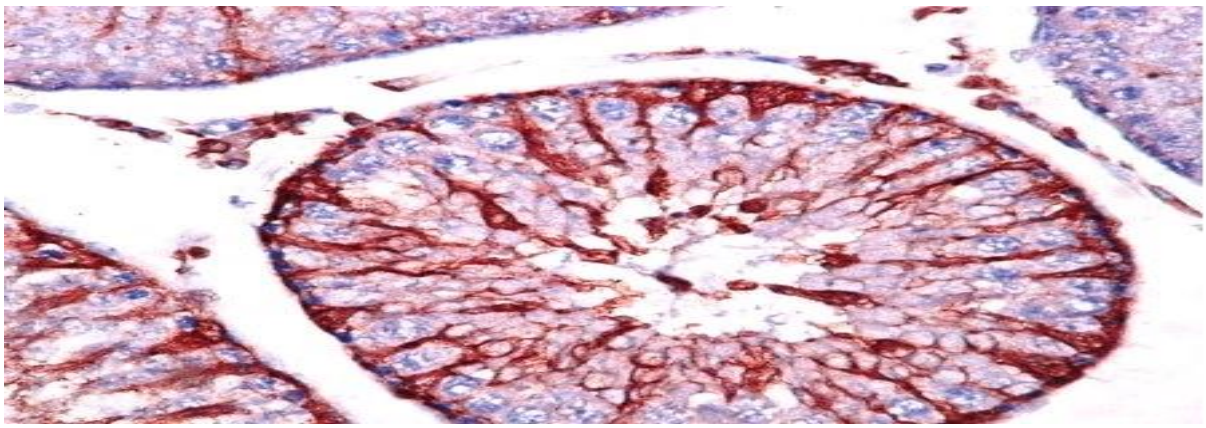

Figure 4.26 (d) x400: Effect of 10.0mg/kg body wt plumbagin on Bax expression in testes of Wistar rats.

Figures 4.26 a-d: Photomicrographs showing effects of varying doses of plumbagin on Bax expression in testes of Wistar rats.

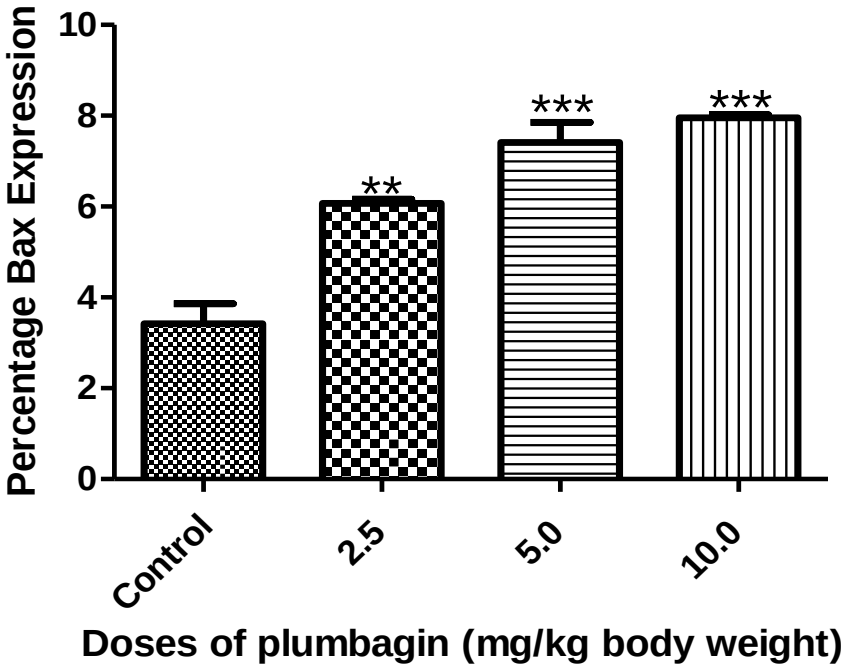

Figure 4.27: Effect of plumbagin on Bax Expression in liver

*** p < 0.05, ** p < 0.01, *** p<0.001**

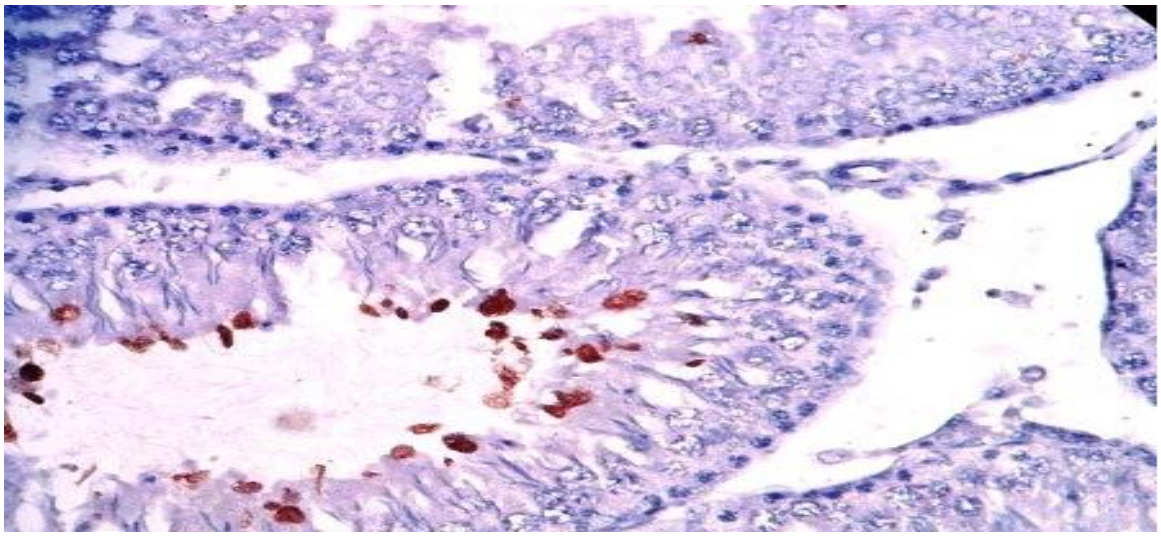

Figure 4.28 (a) x400: Cytochrome C release in testes of normal rats (control).

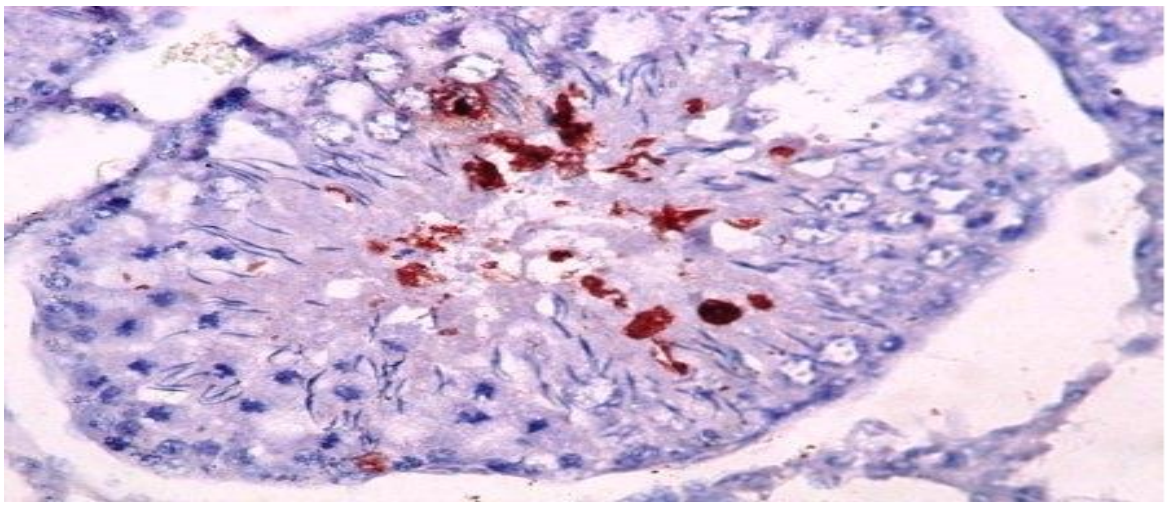

Figure 4.28 (b) x400: Effect of 2.5mg/kg body wt plumbagin on cytochrome C release in testes of Wistar rats.

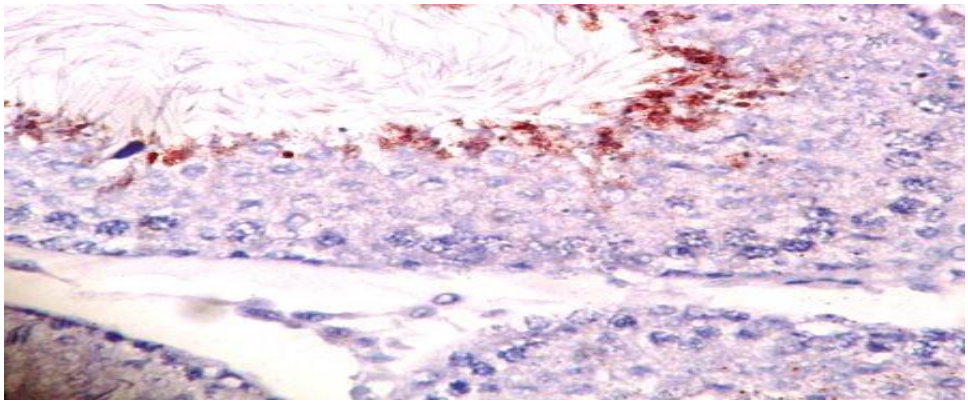

Figure 4.28 (c) x400: Effect of 5.0mg/kg body wt plumbagin on Cytochrome C release in testes of Wistar rats.

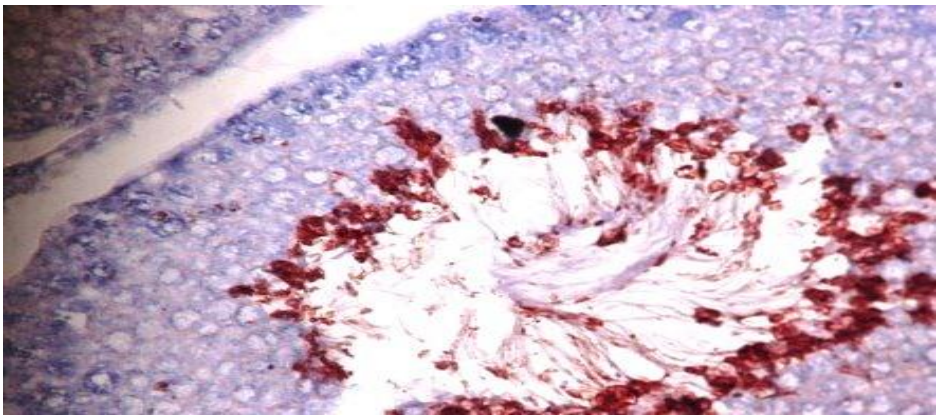

Figure 4.28 (d) x400: Effect of 10mg/kg body wt plumbagin on cytochrome C release in testes of Wistar rats.

Figure 4.28 (a-d) Photomicrographs showing effects of varying doses of plumbagin on cytochrome C release in testes of Wistar rats.

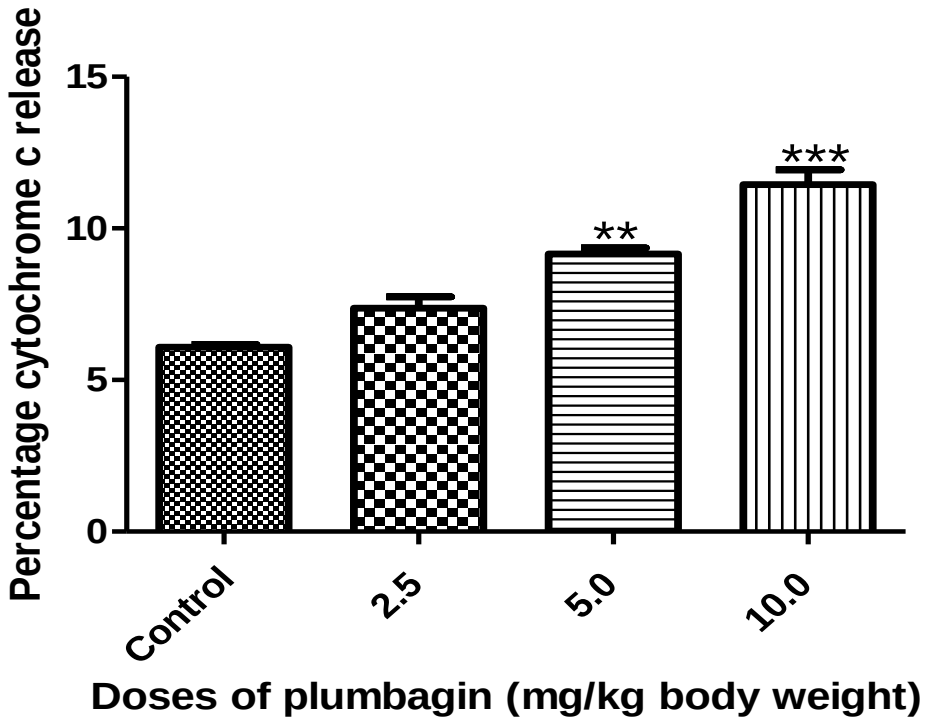

Figure 4.29: Effect of plumbagin on cytochrome C release in testes of Wistar rats

*** p < 0.05, ** p < 0.01, *** p<0.001**

EXPERIMENT 19: Immunohistochemical Examination of Expresssions of Apoptotic Biomakers in Livers of Wistar Rats induced by plumbagin

Introduction

Apoptotic biomarkers namely: p53, cytochrome C, bax and bcl-2 protein were examined to access impact of plumbagin on the experimental animals. These proteins contribute significantly in the apoptotic signaling cascades and as such their expressions determine level of commitment of cells to survival or execution.

Procedure

This involves immunostaining of deparaffinized liver sections with specific antibodies. The procedures involved are same as previously described in Experiment 18.

Results

Figures of photomicrographs, its quantification and statistical analysis are displayed and highlighted as follows to show expressions of apoptotic biomarkers in liver of experimental animals. Figures 4.30 a-d present photomicrographs of Bcl-2 expressions and Figure 4.31 depict statistical analysis of Bcl-2. The result shows dose-dependent decrease in Bcl-2 expression in liver by 36, 20 and 10% for doses of 2.5, 5.0 and 10.0 mg/kg body wt of plumbagin administration respectively.

Measure of Bax expressions quantified and statistically analysed were presented in Figures 4.34 a-d and 4.35 respectively. The Figures show that Bax expression in livers of Wistar rats increases with dose (dose-dependent). Bax expression increases in liver by 22, 27 and 31% for doses of 2.5, 5.0 and 10.0 mg/kg body wt of plumbagin respectively.

Figures 4.36 a-d show quantification of Cytochrome C release in which dose-dependent increase in Cytochrome C were observed from Figure 4.37 statistical analysis presentation vis: 17, 27 and 31% for doses of 2.5, 5.0 and 10.0 mg/kg body wt. plumbagin administration respectively. Similarly, Figures 4.32 a-d showed quantified expressions of p53. Figure 4.33 presents increasing expression of p53 in liver of Wistar rats by 22, 27 and 38% for doses of 2.5, 5.0 and 10.0 mg/ PL kg body weight administered.

Conclusion

Immunohistochemistry expressions of apoptotic biomarkers in liver of experimental animals show that pro apoptotic biomarkers and players namely: p53, Bax expressions and Cytochrome C release were all increasingly expressed in a dose-dependent manner. Moreover, Bcl-2, an anti apoptotic biomarker expression decreased as dosage regimen increases from 2.5, 5.0 and 10.0 mg/kg body wt plumbagin respectively relative to control. The result is indicative of plumbagin toxic potential on liver of experimental animals. This is similar to result obtained for the testes in experiment 18. Hence, toxic effects of plumbagin in both testes and liver induced apoptosis in the organs via the intrisinc pathway with consequential damage in the testes of experimental animals (Chengyong *et al*., 2018).

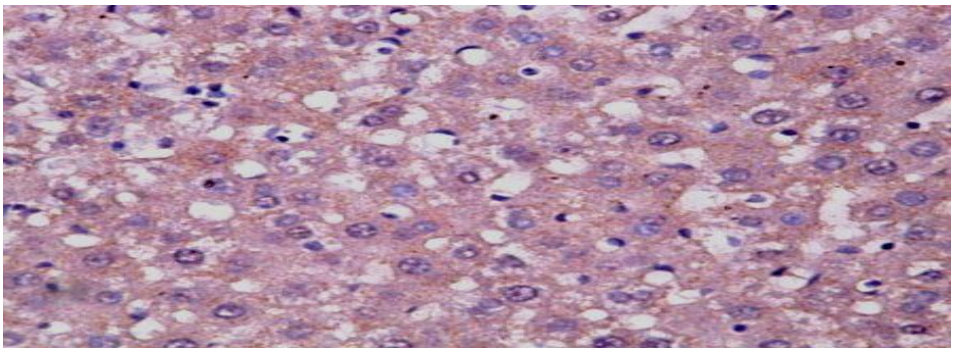

Figure 4.30 (a) x 400**:** Bcl-2 expression in liver of normal rats (control).

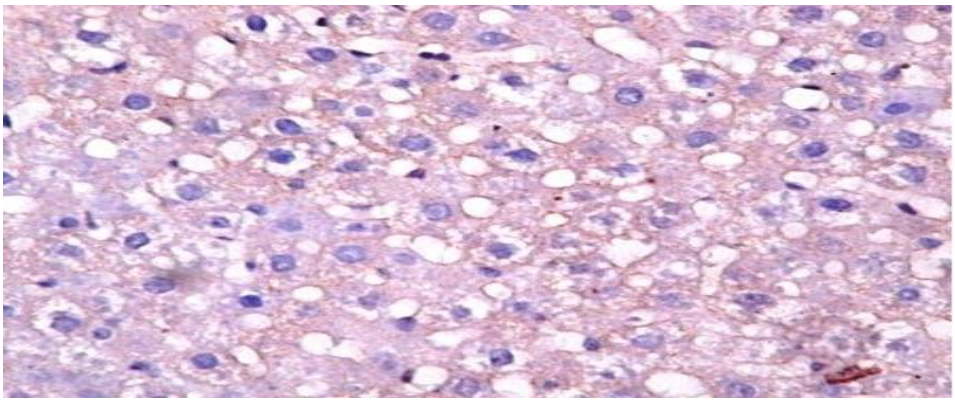

Figure 4.30 (b) x400: Effect of 2.5mg/kg body wt plumbagin on Bcl-2 expression in liver of Wistar rats.

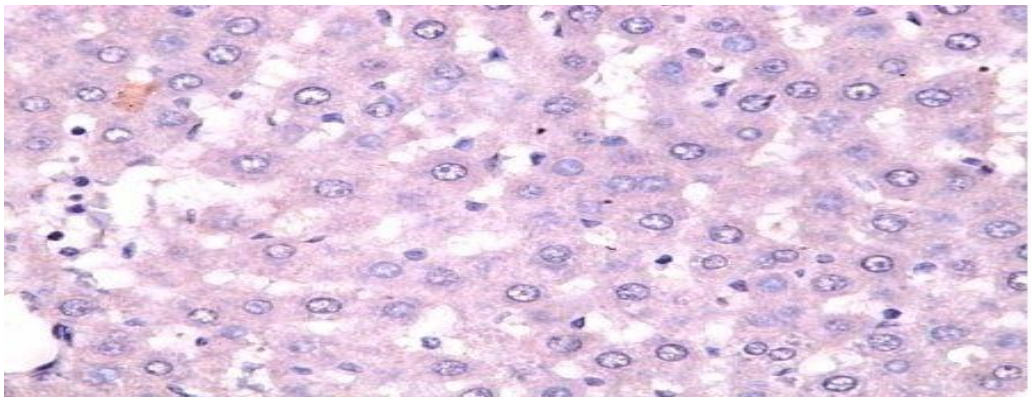

Figure 4.30 (c) x400: Effect of 5.0 mg/kg body wt plumbagin on Bcl-2 Expression liver of Wistar rats.

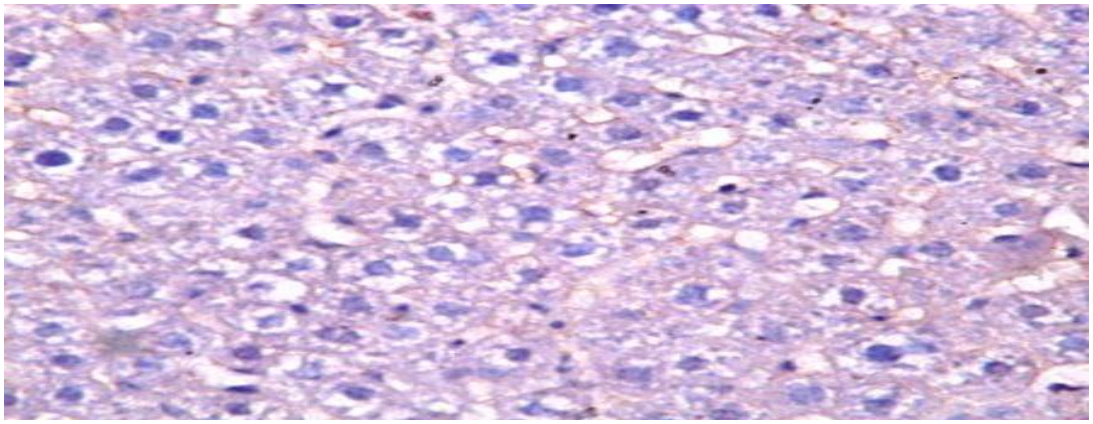

Figure 4.30 (d) x400: Effect of 10.0 mg/kg body wt plumbagin on Bcl-2 expression In liver of Wistar rats.

Figures 4.30(a-d): Photomicrographs showing effects of varying doses of plumbagin on Bcl-2 expressions in the liver**.**

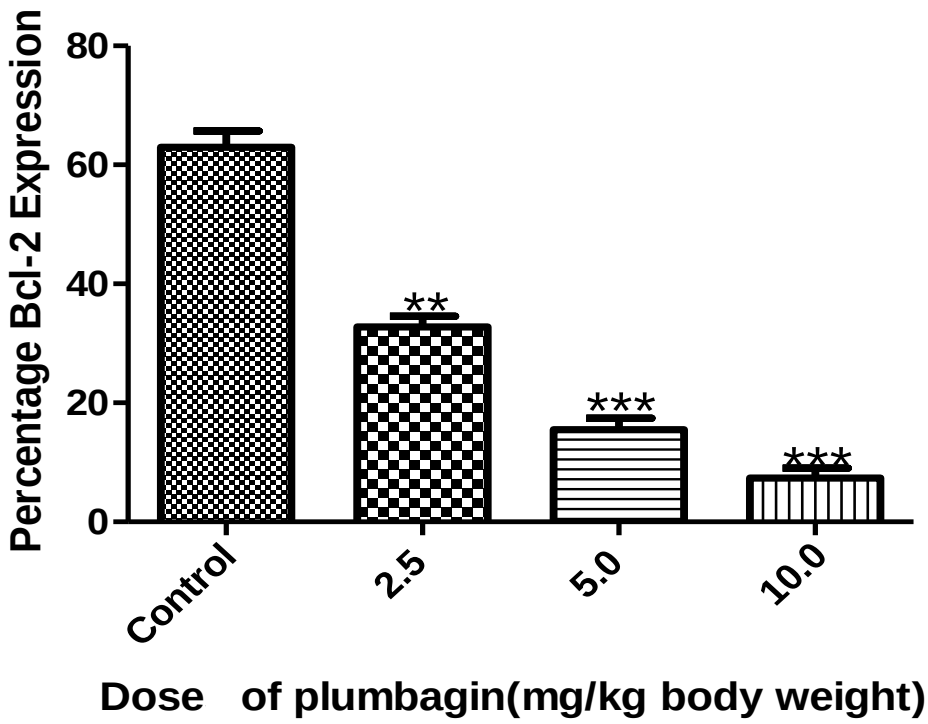

Figure 4.31 Effects of plumbagin on Bcl-2 Expression in liver of Wistar rats.

** $p < 0.01$, *** $p<0.001$

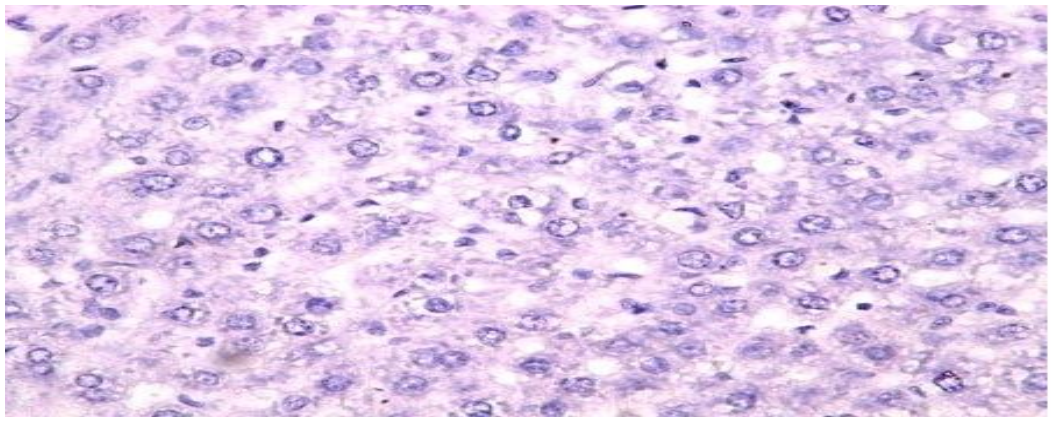

Figure 4.32 (a) x400: p53 expression in liver of normal Wistar rats (control).

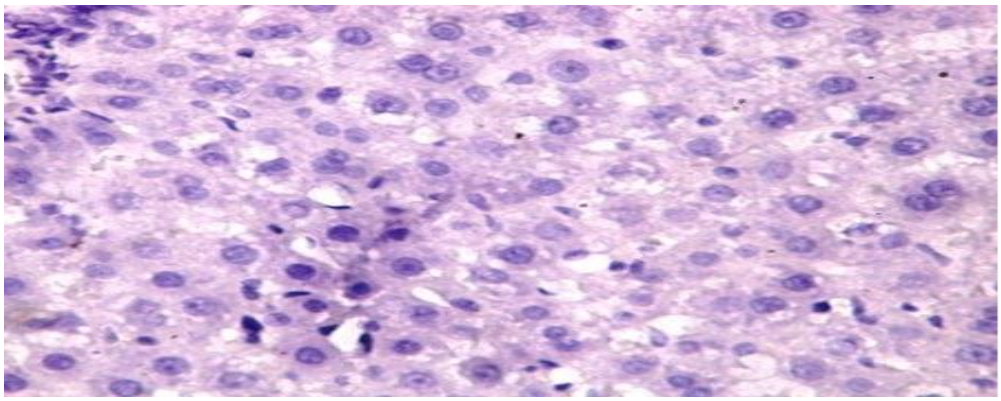

Figure 4.32 (b) x400: Effect of 2.5 mg/kg bwt plumbagin on p53 expression in liver of Wistar rats

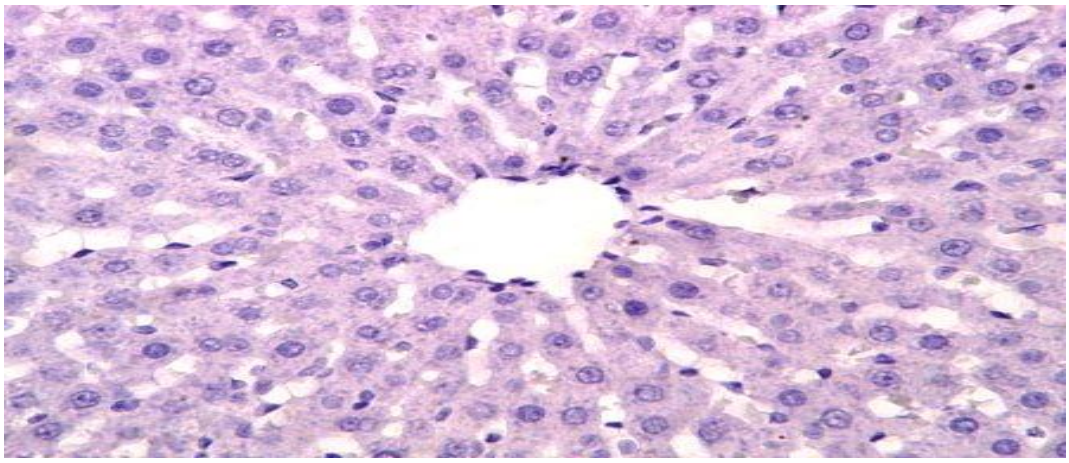

Figure 4.32(c) x400: Effect of 5.0 mg/kg bodywt. plumbagin on p53 Expression in liver of Wistar rats.

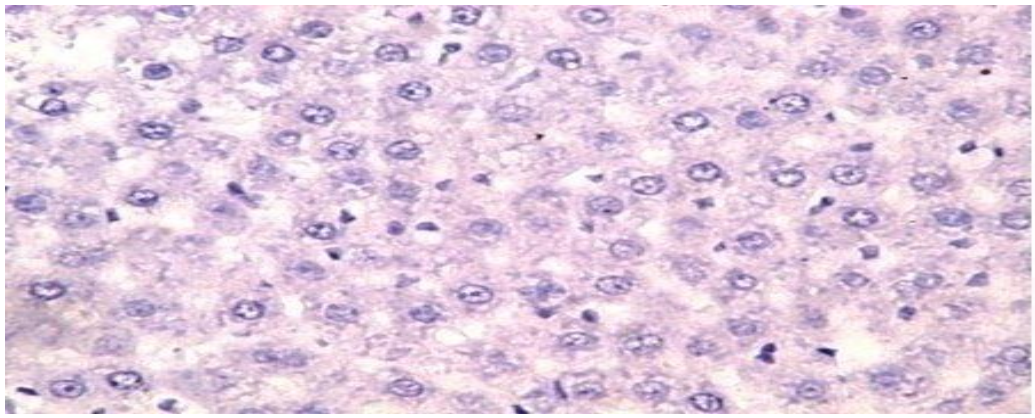

Figure 4.32 (d) x400: Effect of 10.0 mg/kg bwt plumbagin on p53 expression in liver of Wistar rats.

Figures 4.32(a-d): Photomicrographs showing effects of varying doses of plumbagin on p53 expression in the liver of Wistar rats.

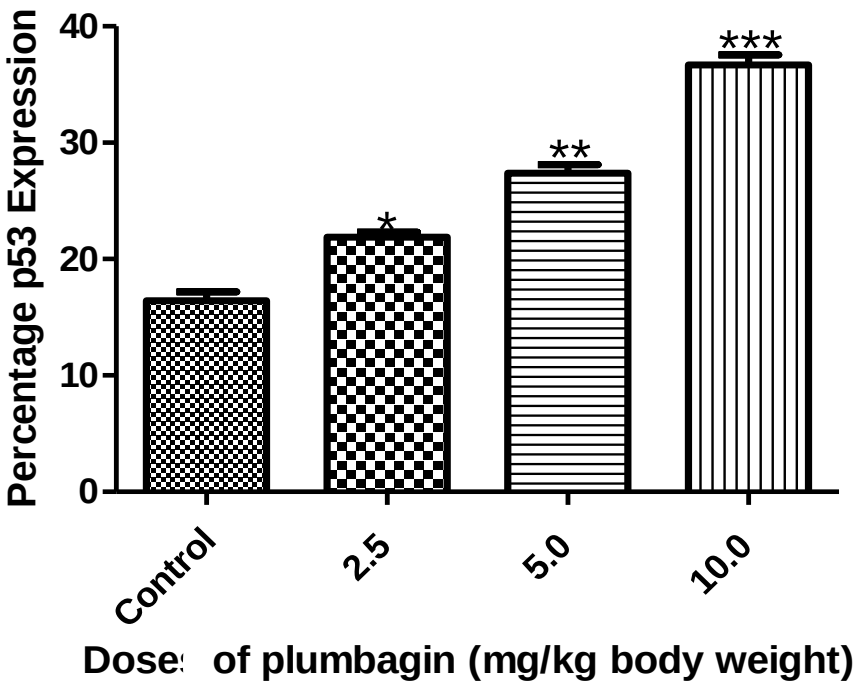

*** p < 0.05, ** p < 0.01, *** p<0.001**

Figure 4.33: Effect of Plumbagin on p53 Expression in liver

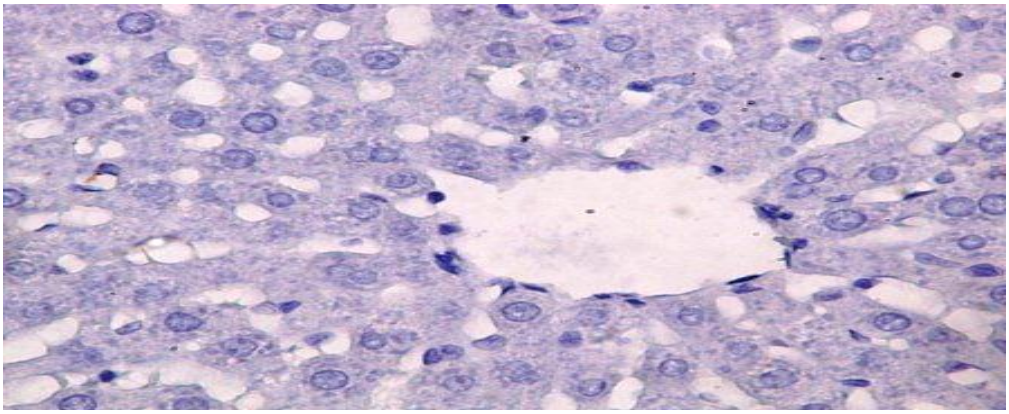

Figure 4.34: (a) x400: Bax expression in liver of normal Wistar rats (control).

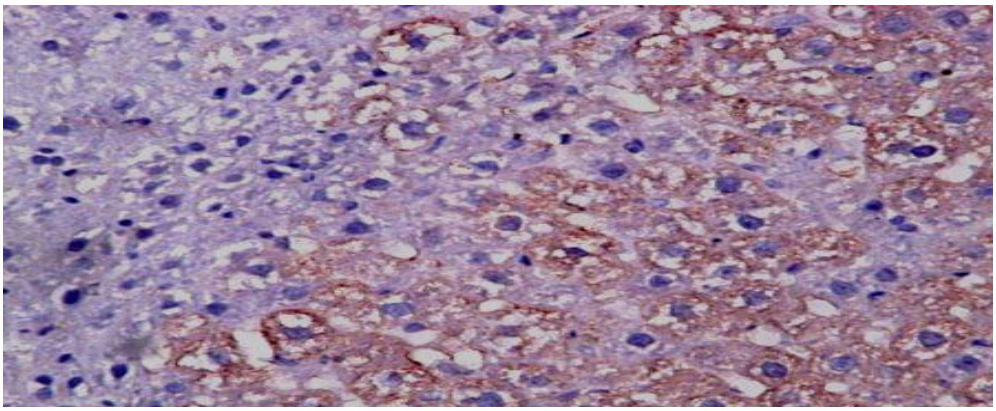

Figure 4.34 (b) x400: Effect of 2.5mg/kg bwt plumbagin on Bax expression in liver of Wistar rats.

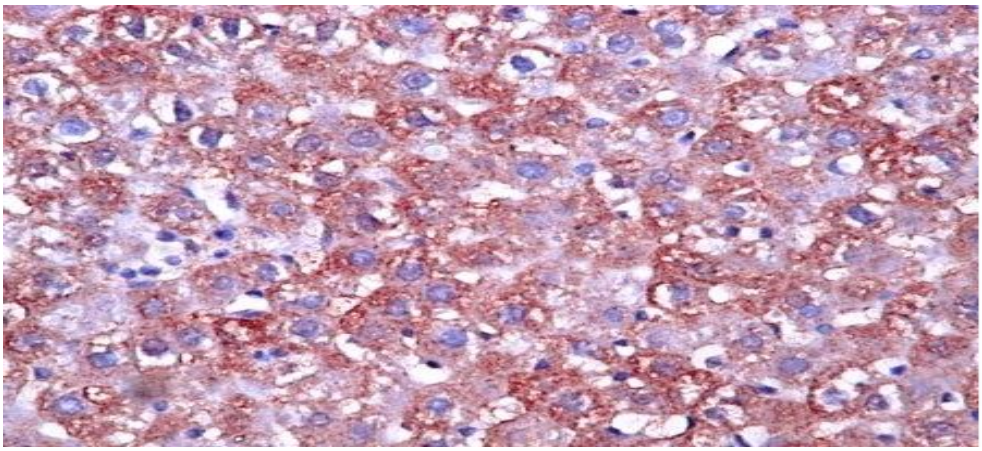

Figure 4.34 (c) x400: Effect of 5.0mg/kg bwt plumbagin on Bax expression in liver of Wistar rats.

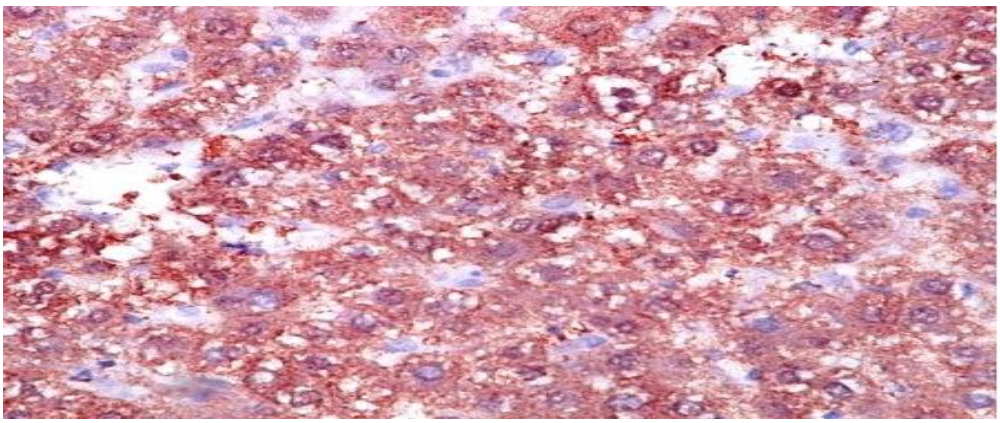

Figure 4.34 (d) x400: Effect of 10.0 mg/kg bdwt plumbagin on Bax expression in liver of Wistar rats.

Figures 4.34 (a-d): Photomicrographs showing effects of varying doses of plumbagin on Bax expression in liver of Wistar rats quantified and analysed by Image J and graph pad prism 5.

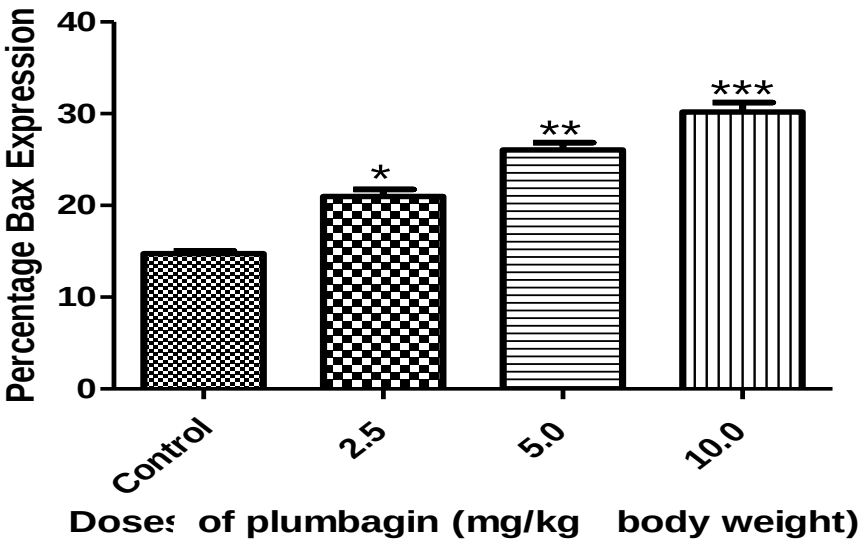

Figure 4.35: Effect of plumbagin on Bax expression

***p < 0.05, ** p < 0.01, *** p<0.001**

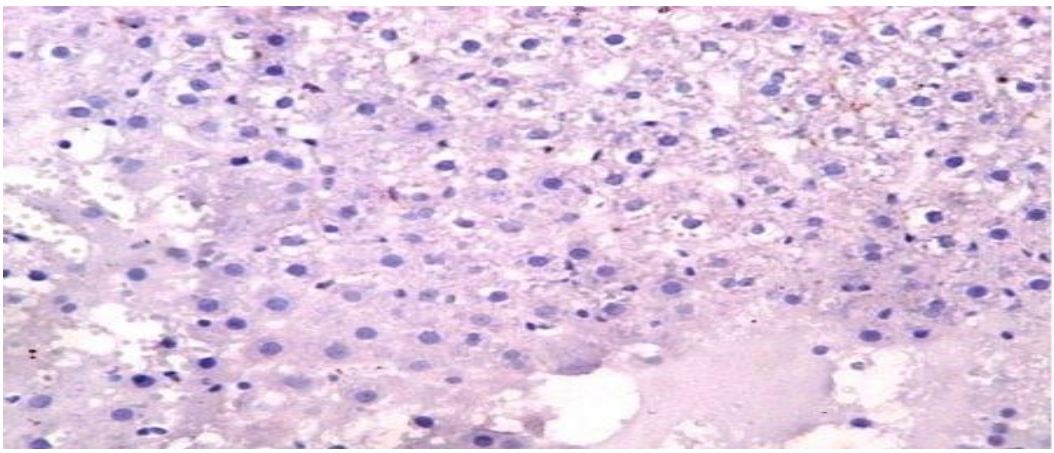

Figure 4.36 (a) x400: Cytochrome C release in liver of normal Wistar rats.

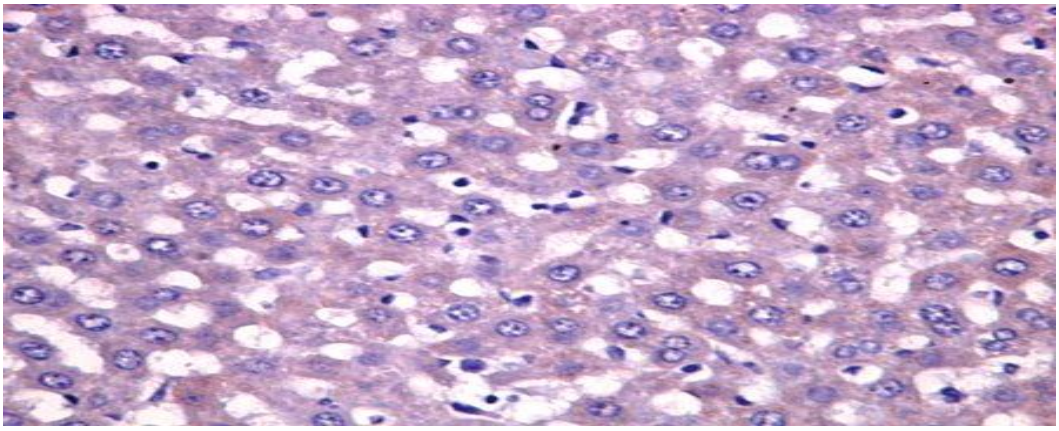

Figure 4.36 (b) x400: Effect of 2.5mg/kg bwt plumbagin on cytochrome C release in liver of Wistar rats.

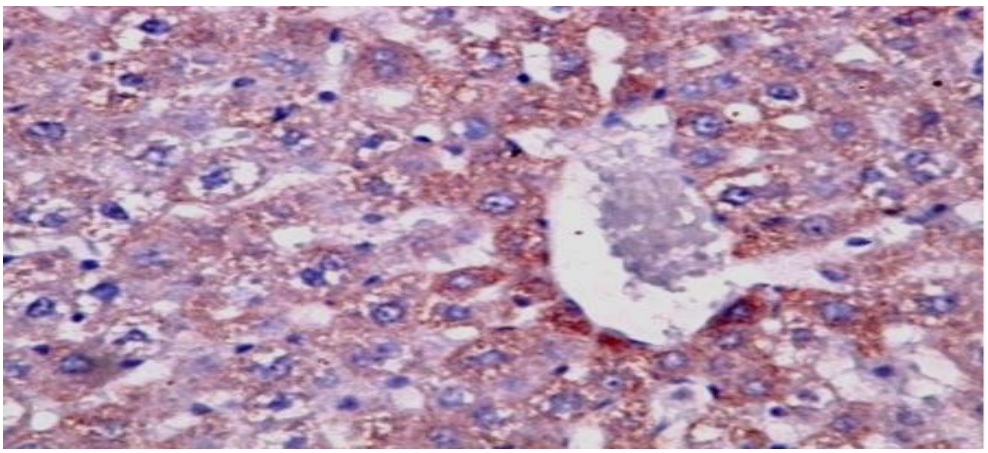

Figure 4.36 (c) x400: Effect of 5mg/kg bwt plumbagin on Cytochrome C release in liver of Wistar rats.

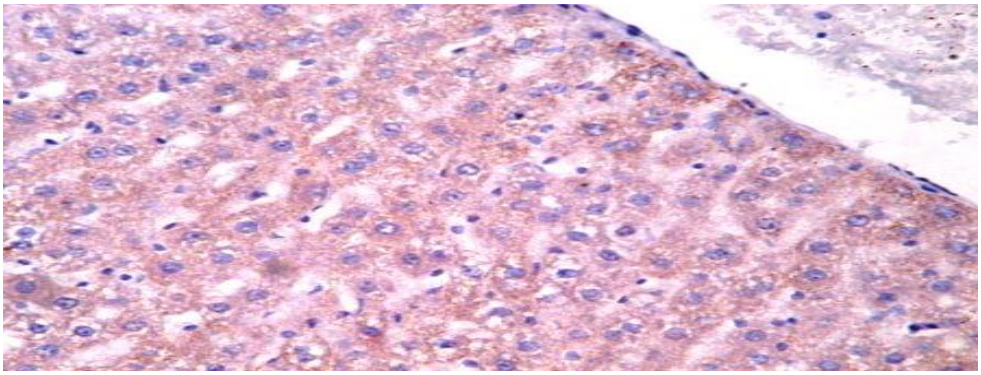

Figure 4.36 (d) x400: Effect of 10mg/kg bwt plumbagin on Cytochrome C release

Figures 4.36 (a-d): Photomicrographs showing effect of changing doses of plumbagin on Cytochrome C release in liver of Wistar rats.

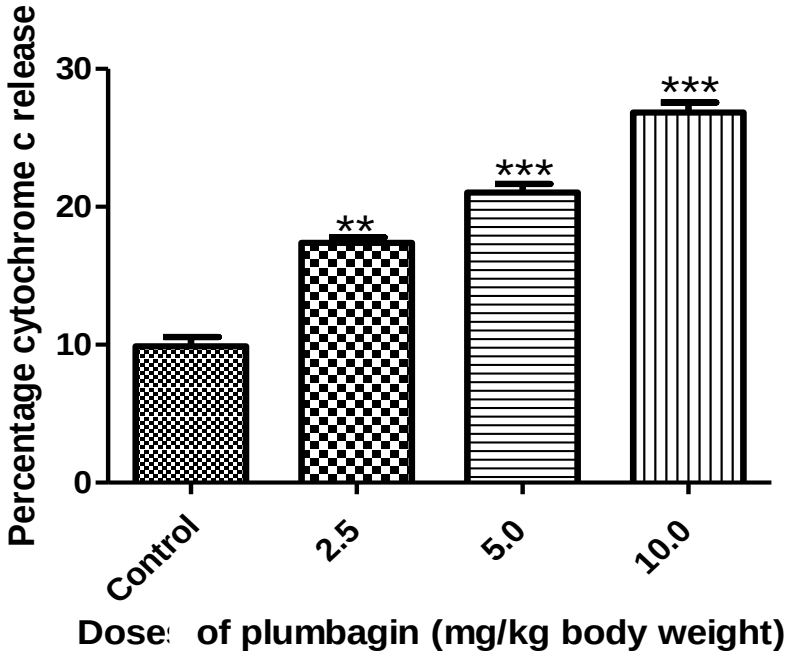

Figure 4.37: Effect of plumbagin on Cytochrome C release in liver of Wistar rats expressed in percentage

**** p < 0.01, *** p<0.001**

EXPERIMENT 20: Molecular Assessment of Testicular Functions in Plumbagin *Treated Rats*

Introduction

Probing further beyond the cellular level, effect of plumbagin on reproductive function and expression of molecules in the testicular organ were examined using the principle of semi-quantitative gene expression studies.

Since the testes remain the major reproductive machinery in the male reproductive system, molecules that are cardinal to its functions and expressions can be examined to verify how they are being affected as a result of plumbagin administration. The testicular organ functions under control and regulation of hormones and enzymes which are expressed as an index of its functionality. The expressions of testes specific protein kinase-1 (TESK-1) and Aromatase enzymes, follicle stimulating hormone (FSH) and progesterone receptors (PGR) were investigated in this experiment and their relative activities or expressions measured.

Procedure

The experiment involves oral administration of male Wistar rats with varying doses of plumbagin: Control (10 ml distilled water, 30 and 100 mg/kg body wt PL for groups II and III respectively) they were so given to saturate their tissues and allow general effect on gene transcription within the space of 72 hours. Testes were removed and homogenized in TRIzol reagent and RNA isolated according to the method described by Omotuyi *et al.*, (2018) in chapter 3.

Results

The result of semi quantitative gene expression studies includes: Follicle stimulating hormone (FSH) and progesterone receptors (PGR) presented in Figures 4.38 and 4.39 indicate that increasing plumbagin doses at 30 and 100 mg/PL kg body weight decreases significantly the expressions of the receptors relative to control. Consequently, the same dosage regimen of plumbagin elicit relative decrease in expressions of TESK-1 and aromatase as presented in Figures 4.40 and 4.41 respectively. Hence, reduced expressions of reproductive receptors and enzymes will restrict reproductive processes and thus affect fertility potential in the testes of Wistar rats.

Conclusion

Proteins inform of receptors, enzymes and hormones play significant roles in reproductive processes. The mammalian gametes are designed and vested with proteins which render crucial functions at each stage of gamate formation, development and eventual function for fertility.

Gene expression studies of receptors and enzymes which influence reproductive potentials of experimental animals as presented in Figures 4.38 - 4.41 show that plumbagin induced decreased expressions of FSH and PGR receptors. Similarly, there were observed significant reduction in TESK-1 and Aromatase expression at 100 mg/kg body weight. These results show significant reduction in relative manifestation of key hormonal markers and enzymes of testicular functioning. Hence, the entire result confirms the toxic nature and potential of plumbagin to precipitate infertility in the testes of experimental animals.

This result confirms emperical studies by Scorilas (2001) and Harvefield *et al.*, (2011) showing that reproductive hormones and enzymes such as aromatase, testosterone and FSH all play regulatory roles in apoptosis and spermatogenesis thus influencing reproductive potentials in experimental animal models.

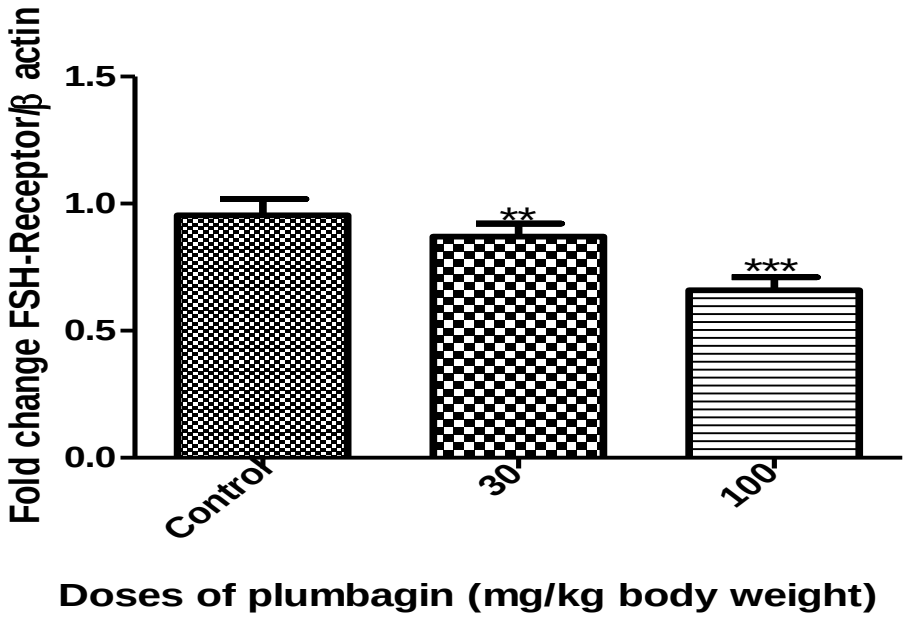

Figure 4.38: Effect of plumbagin on relative expression of FSH receptor.

**** p < 0.01, *** p<0.001**

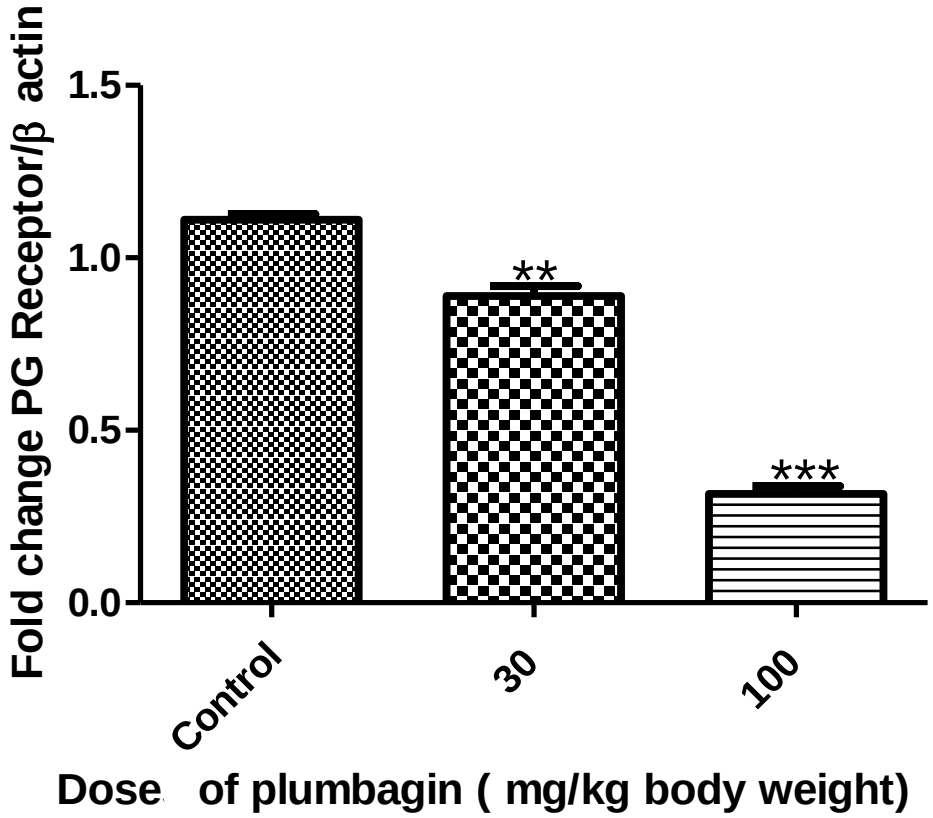

Figure 4.39: Effect of plumbagin on relative expressions of progesterone receptor in testes of Wistar rats

**** p < 0.01, *** p<0.001**

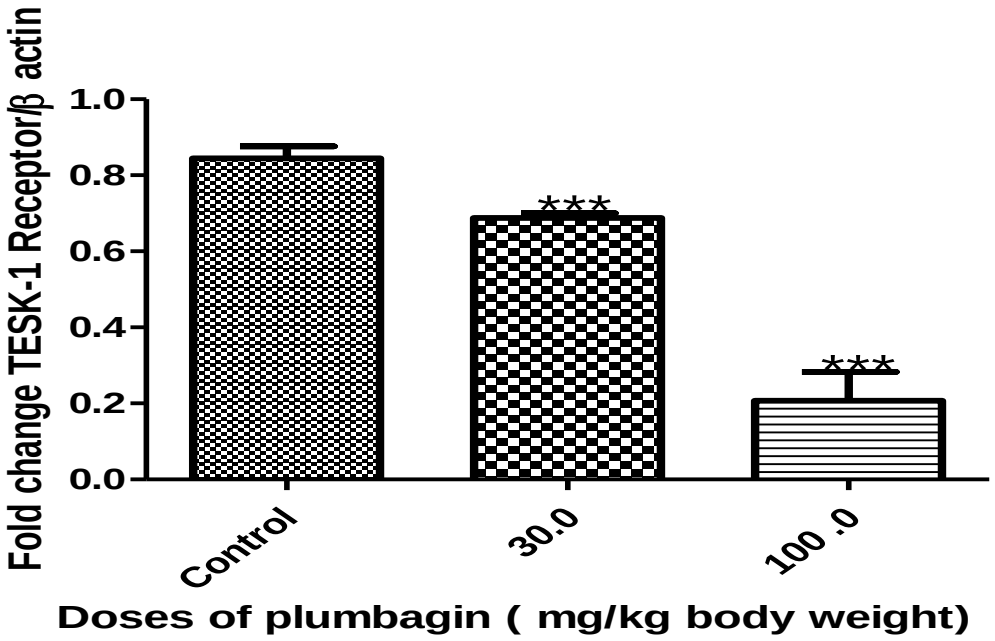

Figure 4.40: Effect of plumbagin on relative expressions of TESK-1.

***** p<0.001**

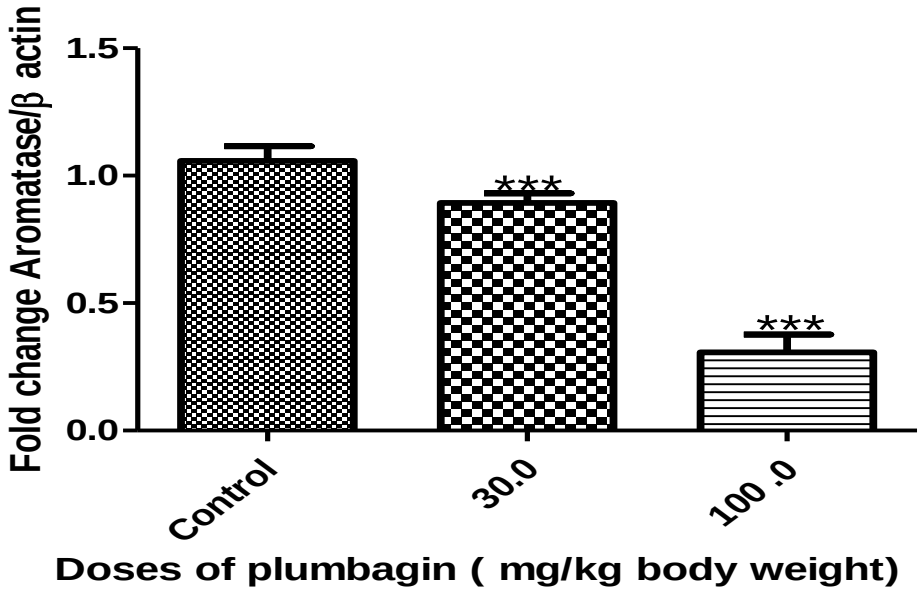

Figure 4.41 Effect of plumbagin on relative expressions of Aromatase enzyme

***** p<0.01**

EXPERIMENT 21: Molecular Docking of Plumbagin with likely Apoptotic Players

Introduction

Plumbagin has been established to interact with certain relevant protiens to elicit induction of apoptosis. The study of such mode of interactions and conformation of biomolecules inform of drug-ligand complex has become a necessary clue in understanding the working of drug and its kinetics. This idea is an important concept in drug development. The subject and mechanism by which drugs interact with certain biomolecules to achieve desired conformation which result to its effective healing potential is known as docking. In docking process, binding and interaction do take place and amino acids are involved in binding with enegy dissipation.

Since plumbagin elicits a variety of chemotheraupeutic properties, it is likely feasible to study the level and mechanism of its binding and possible pharmacokinetics in its interractions with target proteins to provide healing. The binding of plumbagin with some common apoptotic players including: Bcl-2, Bcl-xL, Bcl-W, Mcl-1, MDM2 and A1 will form basis for the present study using molecular docking and ligand (un)binding simulation approach. This approach is preferentially acceptable in situations where potential of drug efficacy is being monitored for pharmacokinetics of its theraupeutic properties with docking scores which measures the extent and effectiveness of binding (Yunta, 2016).

There are two types of docking, namely: 1. The Flexible ligands and target protein docking and 2. The Rigid body docking where both the ligand and the target are all rigid molecules. However, the present study will adopt the flexible ligands and target protein docking because of its relevance as it clearly illustrates ligands (drug) -target protein interaction depicted in this study (Dar and Mir, 2017).

Molecular interractions with protiens involves amino acids which are released or conformed to certain orientation fit for bounding to drug in a ligand-target protein relationship.

It has been documented that the Bcl-2 groups of proteins are major regulators of apoptosis as excessive expression of Bcl-2 has been recorded in numerous and varied cancer types which add up to drug resistance (Du *et al.*, 2018) Therefore, antagonists of Bcl-2 protein can act as potential anti cancer drug. It has been shown that plumbagin also induce apoptosis by down-regulation and inactivation of Bcl-2 in human breast cancer cells. This makes it a target in the

present study, hence docking of plumbagin with these protein families which influence apoptosis were studied.

The objective of the study is to identify negative or deregulators of apoptosis molecule that interact effectively with plumbagin to induce cell death. Hence, best docking pose of interaction with corresponding binding energy were determined among other factors.

Procedure

Chemical structure of plumbagin was downloaded from PubChem software and target protein molecular structures viz: Bcl-2, Bcl-XL, Bcl-W, Mcl-1, MDM2 and A1 were retrieved from the Protein Data Bank.

Molecular docking simulation was done using Glide platform on Schrodinger suite, for each target protein with Gibbs free energy scores (G-score) calculated for each target with their best docking pose and orientation. Pro- apoptotic proteins docked with plumbagin were measured in Kcal/mol relative to a standard drug -7 hydroxyl methylcoumarin.

Results

Results of docking pose of plumbagin with molecular targets of anti apoptotic proteins are stated with their corresponding Gibbs free energy scores as follows: Figures 4.43 -4.49 features: 7 HC standard ligand with a Gscore -10.963, Bcl-xl -3.89; Bcl-w -3.005; Mcl-1 -5.82; MDM2- 6.000; CyclinA1-3.933 Kcal/mol respectively.

The entire result indicates that plumbagin interaction potential with the anti apoptotic protein targets are in the following order (decreasing order) MDM2, Mcl-1, Bcl-2, Bcl xl, A1 and Bcl-w with respect to their G-scores. Hence, plumbagin interaction is most effective with MDM2 anti apoptotic protein to precipitate apoptosis. Moreso, Bcl-2, Mcl-1 and Bcl-xl also show tendency for effective interactions with the respective G scores of -5.886., -5.820 and -5.770 kcal/mol.

Conclusion

Molecular docking results show that plumbagin is likely to interact with anti-apoptotic proteins: Bcl-2, Bcl-XL, Bcl-w, Mcl-1, MDM2 and AI with the binding energies: -5.886, -3.899, -3.005, -5.820, -6.000 and -3.933 kcal/mol respectively. It can be concluded that MDM2 interaction with PL is more effective relative to other targets. This interaction is likely feasible due to the amino acids involved in providing electrostatic/ hydrophobic interactions for the docking process.

Therefore, MDM2 (with the highest docking score) was adopted for further studies to elucidate basis for its effective inhibition by plumbagin in a series of molecular dynamics simulation studies (Kumari, 2014; Yunta, 2016). It is interesting to note that MDM2 is a natural antagonist of p53 tumor suppressor protein and sequestered in its inactive form as a complex in the form- MDM2-p53. It is only possible to disengage p53 because there is a stronger affinity between PL and MDM2. This can only take place because the complex is distrupted and p53 released when there is stress signal or DNA damage. Hence, the toxic effect of plumbagin is being responded to by cell when p53 is released from the complex to activate the apoptotic cascades during stress signal or DNA damage in cell.

Similarly, Bcl-2 has -5.886 Kcal/mol energy score (Figure 4.44) following MDM2 (Figure 4.48) closely. The observed affinity in the docking score also justifies its function in Bax-dependent testicular degeneration and restriction of pro apoptotic protein BIM. Basically, various amino acids are responsible for the recorded interactions.

In Figure 4.47, Mcl-1 records a peak of -5.820 Kcal/mol energy score and this is a reflection of its response to toxic potential of plumbagin as well closely following Bcl-2. In all these observed increased G-scores of protein targets with plumbagin, it shows that various amino acids are involved in the binding interractions especially for MDM2, Bcl-2 and Mcl-1.

On the whole, anti apoptotic proteins particularly, MDM2 in complex with p53, Bcl-2 and Mcl-1 engaged with plumbagin in relative interaction with the results showing that effective interractions with these target proteins confirms toxic potentials and affinity of plumbagin for these target anti apoptotic proteins to inhibit their actions and thus promote apoptosis under various conditions mentioned earlier with amino acids actively involved in their interactions with plumbagin.

Figure 4.42: Plumbagin molecular structure showing its orientation in space for docking procedure.

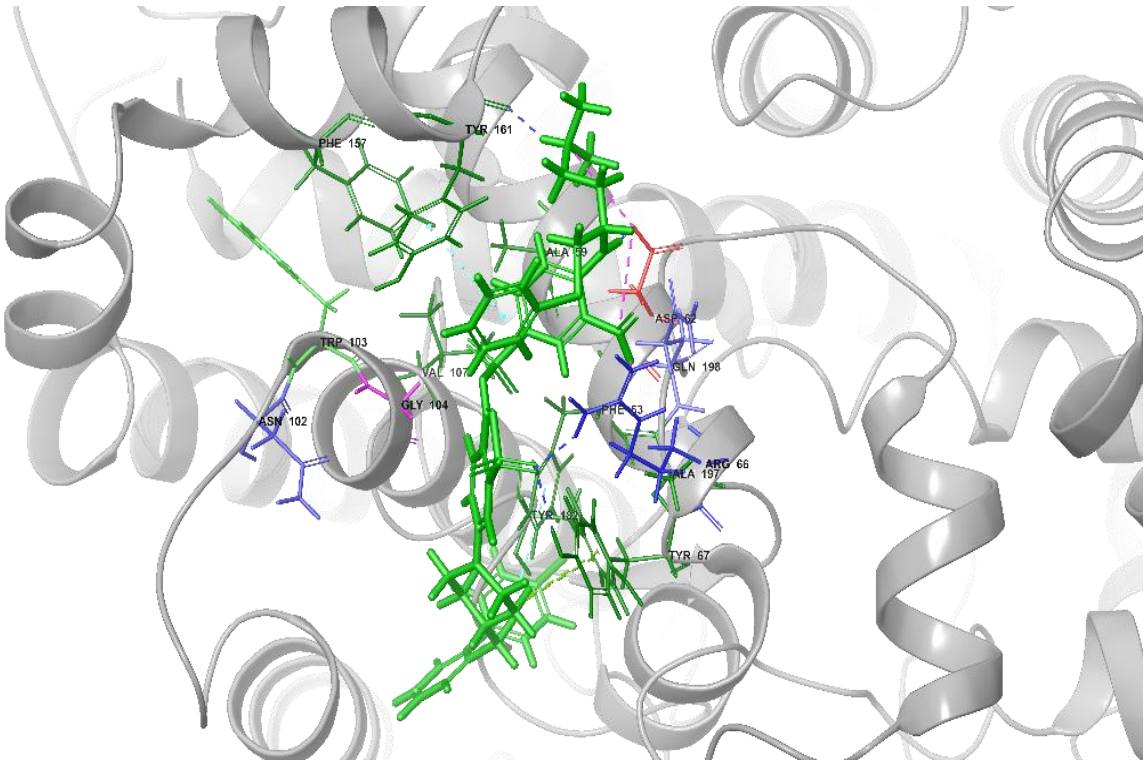

Fig 4.43: Photomicrograph of co-crystallized ligand G-score (kcal/mol): -10.963

7 HC used as standard with docking score -10.963 kcal/mol

Plumbagin docking with all anti apoptotic protein were done relative to 7HC docking score.

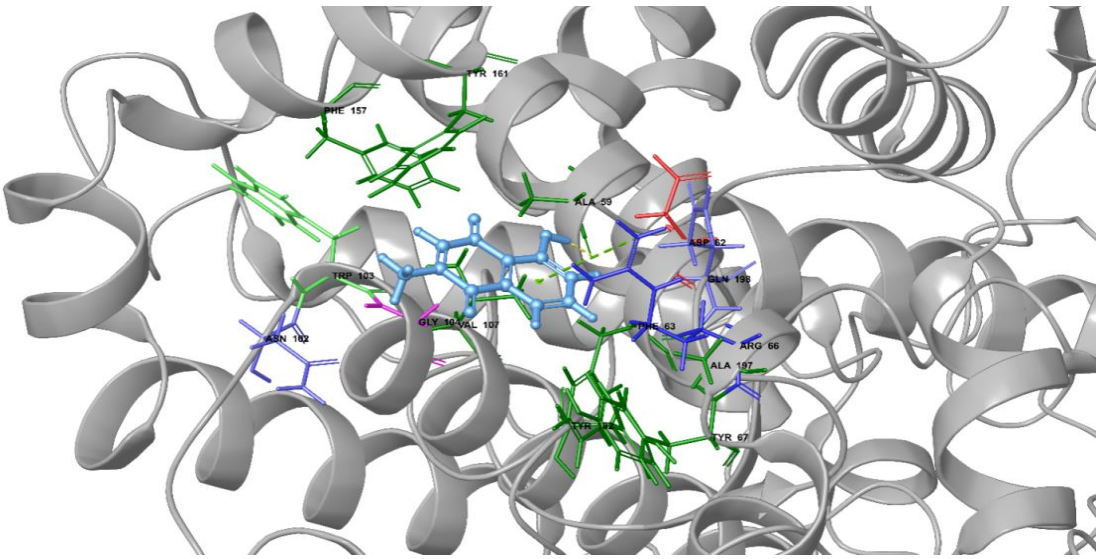

Figure 4.44: Plumbagin Gscore with Bcl-2 (kcal/mol): -5.886

The Bcl-2 is an antagonist protein which restrains the action of pro-apoptotic BIM and is associated with Bax dependent testicular degeneration.

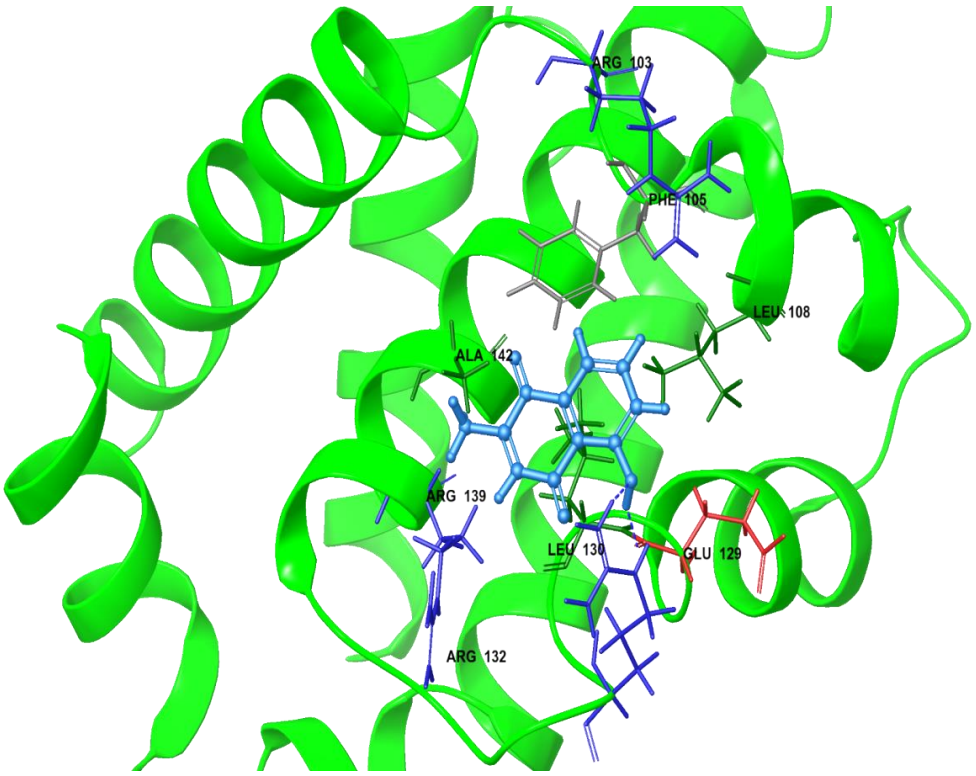

Figure 4.45 Plumbagin: Gscore with bcl-xL (kcal/mol): -3.899

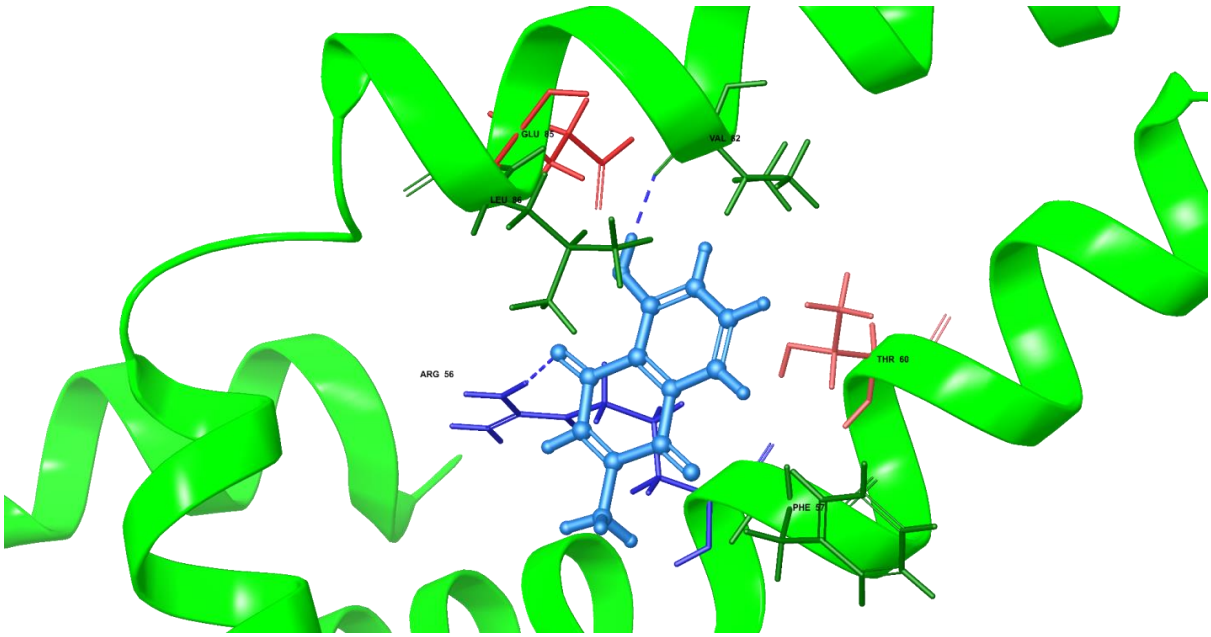

Figure 4.46: Plumbagin Gscore with bcl-w (kcal/mol): -3.005

This protein functions to promote testicular survival but otherwise appears redundant during development.

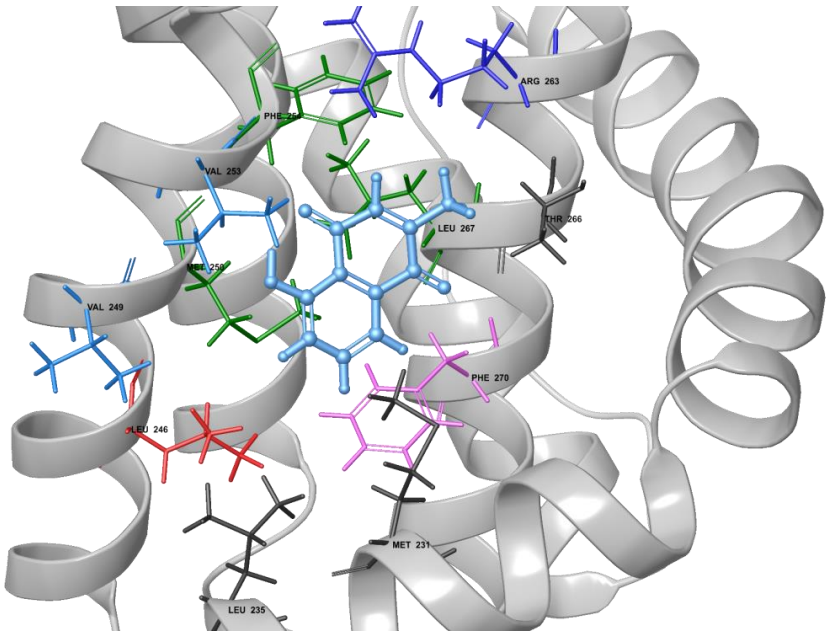

Figure 4.47: Plumbagin G score with Mcl-1 (kcal/mol): -5.820

This protein is essential for promoting development during embryogenesis; targeting this molecule may cause enormous toxic potential.

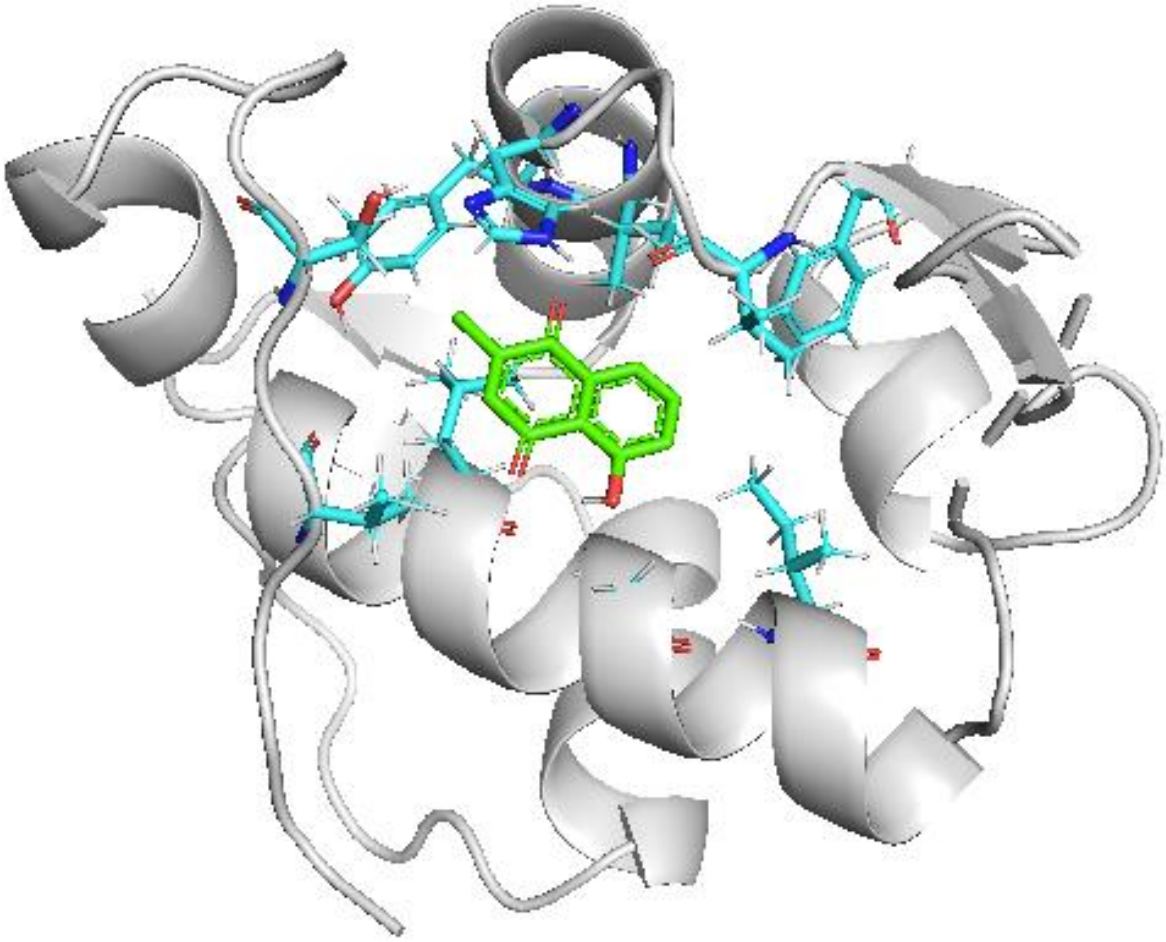

Figure 4.48: Plumbagin G score with MDM2 (kcal/mol): -6.000

`

MDM2 is a natural antagonist of p53 tumor suppressor protein. It is found as MDM2-p53 complex and is only released when there is stress signal or DNA damage.

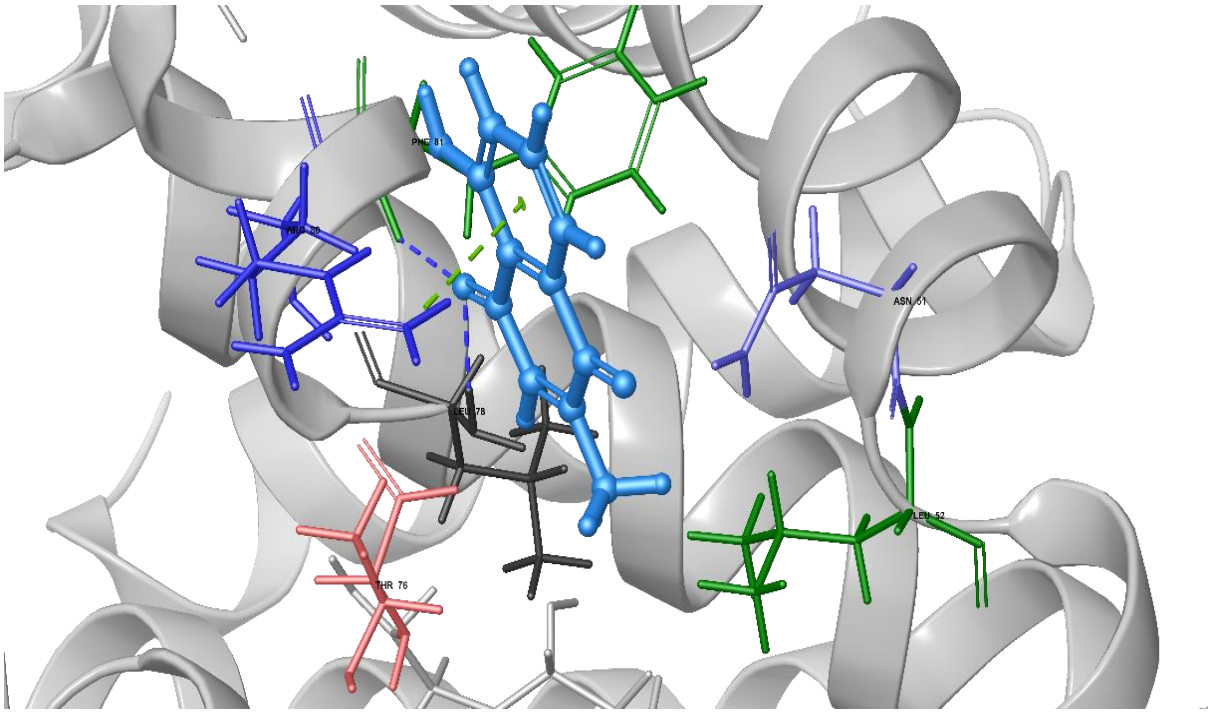

Figure 4.49: Plumbagin Gscore with Cyclin A1 (kcal/mol): -3.933

This is known as cyclin A1 and is expressed in male gametopoiesis. It is recognised in testicular and ovarian cancer especially in epithelial ovarian cancer (EOC).

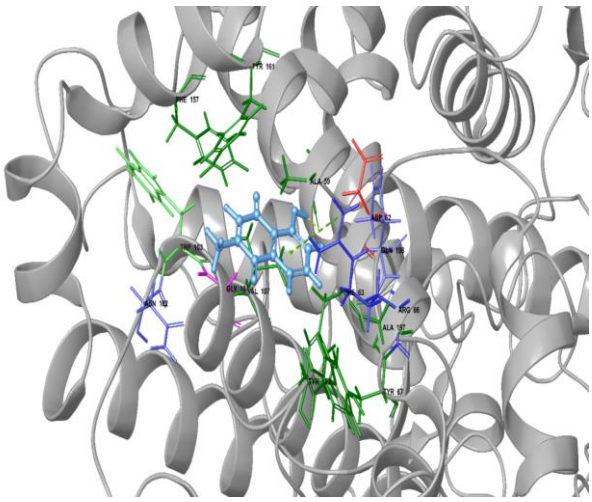

Plumbagin Gscore (kcal/mol): -5.886

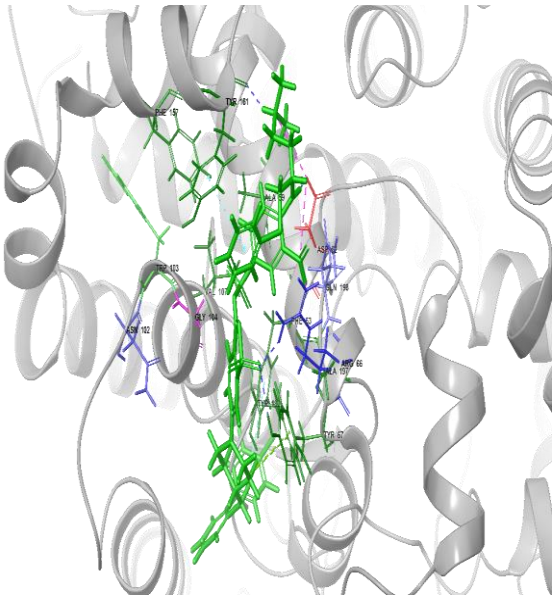

Fig 4.50: Co-crystallized Ligand Gscore (kcal/mol): -10.963

Figures 4.50 a-b: Plumbagin G score with Bcl-XL relative to 7HC

: **Gscore (kcal/mol): -3.899**

73

Figure 4.51 Plumbagin G score with Bcl-xl relative to 7HC

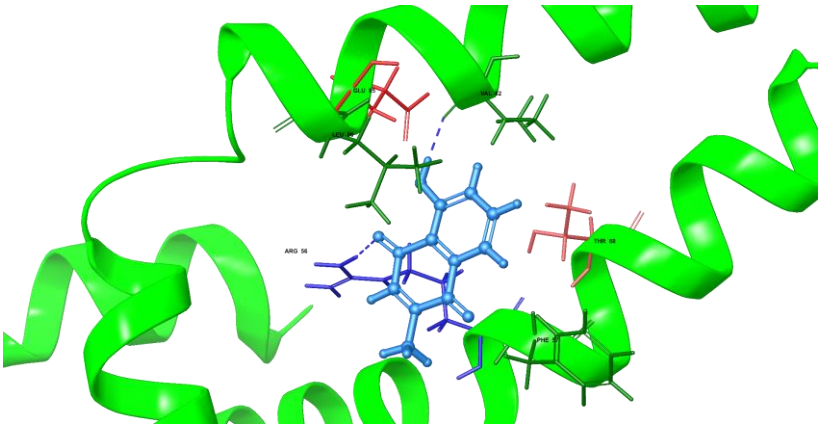

Fig 4.53: Plumbagin Gscore (kcal/mol): -3.005

Figure 4.52: plumbagin docking Gscore with Bcl-W relative to 7HC

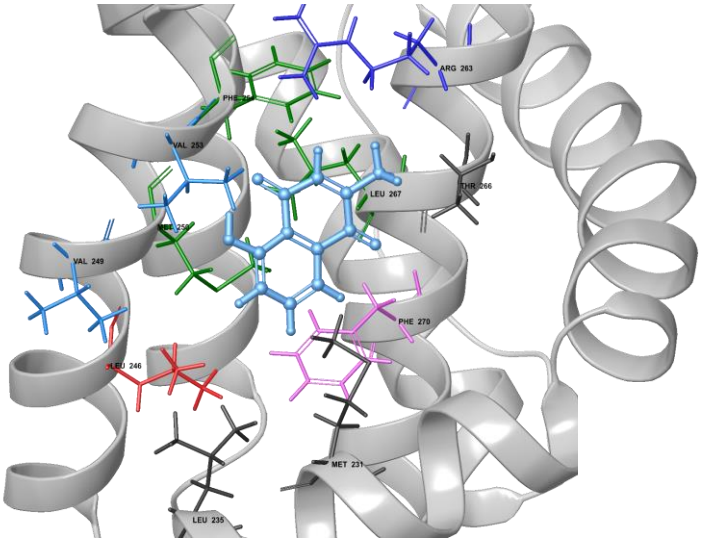

Fig 4.53: Plumbagin G score (kcal/mol): -5.820

75

Figure 4.53: Plumbagin Gscore with MCl-1 relative to 7HC

EXPERIMENT 22: Molecular Kinetics, Simulation Studies and Atomistic Basis for MDM2 Inhibition by Plumbagin

Introduction

Based on previous docking studies, docking score for MDM2 with plumbagin (- 6.00 kcal/mol) is most effective and as such further studies would be necessary to establish the atomistic basis for the predicted interactive inhibition of MDM2 with plumbagin (Dar and Mir, 2017).

Noted that MDM2 is an anti apoptotic protein sequestered in its inactive form as a complex with p53 protein. Its engagement and release from the complex can potentiate and activate p53 protein to kick-start apoptosis in the intrinsic pathway.

p53 Inhibition of anti apoptotic protein targets are generally feature characteristics of anti cancer agents. Therefore, subjecting 7HC and plumbagin to similar molecular dynamics simulation will reflect the shared properties qualifying plumbagin as an anti-cancer agent via its induction of the intrinsic pathway of apoptosis.

Procedure

Pictorial presentation of MDM2, p53 unisolated state and 7HC linked state with Plumbagin were used as starting models for molecular kinetics and simulations. Molecular dynamic simulation was done on GROMACS version 4.1.0. The result and visualization were done using VMD and pyMOL software.

Results

Results as observed in Figure 4.54 displays similar spatial orientations as shown in a cartoon representation for 7HC and Plumbagin. In Figure 4.55, plumbagin and 7HC show similar interractions with MMPBSA value while in Figure 4.46 the rmsd trajectories show that both 7HC and plumbagin can reproduce similar conformations adopted by MDM2 when bound to submicromolar inhibitor. Furthermore, in Figure 4.57 salt bridge distribution profile ruptured by p53 interraction was re established by both 7HC and Plumbagin.

In Figure 4.58, the secondary structures of MDM2 stabilised by p53 interraction in ligand bound state was distabilised in both 7HC and plumbagin bound states.

Conclusion

The results as displayed in Figures 4.55, 4.56 and 4.57 showing root mean square deviation trajectories, salt bridge distribution profiles and secondary structure distabilised by both plumbagin and 7HC clearly indicate that plumbagin and 7HC show similarity in their interactions with relevant protein to induce cellular responses.

Precisely strong affinity between plumbagin and MDM2 is effective enough to trigger physiological responses as p53 is released resulting in activation of bax and other associated proteins in the intrinsic pathway. It is thus revealing, that plumbagin and 7HC can reproduce similar effects that characterize drug kinetics and molecular interactions between drugs and protein targets.

Plumbagin actually reproduces similar conformation by the standard as demonstrated in the time series trajectories of rmsd in Figure 4.56, salt brigde rupturing potential in Figure 4.57 and destabilization of p53 interraction in ligand bound state by both 7HC and plumbagin in Figure 4.58 (Yunta, 2016).

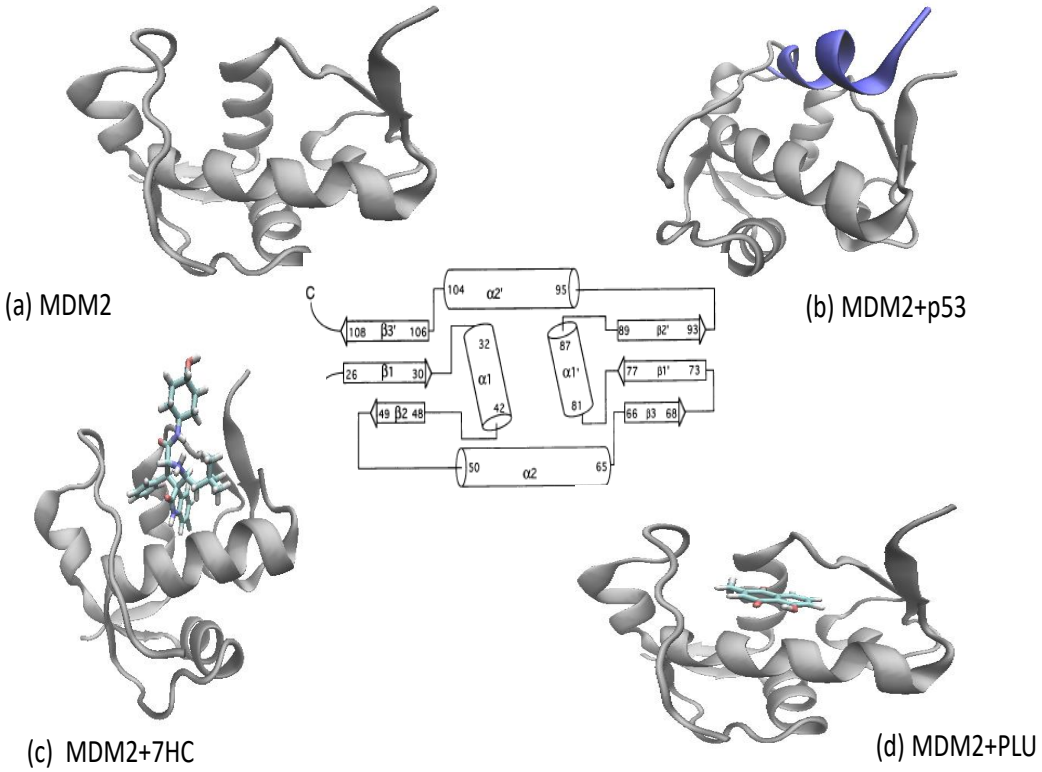

Figures 4.54: Cartoon representation of MDM2, MDM2 + p53, MDM2 + 7HC and MDM2 + plumbagin

MDM2-ligand Binding Energy calculated from classical MD simulation

Energy terms (Kj/mol)	p53	7HC	PLU
Electrostattic energy	-557.496±12.368	-25.475±3.704	-8.123± 0.832
Polar solvation energy	332.319 ± 8.065	82.695±3.117	32.962 ± 0.938
SAV energy	-237.285± 3.245	-117.831±2.665	-57.464± 1.288
Binding energy	**-462.425± 8.608**	**-60.611±3.005**	**-32.665± 1.258**

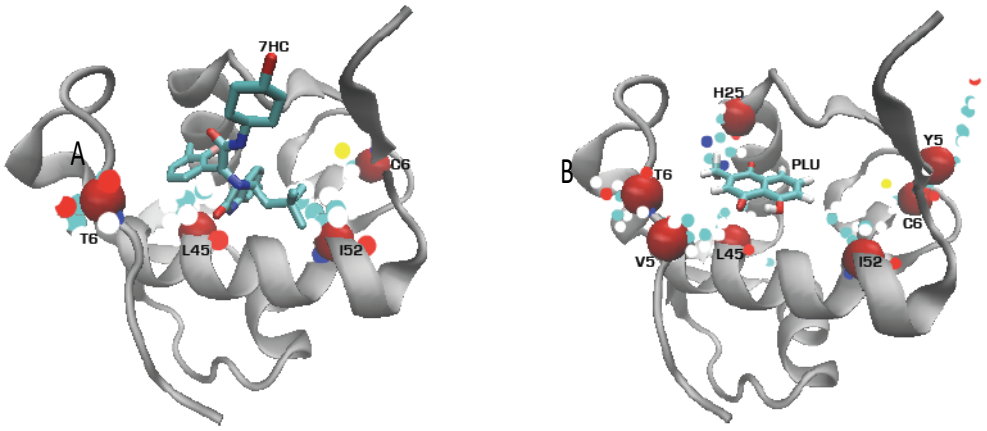

(a) 7HC interaction (b) Plumbagin interaction

Tabular representation of free energy of binding estimate of p53, 7HC and PLU from molecular dynamics simulation trajectories and Molecular Mechanics Poisson-Boltzmann Surface Area free energy calculations.

Fig 4.55 Cartoon (MDM2) and stick (blue) representation of key MDM2 amino acids involved in 7HC (A) and Plumbagin interaction (B).

81

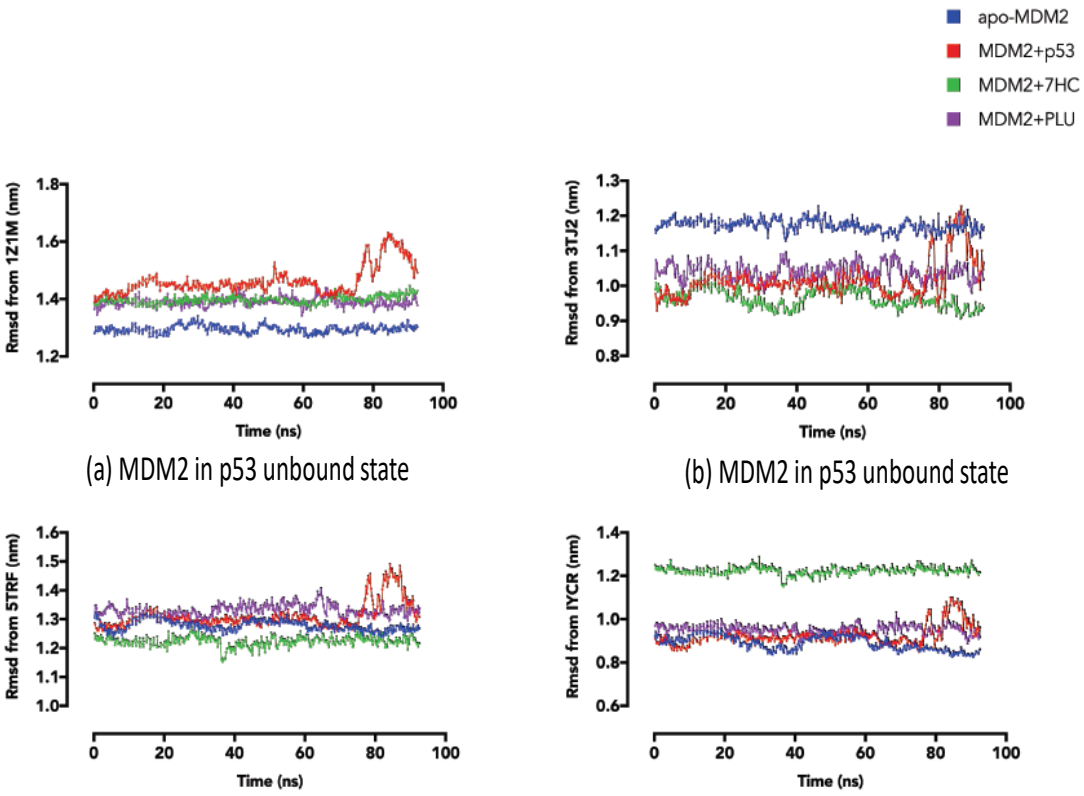

(a) MDM2 in p53 unbound state

(b) MDM2 in p53 unbound state

(c) 7HC ligand bound state

(d) Plumbagin ligand bound state

Fig 4.56:Time-series representation of root mean square deviation of trajectories of MDM2 in ligand bound states. Rmsd value from 3TJ2 indicates that both 7HC and Plumbagin can reproduce similar conformation adopted by MDM2 when bound to sub-micromolar inhibitor.

82

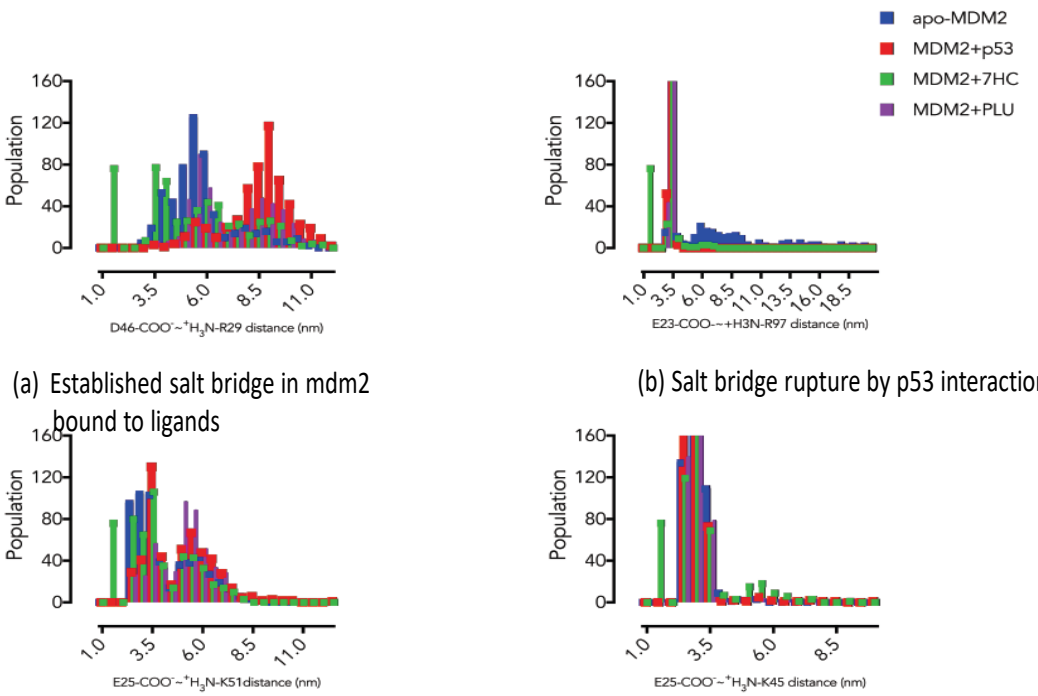

(a) Established salt bridge in mdm2 bound to ligands

(b) Salt bridge rupture by p53 interaction

(c) Salt bridge re established by 7HC

(d) Salt bridge re established by plumbagin

Fig 4.57: Distribution of salt bridge profile in MDM2 bound to ligands. Asp-64/Arginine-29 salt-bridge ruptured by p53 interaction is re-established in 7HC and Plumbagin bound states.

83

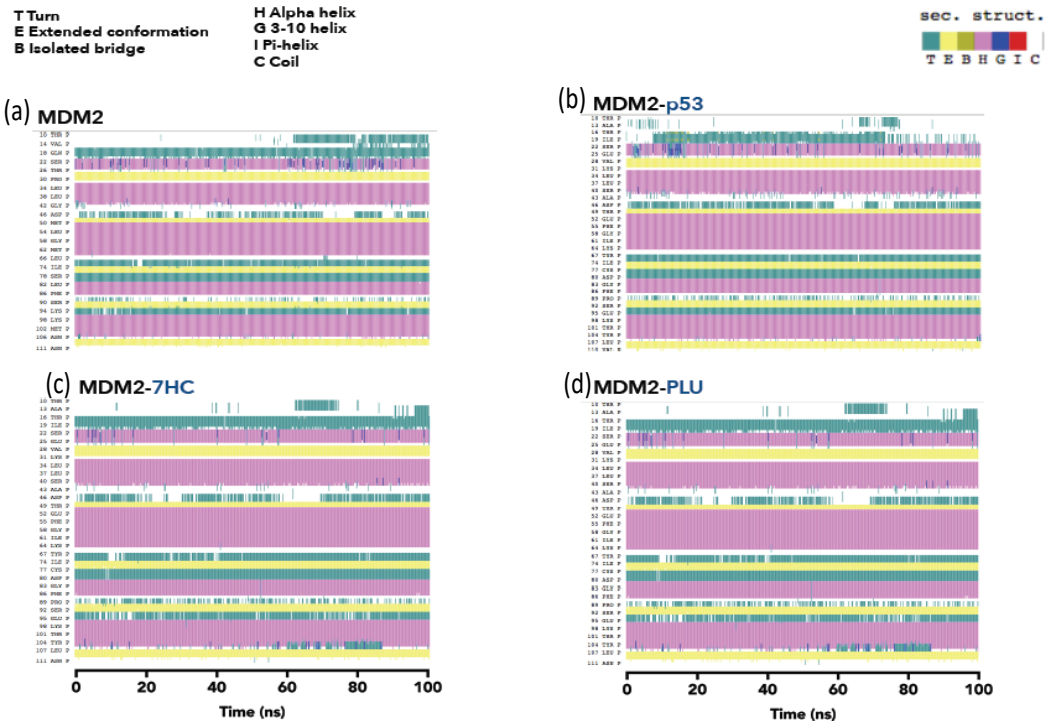

Fig 4.58: Diagramatic representation of secondary structure of MDM2 in ligand bound states. Secondary structures otherwise stabilized by p53 interaction is destabilized in 7HC and plumbagin bound states.

CHAPTER FIVE

DISCUSSION

Mitochondria are identified as cellular organelles known to exhibit multitasking functions and basically involved in vast physiological processes including cell death. Consequently, mitochondrial defects are known to precipitate varieties of malfunctions ranging from tissue wastage, Parkinson's disease, cancer and even infertility among others (Sukardi *et al.,* 2009; Zhao *et al.*, 2014). The study presents detailed biochemical mechanism that unravels adverse effects of plumbagin in adult rat testes in an attempt to explain the participation and roles of molecular target in the entire apoptotic process (Sinha *et al*., 2003).

In the study, toxic effects of plumbagin were investigated on testes and liver mitochondria of male adult Wistar rats while it also addressed the molecular targets involved in its toxicity. This study indicated that oral regimen of plumbagin doses induced apoptosis in testicular germ cells and in the hepatocytes. In both cases, the intrinsic pathway is involved having its various apoptotic molecules activated or autoactivated leading to down stream responses and cascades of events ultimately resulting in cell demise (Li *et al*., 2019).

To establish toxic effects of plumbagin in the animal models, certain suspected target organs were examined preliminarily as a clue for further indepth studies. These are all necessary steps towards unraveling possible adverse effects precipitated by plumbagin administration.

Mitochondria are known to respond to toxicants, hypoxia, UV light, radiation and ROS through cytochrome C release and ultimately cell death (Jezek, 2017). In this study, mitochondria response to plumbagin toxicity was examined and the responses involved initially originates from within the cell and precisely from the mitochondria. Experiments 5 and 6 confirm that the permeabilization of the mitochondrial membrane is a starting point for the intrinsic apoptotic responses.

Moreso, increased ATPase activities in Experiments 7 and 8 which follow dose-dependent pattern result, show that apoptotic responses in the cell requires energy for execution of its multiple activities. In Experiments 9 and 10, toxic effects of plumbagin precipitates peroxidation of lipid membrane in liver and testes of experimental animals. The resultant effect will necessarily affect the integrity of the membrane and its potential in all ramifications.

According to Yu *et al.,* (2019) and Bello *et al.,* (2021) gross decline in testicular ATP levels with corresponding upsurge in inorganic phosphate levels tend to impact significantly on key reproductive functions and as such at ambient and physiological pH, ATPase activities promote reproductive functions. Specifically, ATP synthase may be required for male reproductive potential and germ cell maturation in Drosophila testes (Li *et al*., 2017).

To further establish toxic effects and apoptotic response of Wistar rats to plumbagin at cellular levels, caspases 3 and 9 were assessed in Experiments 11,12,13 and 14. The results obtained show consistent dose-dependent increases in the caspases activities- showing that plumbagin administration trigger the initiation and execution of apoptosis in the animals. Hence, plumbagin fosters the activities of players and promoters of apoptosis especially in the intrinsic pathways.

In pragmatic and quantitative terms, Experiment 15 reveals that reproductive parameters such as sperm motility, mean count and morphology were adversely affected as a result of plumbagin administration in a dose dependent manner. This in particular provide evidence and explanation for previous results in Experiment 3-5. The explanation put in a simple analogy can be stated thus: sundry cellular effects of plumbagin within the mitochondria and at cellular level result to observed practical quantitative and qualitative reduction in sperm count, motility and morphology in Experiment 15.

A significant indicator of toxic propensity of PL was obtained from characteristic dose-dependent decrease in basic reproductive parameters including sperm count, motility and morphology in all animals administered plumbagin compared with control (Figures 4.16, 4.17 and table 4.0) in which the bioactive compound adversely impacted on the reproductive machinery and this result is supported by earlier reports (Carreau *et al*., 2010; Li *et al.,* 2017) that plumbagin alters reproductive capability in experimental animals.

Further investigations in the study included histological examinations of liver and testes after varying doses of the bioactive compound-plumbagin were administered to animal models. Results of these studies showed evidence of progressive vascular congestions, dose dependent alterations in both liver and testicular architecture with maturation arrest in the testicular germ cells (Figures 4.20 and 4.21). These results open avenue for further probings and indepth studies of the effect of plumbagin on the toxicity potential and impact on reproductive machinery in experimental animals.

The next level of study also corroborates initial results from reproductive parameters; this precisely includes assessment of levels of hormones and receptors contributing essential regulatory and reproductive control. Since experimental results show consistent and significant dose-dependent reduction in FSH, PR, TESK-1 and aromatase in Figures 4.38, 4.39, 4.40 and 4.41 respectively. This account for the practical reduction in sperm count, motility and morphological disorders indicated earlier and in concord with the findings of Mahdi *et al.,* 2012; Oduwole, 2018).

TESK-1 and aromatase are reproductive enzymes, while TESK-1 is known to foster reproductive propensity, its reduced expression has been attributed to altered testicular function in plumbagin fed rats (Scorilas *et al.,* 2001). Result on table 4.0 showed increased altered testicular morphology indicative of reproductive dysfunction as recorded and supported by related results including reduced sperm count and motility all of which attest to adverse effect of plumbagin on the entire reproductive machinery. Hence all the reproductive enzymes and receptors assessed in the study were all negatively affected by plumbagin administration (Bello *et al*., 2021).

Mitochondrial membrane functions to compartmentalize essential molecules which can be selectively released via pore opening. Therefore, mitochondrial membrane permeability transiton pore opening was assessed as an index of plumbagin adverse effect to permeabilise the membrane thus releasing molecules such as cytochrome C which inevitably kick starts the apoptotic process through the intrinsic pathway. Result obtained in the study as indicated on Figures 4.30, 4.40, and 4.5 showed that plumbagin induced dose-dependent pore opening. This corroborates previous report that toxic molecules can induce apoptosis leading to cell death in diseased cells such as cancer cells which are already primed to die (Bello *et al*., 2021).

PL precipitates distruption of mitochondrial membrane permeability thus activating pore opening in treated animals. Further biochemical and membrane investigation attest to enhanced ATPase activities expressed as an index of ATP production. Basically, mitochondrial ATP plays crucial role in regulation of male germ cell via apoptosis and in spermatogenesis (Erkkila *et al*., 2006).

Furthermore, plumbagin increased expressions of liver ATpase activities in dose-dependent manner as shown in Figure 4.7 is indicative of its ability to induce apoptosis (since apoptosis is an energy dependent process), increased dose-dependent mitochondrial lipid peroxidation in liver of experimental animal (Figure 4.9) are all indicators that plumbagin qualifies as anticancer drug candidate and has been corroborated in literature (Chen, 2016). Plumbagin by engaging MDM2 and bcl-2 as shown in Figure 5.1 provide avenues for activation and interaction of the p53 protein with apoptotic molecules leading to formation of mPT pore with consequent release of cytochrome C. In similar pattern, bcl-2 engaged by plumbagin also promotes activities and interractions of the bax and bak molecules as they are autoactivated to induce the mPT pore opening.

Anticancer claims of plumbagin have been further established in the immunohistochemical studies results in liver of Wistar rats where apoptotic biomarkers namely: cytochrome C release, p53 and bax expressions were observed to be dose-dependent (Figures 4.60, 4.50 and 4.55) while bcl-2 was observed to decrease with increasing dose of plumbagin (Figure 4.45). Hence, this is in agreement with findings that bcl-2 family proteins are key players in the intrinsic pathways and as such they are critical death regulators (Danial, 2017; Bejarano *et al.*, 2018).

In terms of affinity for interaction, MDM2 is likely to interact most effectively with PL amongst other anti apoptotic molecules (MDM2 having a high negative value of 6.000 kcal/mol) hence, docking and simulation studies revealed that amino acid interactions involving Asp-64/Arginine-29 are involved in the binding of plumbagin to MDM2. This also is in tanderm with the submission of Yang *et al*, (2015) relating taurine increased testicular function via inhibition of oxidative stress and apoptosis in Wistar rats.

Although, docking is not part of the wet laboratory experimental study; docking studies in the virtual lab on its own provide insight into the possibility of predicting the effect of drug or xenobiotics in the treatment of diseases and as such it is an essential aspect applied in drug

development to explain the molecular concept and workings of drug in terms of its interactions, binding and possible orientation to elicit its chemotherapeutic effects (Grant *et al.*, 2006; Omotuyi, 2015b).

To further examine the working principle of plumbagin as an anti cancer agent, a standard anticancer drug 7- methylcoumarin (7HC) was subjected to simulation studies to examine if there are similarities in their mechanisms or working and conformation at the molecular level.

Coroborating the result on immunohistochemical studies where pro and anti apoptotic proteins were assessed, p53 protein was implicated in its role to foster apoptotic responses via the intrinsic pathway as plumbagin inhibits MDM2, it releases p53 to activate apoptotic responses by activating bax expression. Hence, with the result of the simulation studies, free energy binding estimate of p53, 7HC and PL from Molecular Dynamics Simulation trajectories and Molecular Mechanics Poison Boltzman Surface Area (MMPBSA) free energy calculations all showed similar relativities (Kumari, 2014).

Further simulation showed that, it is possible to re-establish salt bridge profile distrupted or ruptured by p53 interraction when bound to MDM2 by 7HC as well as plumbagin at Asp-64/Arg29 (Figure 4.82). Hence, there are confirmed similarities between 7HC and Plumbagin. It was noted that the secondary structure of MDM2 stabilised in its ligand bound state by p53 interraction is destabilized in both 7HC and plumbagin bound states (Figure 4.53). These properties are useful tools employed as criteria in modern drug development which enables predictions of potential drug effectiveness in treatment of disease conditions having known their molecular profiles (Omotuyi, 2021).

In Experiment 16, Liver enzymes activities were observed to increase in dose dependent fashion. The increase which is indicative of potential of plumbagin to cause liver damage in Wistar rats attest to its toxic effect as well.

Experiments 17, and 18-19 feature histology and immunohistochemical examinations respectively. The results present practical effects of plumbagin doses on Wistar rats with corresponding expressions of apoptotic biomarkers and players in the intrinsic pathways of apoptosis. Hence, cytochrome C and p53 release, including Bax expressions are all indices of plumbagin potential to induce apoptotic process via the intrinsic pathway as their expressions were dose-dependent.

Docking experiment confirms in particular that p53 expression is involved in the intrinsic apoptotic process since it is disengaged as a result of stronger affinity between plumbagin and MDM2. Therefore, the release of p53 in Experiments 18-19 clearly justify and corroborates the docking result in Experiment 21. Similarly, Bcl-2 and Mcl-1 are soft targets for plumbagin as revealed in their respective docking scores.

It is worth noting that MDM2-p53 complex triggers and activates a downstream apoptotic response in the intrinsic pathway occasioned by permeabilisation of the outer mitochondrial membrane leading to the release of cytochrome c to kick start the cell-death cascade. Proteins and molecules interact in form of players and prosecutors to ensure death sentence on marked cells are irreversible. Identified proteins and agents in the pathway leading to cell demise include cytochrome C, Bax, p53, Bcl-2 and MDM2 and represent a host of molecules interacting as anti apoptotic agents in the animal model.

The results in Experiment 22, affords a model template for plumbagin interaction in the entire scenario to explain possible mechanisms of plumbagin toxic effect on testes of animal model used in the study. It begins with the toxic propensity of plumbagin to induce permeabilization of the mitochondrial membrane with the release of cytochrome C which initiates Apaf-1 forming apoptosome complex with consequent down stream activation of the initiator and effector caspases resulting to cell death.

Finally, Experiment 22 unequivocally provides summary with possible comprehensive mechanisms for the toxic response in inhibition and release of target proteins regarded as players and promoters in the intrinsic pathway. These players are activated simultaneously by a single action of inhibition of MDM2 which releases the p53 protein to kick start other apoptotic responses.

CHAPTER SIX

CONCLUSION

To conclude on the study, confirmation of the potential toxic effect of plumbagin in the entire study can be presented as a proposed mechanism for plumbagin induction of apoptosis and toxicity via the intrinsic pathway as shown in the Figure 6.1.

In the entire study, plumbagin presents effectiveness as an anticancer agent suitable in treatment of conditions such as prostate tumour. However, its toxicity indicated by reduced sperm count, increased sperm abnormalities, and alterations in reproductive enzymes and hormones show-case plumbagin as a doubled edge sword agent capable of inflicting significant damage on male reproductive machinery thus precipitating infertility in males (Chen, 2016).

The relationship established in the simulation studies indicated that plumbagin interacts effectively with MDM2 (-6.00KJmol^{-1}) which ordinarily is sequestered in complex with p53 protein in the cell. It was also indicated that Bcl-2 with appreciable G score (-5.886 KJmol^{-1}) next to MDM2 was inhibited by plumbagin. Hence engagement of plumbagin with MDM2 releases p53 from the complex which kick-start its activation and consequent induction of apoptosis. Similarly, inhibition of Bcl-2, an anti apoptotic protein allows apoptosis to proceed in the intrinsic pathway. Hence, plumbagin inhibits MDM2 and bcl-2 to promote cell death in primed cells (Chen, 2003). This is the reason why in the immmunohistochemistry studies, plumbagin reduces Bcl-2 proteins expression and increases p53, Bax and cytochrome c release in dose-dependent manner. The two anti apoptotic proteins (Bcl-2 and MDM2) are well inhibited for the promotion of apoptosis in the intrinsic pathway as illustrated in Figure 6.1

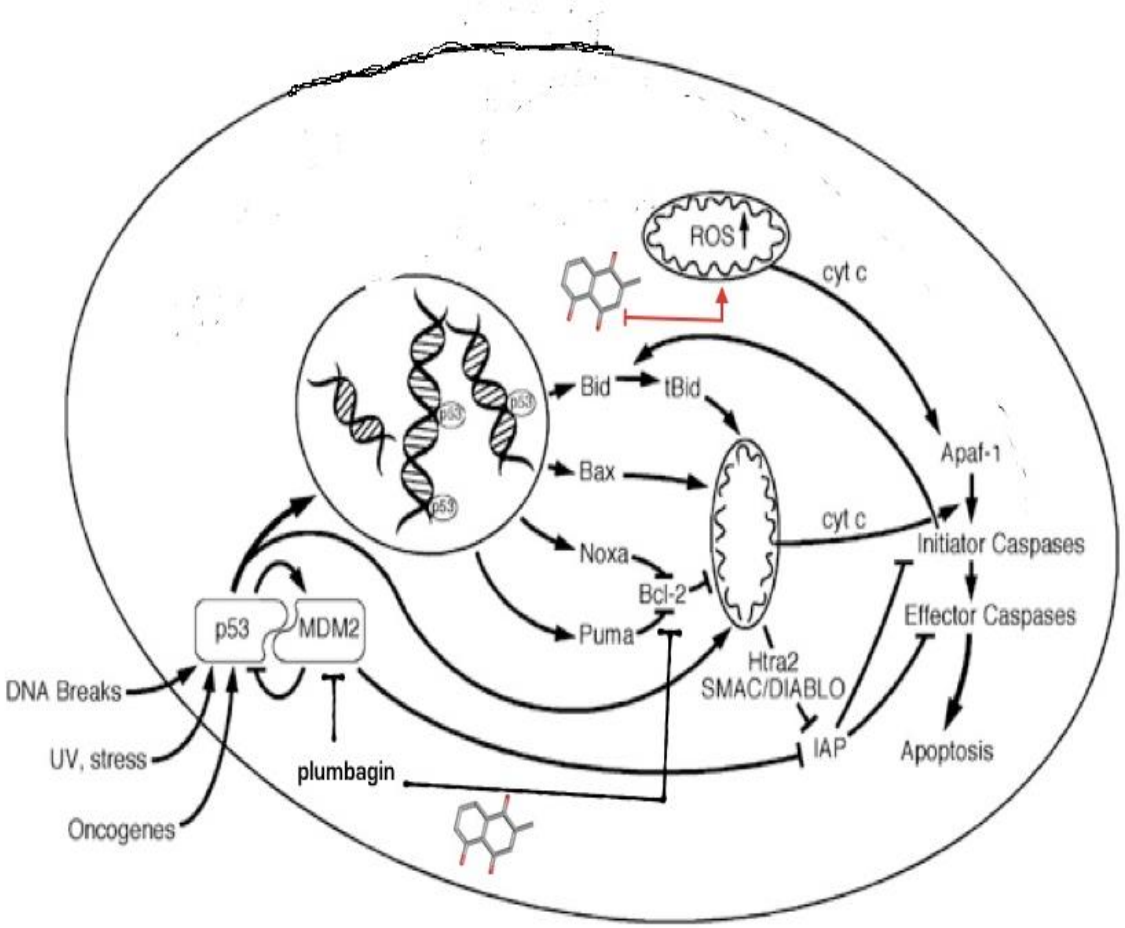

Fig 6.1: Proposed mechanism for plumbagin induction of apoptosis and toxicity via the intrinsic pathway

6.1 Contributions to knowledge

- Plumbagin induced mPT pore opening, increased mLPO, mATPase and caspases -3 and 9 activities in a dose- dependent manner in testes of Wistar rats.
- Plumbagin induced toxicity in the testes of experimental animal is via the intrinsic or mitochondrial-dependent pathway of apoptosis.
- Plumbagin-induced toxicity in the testes caused reduced sperm count, motility and various forms of sperm morphological disorders.
- Down-regulation of reproductive receptors and enzymes in testes is as a result of plumbagin toxicity.
- Plumbagin toxicity on sperm cells is a warning sign of infertility in males.
- Docking and simulation studies showed that plumbagin effectively inhibited MDM2 and bcl-2 protein to foster apoptosis in the intrinsic pathway of apoptosis. This is the consequent toxic effect of plumbagin in causing testicular damage in the reproductive machinery of Wistar rats as confirmed in the study.

REFERENCES

Adam-Vizi, A. and Seregi. R (1982) Receptor-independent stimulatory effect of noradrenaline on Na, K-ATPase in rat brain homogenate: Role of lipid peroxidation, *Biochemistry and Pharmacology.* 31: 2231- 2236.

Aditi, G. (1999) Medicinal plants used in traditional medicine in Jimma zone, *South West Ethopia, Pharm. Biol,* 37: 321-323

Antonio Toninello, Lisa Dalla Via, RobertoStevanato, Shiroki Yagisawa (2000) Kinetics and Free Energy Profiles of Spermine Transport in Liver Mitochondria. *Biochemistry* 39(2):324-31

Ameisen, J. C. (2002). "On the origin, evolution and nature of programmed cell death: a timeline of four billion years.*" Cell Death Differentiation:*9(4): 367-93.

Antonsson, B, Montessuit, S, Lauper, S, Eskes, R and Martinou, JC (2000). "Bax oligomerization is required for channel-forming activity in liposomes and to trigger cytochrome c release from mitochondria." *Journal of Biochemistry* 345(Pt 2): 271-8.

Aziz, M. H. Dreckschmidt, N.E. and Verma, A.K. (2008) Plumbagin, a medicinal plant-derived naphthoquinone, is a novel inhibitor of the growth and invasion of hormone refractory prostate cancer. *Cancer Research* 68(21):9024-9032

Bae, K.J., Soon,Y.L. and Kim, J.K. (2016) Plumbagin exerts immunosuppressive effects on human T-cell acute lymphoblastic leukemia Molt-4 cells. *Biochemical and Biophysical Research Communications* 473(1): 272-277

Barbagallo, G.A. Cain, K and Cohen, G. M. (2020) Effect of bisphenol on testicular steroidogenesis. *Frontiers in Endocrinology*. 11: 373-381

Barret, K. E., Barman, S. M., Boitano, H. and Brooks, R. S. (2013). Physiology of the male reproductive system. In: Barret, KE, Barman, SM, Boitano, S, Brooks, H. Ganong medical physiology. Twenty-fourth edition. MacGraw-Hill p: 419.

Bassir, O. (1963) Hand book of practical Biochemistry. University of Ibadan Press.23-30

Bauer, T. M. and Murphy, E. (2020) Role of mitochondrial calcium and the permeability transition pore in regulating cell death, Circ Res. 126 (2) 280–293.

Bello, I.J., Oyebode, O.O., Olanlokun, J.O., Oluwatodimu, O. and Olorunsogo, O.O. (2021) Plumbagin induces testicular damage via mitochondrial dependent cell death. *Chemico- Biological Interactions* 347: 109582.

Bejarano, I., Rodríguez, A.B., and Pariente, J.A. (2018) Apoptosis Is a Demanding Selective Tool during the Development of Fetal Male Germ Cells. *Frontiers in Cell and Developmental Biology,* 6: 65.

Bernardi, P. (2018) Why F-ATP synthase remains a strong candidate as the mitochondrial permeability transition pore, *Frontiers in Physiology.* 9 (2018) 1- 4

Bloom, H. (1948) Procedures in basic histology practice. A text book of histology 476

Bhargava, S. K. (1986) Antifertility effects of embelin and plumbagin in female rats [Embelia ribes, Plumbago zeylenica] Dixit, V.P. 30 In AGRIS 19: 29-3434

Bhargava, S. K. (1984) Effects of plumbagin on reproductive function of male dog, Indian *Journal of Experimental Biology*. 22 :153-156

Boatright, D. and Salvesen R. (2003) Mechanism of caspase3 activation. *Curr. Opin Cell Biol*. 15(6) 725-31

Bouillet, P and Strasser, A (2002). "BH3-only proteins - evolutionarily conserved proapoptotic Bcl-2 family members essential for initiating programmed cell death." *Journal of Cell Science* 115(Pt 8): 1567-74.

Boyer, P.D. (1997) The ATP synthase- a splendid molecular machine. *Annual Review of Biochemistry* 66, 717-749

Bratton, SB, MacFarlane, M, Cain, K and Cohen, GM (2000). "Protein complexes activate distinct caspase cascades in death receptor and stress-induced apoptosis." Experiment in Cell Research. 256(1): 27-33.

Bratton S., and Salvesen G. (2010) Regulation of the Apaf-1 caspase-9 apoptosome. *Journal of cell science* 123, 3209-3214

Carreau, S. Wolczynski, S Galeraud-Denis,I (2010) Aromatase, oestrogens and human male reproduction. Philosophical Transactions of the Royal Society of Biological Sciences, 365 (2010) 1571–1579

Chengyong Du, Xiaochen Zhang, Munya Yao, Kezhen Lv, Jiannan Wang and Luyan Yi (2018) Bcl-2 promotes metastasis through the epithelial to mesenchymal transition in the Bcap37 Medullary breast cancer cell line. *International Journal of Oncology* 15(6) 1189-1201

Chen, J. Wang, J., and Hui,C., (2016) Mechanisms of Heshouwuyin in regulating apoptosis of testicular cells in aging rats through mitochondrial pathway, BMC *Complementary Alternative Medicin*e 16 : 337

Chen, P. (2003). "Inhibiting the p53-MDM2 interaction: an important target for cancer therapy." Nat Rev Cancer 3(2): 102-9.

Christudas, S, Duraipandiyan, V. Agastian, P. and Ignacimuthu,S.(2012) Antidiabetic effect of plumbagin isolated from *Plumbago zeylanica* L. root and its effect on GLUT4 translocation in streptozotocin-induced diabetic rats. *Food and Chemical.*123: 288-301

Colombini, M. (2004) VDAC: the channel at the interface between mitochondria and the cytosol *Cell Biochemistry* 256: 107-115

Crompton, M. (1999) The mitochondrial permeability transition pore and its role in cell death *Biochemical Journal*, 341(2) 233-249

Danial, N.N. (2017) Bcl-2 family proteins: Critical check points of apoptotic cell death. *Clinical Cancer Research* 13(24):7254-7263

Ding, C. Wang, Q., Hao, Y. Ma, X. Wu, L. Du, M. Li, Y Wu, Y,Guo, F. and Ma, S (2016) Vitamin D supplement improved testicular function in diabetic rats. *Biochemical and Biophysical Research Communications,* 473 (2016) 161–167.

Dar, A.M. and Mir, S. (2017) Molecular Docking: Approaches, Types, Applications and Basic Challenges. *Anal. Bioanal. Tech*. 8: 356-364

Dominic P. Del Re, Dulguun Amgalan, Andreas Linkermann, Qinghang Liu, Richard N. Kitsis (2019) Fundamental Mechanisms of Regulated Cell Death and implications for Heart Disease", *Physiological Reviews,* 2019:445-466

Du, K.D.,Clarke , S.J., Javadov, S. A, Wagner D.A and Krrist, M.A (2018) Bcl-2 promotes metastasis through the epithelial to mesenchymal transition in the medullary breast cancer cell lines. *Oncology letter*. 342: 8891-8898

Erkkila, K., Kyttanen,S., Wikstrom , M., Taari, K., Hikim,A.P, Swerdloff, R.S., Dunkel , R (2006) Regulation of human male germ cell death by modulators of ATP production, *American Journal of Physiology ,Endocrinology and Metabolism* 290:1145–1154

Gazzotti, P., Malmstron, K. and Crompton M. (1979). Preparation and assay of animal mitochondria and submitochondrial vesicles. In: Carafoli E, Sememza G, editors. Membrane biochemistry: a laboratory manual on transport and bioenergetics. New York (NY): Springer-Verlag, p. 62–69.

Grant, B.J., Rodrigues, A.P. ElSawy, K.M., McCammon, J. A., and Caves, L. S. (2006). Bio3d: an R package for the comparative analysis of protein structures. *Bioinformatics, 22*(21), 2695-2696.

Giorgio, V, Federico Fogolari, Giovanna Lippe and Bernardi P. (2016) Subunit of Mitochondrial ATPase synthase: Role in regulation of Enzyme function. *British Journal of Pharmacology* 176:4247-4257

Green, L.C, Wagner D.A, Glogowski, J. and Wishnok, J.(2008)Chemical inhibition of mitochondrial division and its role in Bax/bak- dependent mitochondrial outer membrane permeabilisation *Developmental Cell* 14(2) 193-204

Grasberger, B.L. Lu,T. Schubert,C, Parks, D.J.T. Carver, E , Koblish,H.K. and Bone.R.F, (2005) Discovery and cocrystal structure of benzodiazepinedione HDM2 antagonists that activate p53 in cells, *Journalof Medical Chemistry* 48(4) (2005) 909-912.

Hafeez, B. B., W. Zhong, A. Mustafa, J. W. Fischer, O. Witkowsky, and A. K. Verma (2012) "Plumbagin inhibits prostate cancerdevelopment in TRAMP mice via targeting PKC , Stat3 and neuroendocrine markers",*Carcinogenesis, 2012*.288-297

Haverfield, S. Ham, K. A. Brown, E. R. Simpson, and S. J. (2011) Meachem, Teasing out the role of aromatase in the healthy and diseased testis, *Spermatogenesis1* (3) (2011) 240–249.

Hildebrand, P. W., Rose, A. S. and Tiemann, J. K. S. (2019). Bringing Molecular Dynamics Simulation Data into View. *Trends Biochem Sci, 44*(11), 902-913. Retrieved from https://www.ncbi.nlm.nih.gov/pubmed/31301982. doi:10.1016/j.tibs.2019.06.004

Huang, J. and MacKerell, A. D., Jr. (2013). CHARMM36 all-atom additive protein force field: validation based on comparison to NMR data. *Jounal of Computational Chemistry,34*(25), 2135-2145.,

Halestrap, A.P., Clarke , S.J. and Javadov, S. A. (2004) Mitochondria Permeability transition pore opening during myocardial reperfusion- a target for cardioprotection. *Cardiovascular Research* 6(3) 372-385

Itoigawa, M, Takeya, H. and Furukawa, T. (1991) Cardiotonic action of plumbagin on guinea-pig papillary muscle, Planta Med. 57**:** 317– 319.

Jeffery G., Gkotsi. D, Salt T., Hogg. C and Chau K.(2014) Recharging mitochondrial batteries in old eye. Near infra red increases ATP Exp 122: 50-53

Jezek, J., Katrina, F.C, and Randy S.(2017) Reactive oxygen species and mitochondrial dynamics, *Antioxidants* 7:13

Johnson D. and Lardy,H. (1967) Isolation of liver or kidney mitochondria. *Methods in Enzymology* 10; 94-96

Juárez-Rojas, A.L. García-Lorenzana, M. Aragón-Martínez, A. Gómez-Quiroz, L. and Retana-Márquez, M.(2015) Intrinsic and extrinsic apoptotic pathways are involved in rat testis by cold water immersion-induced acute and chronic stress,Systems Biology in Reproductive Medicine, 4 : 211-221

Kale R.A. (1990) Radiation induced lipid peroxidation in liposomes. *International Journal of Radiation Biology* 54(78): 356-361

Kiess, W. and Gallaher. B. (1998) Hormonal control of programmed cell death/apoptosis. *European Journal of Endocrinology.* 138 (5) 482-491.

Kirtikar, K.R, Basu, B.D. (1993) Indian medicinal plants, Shiva publishers Dehradun 1466-1468

Koff, Ramachandiran and Bernal-Mizrachi, (2015) Programme cell death as a defence against infection. Nat. Rev. Immunol 3; 151-164

Kumar, A.P, and Sethi G. (2011) Plumbagin inhibits invasion and migration of breast and gastric cancer cells by downregulating the expression of chemokine receptor CXCR4, *Molecular Cancer Research*, 10: 107.

Kumari, R. Kumar, C. and Lynn, A.(2014) GROMACS tool for high-throughput MM-PBSA calculations, *J Chem Inf Model* 54 (7) : 1951-1962.

Kumari, R., Kumar, R., Open Source Drug Discovery, C., and Lynn, A. (2014). gmmpbsa--GROMACS tool for high-throughput MM-PBSA calculations.2:23

Kwong, J.Q. and Molkentin, J.D. (2015) Physiological and pathological roles of the mitochondrial permeability transition pore in the heart, *Cell metabolism*, (2015) 21(2) 206–214.

Lai, L., Liu, J., Zhai, D., Lin, Q., He, L., Dong, Y., Zhang, J., Lu, B., Chen, Y., Yi, Z. and Liu, M. (2012) Plumbagin inhibits tumour angiogenesis and tumour growth through the Ras signalling pathway following activation of the VEGF receptor-2, *Britain Journal of Pharmacology*. 165 (4b): 1084-1096.

Lardy, H and Wellman. C, (1983) Induction and uncoupling of rat liver mitochondria by oral administered coartemeter. *American Journal of Biochemistry and Molecular Biology* 3(1) 110-118.

Lapidus, M and Sokolve, O.(1993) Spermine inhibition of permeability transition pore. *Archieves of Biochemistry and Biophysics*. 45: 234-241

Li ,T Lv, M Chen ,X Yu ,Y Zang , G and Tang,Z (2019) Plumbagin inhibits proliferation and induces apoptosis of hepatocellular carcinoma by downregulating the expression of SIVA, *Drug Design, Development and Therapeutics*, 13:1289-1300.

Li, D. Ueta, E., Kimura, T. Yamamoto, T. and Osaki, T.(2004) Reactive oxygen species (ROS) control the expression of Bcl-2 family proteins by regulating their phosphorylation and ubiquitination. Cancer science. 95: 644-650.

Li, L. Tan, H and Yang, H. (2017) Reactive oxygen species mediate heat stress-induced apoptosis via ERK dephosphorylation and Bcl-2 ubiquitination in human umbilical vein endothelial cells, Oncotarget. (2017) 12902-12916

Lowry, O.H., Rosebrough, N.J., Farr, A.L. and Randall, R.J.(1951) Protein measurement with the folin phenol reagent. *Journal of Biological Chemistry*. 193 (1) 265–275.

Mahdi, A.A. Rajender, S. and Shukla, K.K.(2012) Apoptosis, spermatogenesis and male infertility. *Frontiers in Bioscience* (Elite edition) 746-754.

Malaiyandi, J, Anandapadmanaban, G. Perumalsamy, H Kilankajae, A Kumar, C Dua,K Girija, S. and Balusamy S.(2020) Corrigendum to “Plumbagin from two Plumbago species inhibits the growth of stomach and breast cancer cell lines”, Industrial Crops and Products. 149 1-2332.

Martin K.R (2006) Targeting Apoptosis with Dietary Bioactive Agents: Society for Experimental Biology and Medicine. Minireview 36 : 136-143

Mortimer, D.C.(2018) The functional Anatomy of the human spermatozoon: relating ultrastructure and function. *Molecular Human Reproduction* 24(12): 567-592

Oduwole, O. (2018) Role of FSH in spermatogenesis. *Frontier in Endocrinology* 14: 273-281

Olorunsogo, O. O. and Malomo, S. O. (1985) Sensitivity of Oligomycin inhibited respiration of isolated rat liver mitochondrial perfluidone, a fluorinated arylalkylsulfonamide. *Toxicology* 35 (1985) (3), 231-40.

Olorunsogo, O. O. Bababunmi, E.A. and Bassir, O. (1979) Uncoupling effect of N-phosphonomethylglycine on at liver mitochondria. *Biochemcal Pharmacology*. 27 (1979) 925- 927

Omotuyi, I. O. (2015a). Ebola virus envelope glycoprotein derived peptide in human Furin-bound state: computational studies. *J Biomol Struct Dyn*, *33*(3), 461-470. Retrieved from https://www.ncbi.nlm.nih.gov/pubmed/25347780.

Omotuyi, O.I., Jun Nagai, Hiroshi Ueda (2015b) Lys39-Lysophosphatidate Carbonyl Oxygen Interaction Locks LPA1 N-terminal Cap to the Orthosteric Site and partners Arg124 During Receptor Activation", Scientific Reports, 2015doi:10.1080/07391102.2014.981207

Omotuyi, O.I, Nash, O Inyang, O.K. Ogidigo, J Enejoh, O. Okpalefe, T. Hamada(2018) Omotuyi, O.I., Jun Nagai, Hiroshi Ueda (2015) Lys39-Lysophosphatidate Carbonyl Oxygen Interaction Locks LPA1 N-terminal Cap to the Orthosteric Site and partners Arg124 During Receptor Activation", *Scientific Reports*, 2015

Omotuyi, I. O, Oyekanmi Nash, O. BasiruAjiboye, C. Gift Iwegbulam (2020) Atomistic simulation reveals structural mechanismsunderlying spike glycoprotein-enhanced fitness in *Journal of Computational Chemistry*, 45:678-687 2020

Omotuyi I. Olaposi (2021) Alteration of ssRNATorsion and Water Influx into ssRNA Pocket inK309A and S247A Mutations", Current Computer-Aided Drug Design, 17: 456-467 2021

Oyebode, O.T., Odejide, T.T., Kukoyi,A.J., Adebisi,A.A. and Olorunsogo, O.O.(2012) Effects of different fractions of *Calliandra portoricensis* root bark on isolated rat liver mitochondrial membrane permeability transition pore, *African Journal of Medicine and Medical Science.* 41 : 399-409.

Oyebode, O.T., Owumi,S.E., Oyelere, A.K. and Olorunsogo, O.O.(2019) *Calliandra portoricensis* Benth exhibits anticancer effects via alteration of Bax/Bcl-2 ratio and growth arrest in prostate LNCaP cells, *Journal of Ethnopharmacology*. 233: 64–72.

Parakh, T.,Hernandez, J.A., Grammer, J.C., Weck, J. Hunzicker-Dunn, M., A. Zeleznik, J. H. Nilson, (2006) Follicle-stimulating hormone/cAMP regulation of aromatase gene expression requires beta-catenin, Proceedings of the National Academy of Sciences of the United States of America103(33) (2006) 12435–12440.

Paras, J., Hanuman, P., Fauziya, and Binit, B.(2014) Pharmacological profiles of ethno-medicinal plant. Plumbago zeylanica- A review. *International Journal of Pharmaceutical Sciences, Review and Research* 24(1):157- 163

Pérez, M.J. and Quintanilla, R.A. (2017) Development or disease: duality of the mitochondrial permeability transition pore. *Dev. Biol*. 426 (2017) (1) 1-7.

Premkumari, P Rathinam, K Santhakumari, G.(1977) Antifertility activity of plumbagin. *Indian Journal of Medical Research*, 65: 829-838.

Rajakrishnan, S.R. Doman, H.J. and Scalar., M.D. (2017) Phytochemical evaluation of the root of *Plumbago zeylanica* and assessement of of its potential as a nephroprotective agent. *Saudi Journal of Biological Science 24:4-12*

Ray, P. Guha, D. and Chakraborty, J. (2016) Crocetin exploits p53-induced death domain (PIDD) and FAS-associated death (FADD) proteins to induce apoptosis in colorectal cancer, *Sci Rep* 6 : 32979

Reitman, K.C and Frankiel, G. (1957) A colorimetric method for determination of serum AST activity. *American Journal of Clinical Pathology* 28(1): 56-63

Roy, A (2017) A review on alkaloids an important therapeutic compound from plants. *International Journal of Plant Biotechnology* 3(2):1-9

Ruberto, G., Baratta M.T., Deans S.G. and Dorman H. J. (2000) Antioxidant and antimicrobial activity of Crithmum Maritimun essential oils. *Plant Med*. 66; 687

Rueden, C.T., Schindelin, J. ,.Hiner, M.De Zonia, A.E.Walter, E.T Arena., K.W.(2017) Eliceiri Image Clarke , S.J. and Javadov, S. A j2: Imagej for the next generation of scientific image data, BMC *Bioinformatics,* 18 (2017) 529.

Ruwanpura, S, M . McLachlan, R.I.Stanton Loveland, K.L. Meachem, S.J.(2008) Pathways involved in testicular germ cell apoptosis in immature rats after FSH suppression. *of Journal Endocrinology*. 197: (1) (2008) 35-43.

Ruwanpura, S.M., McLachlan, R.I., and Meachem, S. J. (2010) Hormonal regulation of male germ cell development, *Journal of Endocrinology*. 205: 117-131.

Sandur, S.K, Ichikawa, H Sethi,G Ahn, K.S. Aggarwal, B.B.(2006) Plumbagin (5-hydroxy methyl-1, 4-naphthoquinone) suppresses NF-kappaB activation and NF- kappa-B regulated gene products through modulation of p65 and l-kappa B alpha kinase activation, leading to potentiation of apoptosis induced by cytokine *Steroid Biochemistry and Molecular Biology.* 52 (1995) 375–381.

Sharma, A. and Singh, N. (2015) A multifarious potent herb: Plumbago Zeylanica. *Int. Journal of Scientific Research* 6(6):4825-4829

Scorilas, A., Yousef, A .K. , Jung, E , Rajpert-De Meyts, S. and Carsten, E.P.(2001) Diamand Identification and characterization of a novel human testis-specific kinase substrate gen which is down regulated in testicular tumors, *Biochemical and Biophysical Research and Communications.* 285(2) (2001) 400-408.

Sinha Hikim, A.P., Lue, P., Diaz-Romero, M., Yen, P.H. and Wang Swerdloff, C. (2003) Deciphering the pathways of germ cell apoptosis in the testis, *Journal of Steroid Biochemistry and Molecular Biology.* 85(2-5) 175-182.

Sukardi, S, Yakub, H, Ganabadi, S. Ahmad, Z. and Abd Hamid, R (2009) Impaired sperm parameters of Balb/c mice fed plumbagin, *Plant Med*. 75 :234-246

Tilak, J.C Adhikari, S, and Devasagayam, T.P.(2004) Antioxidant properties of *Plumbago zeylanica*, an indian medicinal plant and its active ingredient, plumbagin, *Redox Rep* 9: 219 -227.

Van Der Spoel, E. Lindahl, B. Hess, G. Groenhof, A. E. Mark, H. J. and Berendsen, J.S. (2005) GROMACS: fast, flexible, and free. *Journal of Computational Chemistry* 26 (16) 1701-1718.

Vassan S.S (2011) Semen analysis and sperm function tests. *Indian Journal of Urology,* Urology Society of India 27: 41-50

Wacquier, B. Combettes, L. and Dupont, G. (2020) Dual dynamics of mitochondrial permeability transition pore opening, *Sci Rep* 10 : 3924

Walter, H.J. (2000) The role of mitochondrial membrane permeability transition in rotenone induced –apoptosis in liver cells. *Toxicological sciences* 53:(2)340-352

Wang, F. Wang, Q , Zhou, Z.W. Yu, S.N. Pan, S.T He, Z.X Zhang, X Wang,D Y ,Yang,Y.X and Yang, T. (2015) Plumbagin induces cell cycle arrest and autophagy and suppresses epithelial to mesenchymal transition involving PI3K/AKT/MTOR-mediated pathway in human pancreatic cancer cells, Drug Design, Development and Therapeutics. 9 (2015) 537

Xu, W. Guo, G. Li, J., Ding, Z. Sheng, J. and Li. A. (2016) Activation of Bcl-2-Caspase-9 Apoptosis Pathway in the Testis of Asthmatic Mice, Plos one 11(3) (2016) e0149353.

Yang, J., Zong, X, Wu, J. Lin, S. Feng, Y. and Hu, J. (2015) Taurine increases testicular function in aged rats by inhibiting oxidative stress and apoptosis. Amino Acids. 47(2015) 1549–1558.

Ye , J., Coulouris, G. Zaretskaya, I. ,Cutcutache, I. S. Rozen, T. Madden, M.I. (2012) Primer-BLAST: A tool to design target-specific primers for polymerase chain reaction, BMC *Bioinformatics 13 : 134

Yu, J., Chen, B. Zheng, B., Qiao, C., Chen, X., Yan,Y., Luan, X. Xie, B., Liu, J. Shen, C.,He, C., Hu, X., Liu, M., Li, H., Shao, Q., and Fang, J (2019). ATP synthase is required for male fertility and germ cell maturation in Drosophila testes, Molecular medicine reports19 (3) 1561–1570.

Yunta, M. J. R. (2016). Docking and Ligand Binding Affinity: Uses and Pitfalls. *American Journal of Modeling and Optimization*, *4*(3), 74-114.

Zhao, J., Zhai,L., Liu,Z., Wu,S. and L. Xu, (2014) Leptin level and oxidative stress contribute to obesity induced low testosterone in murine testicular tissue, Oxidative Medicine and Cellular Longevity. 190945.

APPENDIX I

1.0 Calculations of BSA concentration curve

1ml contains 4mg = 4mg/ml

If 4mg = 1000 µl

Therefore, 20 µl will contain 80 µg/ml

40 µl = 160 µg/ml

60 µl = 240 µg/ ml

80 µl = 320 µg/ ml

100 ul = 400 µg / ml

Standard protein determination curve

Test tube	BSA (**µg/ µl**)	A	B	Average
1	80	0.041	0.041	0.041
2	160	0.084	0.080	0.082
3	240	0.119	0.117	0.118
4	320	0.152	0.152	0.152
5	400	0.186	0.186	0.186

MITOCHONDRIAL PROTEIN DETERMINATION

Applying the procedures of Lowry et al, 1951 using BSA Curve as standard 10 µl of mitochondria was pipette into test tube and make up to 1ml with water in the ratio 1: 100

Absorbance was read at 750nm and the concentration extrapolated from caliberated curve with serial dilution of stock. The actual protein concentration was obtained by dilution of BSA stock and multiplying with the dilution factor.1:1

Weight of liver ……4g

Volume of buffer used in the ratio 1:10

= 4x 9

= 36 ml

Slope from BSA Curve = 0.001

Average absorbance = 0.5042

Protein concentration = Absorbance / slope

= 0.5042/0.001

= 5041.5 10 μg/ml

Actual concentration = 504.1 X 10

= 504 ug/ml = 5.04 mg/ ml

Determination of volume of succinate needed for swelling assay medium

Sodium succinate

$CH_2COONa.6H_2O$ = standard formular for sodium succinate

Molecular weight = 270 .15g

270. 15 = 1M = 1000ml

0.25 M = 270.15 X 0.25

= 67.5375g

If 1000ml…….67.5375

10 ml……0.675375

0.675g of sodium succinate was dissolved in 10 ml

Initial concentration of succinate in stock C_1 = 250 mM

Final concentration of succinate in assay C_2 = 5Mm

Initial vol of succinate, V_1 = ?

Final volume of succinate in assay, V_2 = 2500 ul

From mole ratio theory:

$C_IV_I = C_2V_2$

250 X V1 = 5 X 2500

= 50 ul

Rotenone

Molar ~~mass~~ of rotenone = 394.4

1M = 394.4g = 1000ml

1M = 3.944 = 10 ml

80 μM = 0.000000316g = 10 ml

Initial concentration of Rotenone stock

$C_1V_1 = C_2V_2$

80 X V_1 = 0.8 X 2500

V_1 = 25 μl

Spermine

Molar mass of spermine = 348.19g

1M = 348.19 = 1000 ml

1 M = 3. 4819g = 10 ml

4mM = 0.013927g in 10ml

Final volume V_2 = **2500**μl

Final concentration of spermine in assay, C_2 = 0.1 Mm

Initial Volume of Spermine neededV1 = ?

Initial Concentration of Spermine in stock Ci = 4 Mm

From

$C_1V_1 = C_2 V_2$

VI = 62.5µl

Calcium

Molar mass of calcium chloride = 147.02g

1M = 147.02 = 1000ml

1M = 1.4702 in 10 ml

12000 µM = 0.017642g = 10ml

Final volume V2= 2500 µl

Initial concentration of Ca^{2+} in stock C1 = 12000Mm

Initial volume of Ca^{2+} neededV1 = ?

Final concentration of assay C_2 = 120 µM

From

$C_1V_1 = C_2V_2$

V_I = 25µl

Induction and inhibition

%induction = Range of test – Range of TA X 100/ Range of absorbance ofTA

% inhibition = Range of test – Range of spermine x 100 / Range of absorbance of spermine

Induction folds

Inhibitory fold with respect to spermine: Induction with respect to TA

Calcium - Spermine TA – NTA

Calcium NTA

REAGENT PREPATION FOR LIPID PEROXIDATION

0.07M $FeSO_4$

Molecular weight FeSO4 = 152g

152g FeSO4 in 1000ml = 1M

0. 07 M = 10.64g in 1000ml distil water

Thiobarbituric Acid

0.8 of TBA+ 1.1 g of SDS in 100ml distil water

20% Acetic acid

20ml of Acetic acid in 1000ml distil water

% inhibition = (100 – (Atest/Acontrol x100)

Plumbagin

Molar mass of PL = 334.19

1M = 334.19 = 1000 ml

1 M = 334.19g = 10 ml

4mM = 0.03349g in 10ml

Final volume V_2 = **2500**µl

Final concentration of PL in assay, C_2 = 0.1 Mm

Initial Volume of PL needed V1 = ?

Initial Concentration of PL in stock Ci = 5 Mm

From

C1V1 = C2 V2

VI = 45µl

Primers and Amplicons for the Expression of Testis Functions

S/N	Primers	Amplicon size (bp)
FSH-R (NM_198783.1)	**CAAAGATCCGGTGCCTTCCT GGCGATTTTCTCAGCAGTCC**	**199**
TESK-I (NM_031326.1)	**TTCCAGGGGGCTAAGGATGA CACACTGCGACGGATGAGAT**	**198**
PG-R (NM_053655.3)	**ACAACAGGGAAGAAAATGG CGTTGGGCGAGAAAACCTTG**	**184**
Aromatase (NM_017050.1	**GCGTCATTCACTTCGAGCAG CCTCTCTTCATCCGCTGGAC**	**191**

APPENDIX II

Preliminary *in vitro* experiment

Mitochondrial absorbance values

0:00	-0.00	-0.000	0	0	0	0	0
0:30	-0.001	0	-0.001	-0.033	-0.023	-0.01	-0.073
1:00	-0.004	-0.047	-0.002	-0.046	-0.038	-0.048	-0.173
1:30	-0.007	-0.132	-0.005	-0.059	-0.085	-0.127	-0.247
2:00	-0.007	-0.227	-0.008	-0.072	-0.131	-0.23	-0.305
2:30	-0.009	-0.317	-0.011	-0.081	-0.177	-0.312	-0.323
3:00	-0.011	-0.359	-0.013	-0.091	-0.209	-0.367	-0.384
3:30	-0.011	-0.376	-0.015	-0.1	-0.246	-0.402	-0.39
4:00	-0.011	-0.412	-0.016	-0.108	-0.292	-0.43	-0.401
4:30	-0.011	-0.432	-0.017	-0.117	-0.346	-0.462	-0.409
5:00	-0.013	-0.442	-0.021	-0.126	-0.36	-0.47	-0.422
5:30	-0.013	-0.452	-0.021	-0.135	-0.37	-0.482	-0.427
6:00	-0.015	-0.46	-0.022	-0.145	-0.386	-0.492	-0.45
6:30	-0.015	-0.472	-0.022	-0.156	-0.393	-0.499	-0.465
7:00	-0.015	-0.472	-0.023	-0.171	-0.408	-0.507	-0.495
7:30	-0.018	-0.479	-0.025	-0.197	-0.417	-0.516	-0.5
8:00	-0.02	-0.511	-0.026	-0.215	-0.425	-0.525	-0.512
8:30	-0.022	-0.532	-0.029	-0.24	-0.429	-0.537	-0.53
9:00	-0.022	-0.532	-0.03	-0.263	-0.435	-0.548	-0.57
9:30	-0.022	-0.532	-0.032	-0.283	-0.445	-0.559	-0.58
10:00	-0.024	-0.532	-0.043	-0.305	-0.45	-0.57	-0.59
10:30	-0.028	-0.538	-0.053	-0.323	-0.453	-0.587	-0.611
11:00	-0.028	-0.544	-0.055	-0.342	-0.465	-0.593	-0.618
11:30	-0.031	-0.557	-0.056	-0.361	-0.474	-0.605	-0.625
12:00	-0.031	-0.554	-0.056	-0.378	-0.482	-0.608	-0.645

Liver *In vitro Experiment*

Mitochondrial absorbance values

TME	NTA	SPERMINE	TA	20µg/ml	40µg/ml	60µg/ml	80µg/ml
0:00	0	0	0	0	0	0	0
0:30	-0.001	-0.001	0	-0.12	-0.055	-0.018	-0.002
1:00	-0.004	-0.002	-0.047	-0.183	-0.133	-0.072	-0.162
1:30	-0.007	-0.005	-0.132	-0.242	-0.225	-0.145	-0.302
2:00	-0.007	-0.008	-0.227	-0.292	-0.305	-0.2	-0.394
2:30	-0.009	-0.011	-0.317	-0.337	-0.385	-0.246	-0.441
3:00	-0.011	-0.013	-0.359	-0.381	-0.452	-0.289	-0.479
3:30	-0.011	-0.015	-0.376	-0.425	-0.509	-0.332	-0.512
4:00	-0.011	-0.016	-0.412	-0.462	-0.558	-0.375	-0.537
4:30	-0.011	-0.017	-0.432	-0.496	-0.597	-0.418	-0.558
5:00	-0.013	-0.021	-0.442	-0.526	-0.627	-0.461	-0.574
5:30	-0.013	-0.021	-0.452	-0.548	-0.64	-0.502	-0.588
6:00	-0.015	-0.022	-0.46	-0.567	-0.653	-0.539	-0.598
6:30	-0.015	-0.022	-0.472	-0.582	-0.663	-0.574	-0.607
7:00	-0.015	-0.023	-0.472	-0.594	-0.669	-0.611	-0.616
7:30	-0.018	-0.025	-0.479	-0.603	-0.67	-0.628	-0.623
8:00	-0.02	-0.026	-0.511	-0.612	-0.673	-0.648	-0.63
8:30	-0.022	-0.029	-0.532	-0.621	-0.674	-0.663	-0.636
9:00	-0.022	-0.03	-0.532	-0.625	-0.675	-0.676	-0.641
9:30	-0.022	-0.032	-0.532	-0.63	-0.675	-0.685	-0.65
10:00	-0.024	-0.043	-0.532	-0.636	-0.675	-0.693	-0.66
10:30	-0.028	-0.053	-0.538	-0.64	-0.675	-0.701	-0.679
11:00	-0.028	-0.055	-0.544	-0.644	-0.675	-0.7	-0.69
11:30	-0.031	-0.056	-0.557	-0.647	-0.675	-0.706	-0.69
12:00	-0.031	-0.056	-0.554	-0.65	-0.675	-0.722	-0.7

APPENDIX III

Mitochondrial absorbance values

Testis *in vitro Experiment*

INH	20µg/ml	40µg/ml	60µg/ml	80ug/ml
0	0	0	0	0
-0.001	-0.001	0	-0.001	-0.012
-0.002	-0.022	-0.03	-0.04	-0.015
-0.008	-0.03	-0.03	-0.06	-0.023
-0.011	-0.04	-0.04	-0.06	-0.245
-0.013	-0.07	-0.04	-0.07	-0.267
-0.015	-0.12	-0.05	-0.067	-0.299
-0.016	-0.17	-0.05	-0.088	-0.378
-0.017	-0.21	-0.06	-0.092	-0.433
-0.019	-0.26	-0.06	-0.211	-0.446
-0.021	-0.28	-0.07	-0.233	-0.455
-0.022	-0.3	-0.08	-0.265	-0.466
-0.022	-0.31	-0.18	-0.275	-0.476
-0.023	-0.32	-0.24	-0.345	-0.477
-0.025	-0.34	-0.32	-0.358	-0.495
-0.026	-0.34	-0.36	-0.368	-0.497
-0.029	-0.36	-0.38	-0.382	-0.498
-0.03	-0.36	-0.39	-0.465	-0.498
-0.032	-0.37	-0.42	-0.487	-0.566
-0.042	-0.38	-0.44	-0.487	-0.578
-0.042	-0.39	-0.46	-0.498	-0.598
-0.042	-0.39	-0.47	-0.524	-0.653
-0.042	-0.4	-0.48	-0.544	-0.668
-0.042	-0.42	-0.48	-0.542	-0.678
-0.042	-0.44	-0.49	-0.533	-0.679

APPENDIX IV

In vivo testis experiment

Mitochondrial absorbance values

SPERMINE	2.5mg/kg	5mg/kg	10mg/kg
0	0	0	0
-0.002	-0.052	-0.06	-0.021
-0.004	-0.091	-0.122	-0.076
-0.009	-0.122	-0.17	-0.134
-0.027	-0.142	-0.215	-0.2
-0.039	-0.159	-0.249	-0.244
-0.051	-0.17	-0.275	-0.292
-0.06	-0.173	-0.294	-0.334
-0.068	-0.179	-0.304	-0.365
-0.07	-0.181	-0.316	-0.377
-0.072	-0.183	-0.318	-0.388
-0.075	-0.187	-0.322	-0.397
-0.078	-0.191	-0.325	-0.404
-0.081	-0.194	-0.329	-0.416
-0.081	-0.196	-0.329	-0.419
-0.083	-0.199	-0.332	-0.423
-0.085	-0.201	-0.334	-0.425
-0.087	-0.203	-0.336	-0.436
-0.088	-0.204	-0.337	-0.44
-0.088	-0.206	-0.339	-0.467
-0.09	-0.208	-0.34	-0.478
-0.092	-0.209	-0.342	-0.498
-0.093	-0.211	-0.344	-0.506
-0.094	-0.212	-0.346	-0.509
-0.095	-0.213	-0.35	-0.512

APPENDIX V

In vivo liver experiment

Mitochondrial absorbance values

TIME	NTA	TA	SPERMINE	2.5mg/kg bdwt	5mg/kg bdwt	10mg/kg bdwt
0:00	0	0	0	0	0	0
0:30	-0.002	-0.084	-0.001	-0.005	-0.02	-0.034
1:00	-0.005	-0.104	-0.002	-0.028	-0.162	-0.064
1:30	-0.006	-0.318	-0.005	-0.039	-0.274	-0.095
2:00	-0.012	-0.447	-0.008	-0.041	-0.274	-0.125
2:30	-0.014	-0.553	-0.011	-0.044	-0.304	-0.155
3:00	-0.014	-0.622	-0.013	-0.048	-0.305	-0.183
3:30	-0.017	-0.675	-0.015	-0.062	-0.307	-0.208
4:00	-0.019	-0.704	-0.016	-0.074	-0.31	-0.235
4:30	-0.021	-0.725	-0.017	-0.083	-0.312	-0.256
5:00	-0.021	-0.738	-0.021	-0.092	-0.312	-0.274
5:30	-0.024	-0.742	-0.021	-0.12	-0.318	-0.29
6:00	-0.026	-0.742	-0.022	-0.164	-0.318	-0.302
6:30	-0.031	-0.742	-0.022	-0.169	-0.32	-0.315
7:00	-0.033	-0.742	-0.023	-0.171	-0.32	-0.327
7:30	-0.033	-0.742	-0.025	-0.172	-0.322	-0.338
8:00	-0.035	-0.744	-0.026	-0.173	-0.322	-0.352
8:30	-0.038	-0.746	-0.029	-0.174	-0.322	-0.358
9:00	-0.038	-0.746	-0.03	-0.175	-0.325	-0.381
9:30	-0.04	-0.747	-0.032	-0.175	-0.325	-0.39
10:00	-0.04	-0.752	-0.043	-0.175	-0.325	-0.4
10:30	-0.04	-0.756	-0.053	-0.181	-0.327	-0.409
11:00	-0.04	-0.758	-0.055	-0.187	-0.327	-0.418
11:30	-0.04	-0.758	-0.056	-0.193	-0.327	-0.428
12:00	-0.04	-0.758	-0.056	-0.193	-0.33	-0.428

List of primers and their properties:

Primer name	Accession number	Length Forward	Length Reverse	Forward Primer sequence (5'-3')	Reverse Primer sequence (5'-3')	Optimum TM	Amplicon size
Follicle stimulating Hormone Receptor (FsHR), mRNA	NM_199237.1	20	20	CACTGGCTGTGTCATTGCTC	CAAACCTCAGTTCAATGGCG	55°C	180 bp
Testis-Specific Kinase 1 (TESK1), mRNA	NM_031578.1	20	21	TGGCAGGCCATAGGTTAAGG	ACGTGTACAGACCTTTTCCCC	58°C	127 bp
progesterone receptor (Pgr), mRNA	NM_022847.1	21	20	GACACAAAATCAGCAGTCGCT	ACCAAGAAGTGATGGCCTCG	61°C	130 bp
Aromatase mRNA	NM_031144.3	20	20	CTGGCTCCTAGCACCATGAA	CGCAGCTCAGTAACAGTCCG	61°C	192 bp
actin, beta (Actb), mRNA	NM_031144.3	20	20	CTGGCTCCTAGCACCATGAA	CGCAGCTCAGTAACAGTCCG	61°C	192 bp

Protocol for Lipid Peroxidation

Test Tube	**Mitochondria (ml)**	**Tris KCl (ml)**	**TCA (ml)**	**TBA (ml)**
1 (Control)	0.4	1.6	0.5	0.5
2	0.4	1.6	0.5	0.5
3	0.4	1.6	0.5	0.5
4	0.4	1.6	0.5	0.5
				After this, place in water bath at 80^{o}C for 45min, centrifuge at 3000rpm for 10min and read absorbance of clear supernatant at 532nm against blank of distilled water.